

**DEVELOPING TISSUE ENGINEERING AND GENE THERAPY APPROACHES
INVOLVING THE USE OF NERVE GROWTH FACTOR AND MUSCLE-DERIVED
STEM CELLS TO IMPROVE THE REGENERATION OF DYSTROPHIC MUSCLE**

by

Mitra Lavasani

B.S., San Jose State University, 1998

Submitted to the Graduate Faculty of

School of Engineering in partial fulfillment

of the requirements for the degree of

Master of Science in Bioengineering

University of Pittsburgh

2005

UNIVERSITY OF PITTSBURGH

SCHOOL OF ENGINEERING

This thesis was presented

by

Mitra Lavasani

It was defended on

June 30, 2005

and approved by

Harvey S. Borovetz, PhD, Professor, Department of Bioengineering

Bruno Péault, PhD, Professor, Department of Pediatrics and Cell Biology

Xiao Xiao, PhD, Professor, Department of Orthopaedic Surgery

Thesis Advisor: Johnny Huard, PhD, Professor, Department of Orthopaedic Surgery, Molecular Genetics and Biochemistry and Bioengineering

Copyright by Mitra Lavasani
2005

**DEVELOPING TISSUE ENGINEERING AND GENE THERAPY APPROACHES
INVOLVING THE USE OF NERVE GROWTH FACTOR AND MUSCLE-DERIVED
STEM CELLS TO IMPROVE THE REGENERATION OF DYSTROPHIC MUSCLE**

Mitra Lavasani, M.S.

University of Pittsburgh, 2005

In recent years, researchers have attempted to use gene- and cell-based therapies to restore dystrophin and alleviate the muscle weakness that results from Duchenne muscular dystrophy (DMD). Our research group has isolated a population of muscle-derived stem cells (MDSCs) from the postnatal skeletal muscle of mice. In comparison with satellite cells, MDSCs display an improved transplantation capacity in dystrophic *mdx* muscle that can be attributed to their ability to undergo long-term proliferation, self-renewal, and multipotent differentiation, including differentiation toward endothelial and neuronal lineages. The overall goal of this study was to investigate whether the use of nerve growth factor (NGF) improves the transplantation efficiency of MDSCs. Two methods of *in vitro* NGF stimulation were used: retroviral transduction of MDSCs with a CLNGF vector to constitutively express NGF and direct stimulation of MDSCs with NGF protein. Neither method of NGF treatment changed the marker profile or proliferation behavior of the MDSCs, but direct stimulation with NGF protein significantly delayed cells' *in vitro* differentiation ability. Stimulation with NGF also significantly enhanced the engraftment efficiency of MDSCs transplanted within the dystrophic muscle of *mdx* mice, resulting in better muscle regeneration. These findings highlight the importance of NGF as a modulatory molecule, the study of which will broaden our understanding of its biological role in the regeneration and repair of skeletal muscle by muscle-derived cells.

DESCRIPTORS

Cell Transplantation

Gene Therapy

Muscle Derived Stem Cells

Muscular Dystrophy

Muscle Regeneration

Nerve Growth Factor

TABLE OF CONTENTS

DESCRIPTORS	v
NOMENCLATURE.....	i
ACKNOWLEDGEMENTS	iv
1.0 BACKGROUND	1
1.1 Adult Skeletal Muscle Characteristics	1
1.2 Morphological Characteristics of Skeletal Muscle Regeneration.....	2
1.3 Duchenne Muscular Dystrophy: A Skeletal Muscle Disorder.....	5
1.3.1 Animal Model of DMD	7
1.4 Current Treatments and Their Limitations	8
1.5 Muscle-Derived Stem Cells: Potential for Muscle Regeneration	11
1.6 Role of Growth Factors in Muscle Regeneration	15
1.6.1 Nerve Growth Factor— NGF	19
1.6.2 NGF Receptors: TrkA and p75 ^{NTR}	20
1.7 MDSCs & NGF as A Remedy for Tissue Engineering	22
2.0 PROJECT OBJECTIVES.....	24
2.1 Objective 1: Examine the Phenotypic Effect of NGF Stimulation on MDSCs <i>in vitro</i>	24
2.2 Objective 2: Evaluate the Effect of NGF Stimulation on MDSCs’ Regeneration Capacity.	25

3.0 INTRODUCTION.....	26
4.0 MATERIALS AND METHODS	29
4.1 Animals	29
4.2 Cell Isolation and Culturing.....	29
4.3 Generation of Retroviral Vector Expressing NGF.....	30
4.4 Stimulation or Retroviral Transduction of MDSCs with NGF	30
4.5 Cell Characterization by Flow Cytometry	31
4.6 Myogenic Marker Expression by Immunocytochemistry.....	32
4.7 Cell Division Analysis	33
4.7.1 Experimental Settings	33
4.7.2 Imaging System	34
4.7.3 Non-exponential Growth Model.....	35
4.8 Myogenic Differentiation.....	36
4.9 Myofiber Regeneration <i>in vivo</i>	37
4.10 Quantification of Dystrophin-Positive Myofibers Using Northern Eclipse	38
4.11 Statistical Analysis.....	41
5.0 RESULTS	42
5.1 Quantitative Detection of NGF	42
5.2 Proliferation Kinetics	44
5.3 In vitro Stem Cell and Myogenic Marker Profiles.....	45
5.4 In vitro Myogenic Differentiation.....	47
5.5 Muscle Regeneration	49
5.6 Morphological Analysis.....	51

6.0 DISCUSSION	58
7.0 FUTURE STUDIES.....	62
8.0 SUMMARY AND CONCLUSIONS	65
APPENDIX A.....	66
PREPLATE TECHNIQUE: ISOLATION OF THREE POPULATIONS OF MUSCLE- DERIVED CELLS.....	66
APPENDIX B.....	68
NON-EXPONENTIAL GROWTH MODEL	68
APPENDIX C.....	74
DYSTROPHIN-POSITIVE MYOFIBERS ANALYSIS USING NORTHERN ECLIPSE.....	74
APPENDIX D.....	85
PROCEDURES FOR QUANTIZATION OF DYSTROPHIN-POSITIVE MYOFIBER USING NORTHERN ECLIPSE.....	85
BIBLIOGRAPHY.....	89

LIST OF TABLES

Table 1.1	The Marker profile comparison between myogenic, stem, and blood cells, adapted from [96, 97]	13
Table 1.2	Effect of growth factors on the proliferation and fusion of myoblasts <i>in vitro</i> , adapted from [130].....	18
Table 5.1	Dimensional characteristics of dystrophin-expressing myofibers	56

LIST OF FIGURES

Figure 1.1	Morphological characteristics of adult mammalian skeletal muscle	2
Figure 1.2	Skeletal muscle repair process	3
Figure 1.3	Membrane stabilization by dystrophin protein interaction with intracellular cytoskeleton, actin filaments, and the extracellular matrix (Adapted from Expert Reviews in Molecular Medicine 2002, Cambridge University Press).....	6
Figure 1.4	Immunohistochemical dystrophin labeling of skeletal muscle biopsies, taken from a normal individual versus a patient with Duchenne's muscular dystrophy (Courtesy of Johnny Huard, PhD, Pittsburgh, PA).....	7
Figure 1.5	Schematic of the mechanism by which growth factors regulate cell behavior, adapted from [111].....	17
Figure 1.6	A schematic drawing of the structural features of Trk and p75 receptor, adapted from www.izn.uni-heidelberg.edu/de/download/LFB2004/Tucker.pdf	22
Figure 4.1	Bioinformatic Cell Culture and Imaging System (Courtesy of Bridget Deasy, PhD, Pittsburgh, PA).....	35
Figure 4.2	Dimensional analyses of immunohistochemically-labeled dystrophin-positive myofibers	40
Figure 4.3	Challenges encountered during thresholding an image	40
Figure 5.1	Schematic representation of the retroviral vector expressing NGF	42
Figure 5.2	Quantitative detection by ELISA of the NGF protein in the cell supernatant	43
Figure 5.3	Proliferation kinetics of MDSCs.....	45
Figure 5.4	Marker profile analysis of MDSCs	47
Figure 5.5	Myogenic differentiation <i>in vitro</i>	48

Figure 5.6	Dystrophin-positive myofiber regeneration elicited by MDSCs transduced with CL-NGF	50
Figure 5.7	Dystrophin-positive myofiber regeneration elicited by MDSCs stimulated with NGF protein	51
Figure 5.8	Representative time-lapsed images of C-MDSCs population demonstrating visualization and morphological recognition of cell morphology in culture (refer to attached video clip by double clicking on first image).....	52
Figure 5.9	Fiber area distribution (FAD) of newly generated (dystrophin-positive) and host myofibers	53
Figure 5.10	A high magnification image of a small portion of an E-MDSC graft shows a large number of centronucleated myofibers	54
Figure 5.11	Morphological features of dystrophin-positive myofiber	55

NOMENCLATURE

ACRONYMS, ABBREVIATIONS, AND SYMBOL DEFINITIONS

ACCW	Automated Cell's CytoWorks™
Bcl-2	A protein associated closely with progenitor cells
b-FGF	Basic fibroblast growth factor
bp	Base pair
BrdU	Bromodeoxyuridine
CD34	Cluster differentiation 34: A transmembrane cell surface glycoprotein restricted to the capillary endothelium and hematopoietic progenitor cells
CD45	Cluster differentiation 45: A transmembrane cell surface glycoprotein used as stem cell and hematopoietic cell marker
c-kit	Bone marrow-derived hematopoietic stem cell marker
CNPase	2', 3'-Cyclic-nucleotide 3'-phosphodiesterase
DMD	Duchenne Muscular Dystrophy
DMEM	Dulbecco's Modified Eagle's Medium
EGF	Epidermal growth factor
ELISA	Enzyme-Linked Immunosorbent Assay
EP cells	Early preplate cells
FACS	Fluorescence Activated cell Sorting

FGF-2	Fibroblast growth factor-2
Flk-1	A mouse homologue of KDR receptor, a VEGF receptor expressed on the common precursors of endothelial and hematopoietic stem cells
HBSS	Hanks' Balanced Salt Solution
H&E	Hematoxylin and eosin
HSC	Hematopoietic stem cells
IGF-1	Insulin-like growth factor type 1
LIF	Leukemia inhibitory factor
LP cells	Late preplate cells
LTP cells	Long-term proliferating cells
M-Cadherin	A transmembrane protein highly expressed in developing skeletal muscle
MDSCs	Unique population of muscle-derived stem cells isolated by researchers in our laboratory
MyHC	Myosin heavy chain
MyoD	A myogenic regulatory factor that is expressed at earlier stages of myogenic progression
NF	Neurofilament
NGF	Nerve growth factor
Pax7	A transcription factor required for satellite cell development
PBS	Phosphate Buffered Saline
PE	Phycoerythrin
PDGF	Platelet-derived growth factor
PM	Proliferation medium

Sca-1	Stem cell antigen-1
SCF	Stem cell factor
TGF- α	Transforming growth factor α
TGF- β	Transforming growth factor β
vWF	von Willebrand factor

ACKNOWLEDGEMENTS

There are so many people who have touched my life to where I am today, and I can't describe how sincerely I want to thank each one of them for their kindness, guidance, patience and joyfulness. First and foremost, I would like to dedicate this thesis to my mother, who, throughout my life has been my guardian angel. I thank her for unconditional love and sacrifices, her dedication as a wonderful role model, and most importantly for being a great friend. I would like to extend my whole-hearted appreciation to my brother for encouraging me to work hard and follow my dreams. He has always known what I was capable of achieving, even when I was not so certain myself. In addition, I would like to thank my sister and nephew for their love and understanding when I needed them the most and my nephew for his computer expertise during my computer crisis. I am thankful of having a wonderful niece and hope I can be an inspiration toward her future academic excellence. Last but not least, I am grateful to my best friend, Nina Shankian, for her unconditional friendship and support.

I would like to gratefully acknowledge the support of my thesis advisor, Dr. Johnny Huard, as an outstanding paragon of commitment and generosity to research endeavors; Dr. Huard has consistently helped me to reach my full potential and beyond, trusting my scientific input, and offering his dedication to his graduate students as a whole. Sincere thanks to Drs. Harvey Borovetz, Bruno Péault, and Xiao Xiao for their willingness to be part of my thesis committee and critique the work presented here, and more. A special thanks to Dr. Borovetz for his

devotion to bioengineering students and his special attention to those of us not coming from an engineering background; I hope by now you have the answer to your question of why I chose University of Pittsburgh for my graduate studies. Many thanks to Dr. David Vorp for organizing and supervising our bioengineering graduate committee, where students' concerns and suggestions are always welcomed. Special thanks to Lynette Spataro for her willingness to help and her patience when faced with questions. Unfortunately I cannot list all the members of the Growth and Development Laboratory. It is truly a pleasure to work with such talented and intelligent individuals with such diverse backgrounds in a friendly and supportive environment. In particular, however, I would like to acknowledge Dr. Aiping Lu for her support and mentoring, Drs. Bridget Deasy, Burhan Gharaibeh, and Jonathan Pollett for participating in helpful scientific discussions and reinforcing my pursuit of my goal with their emotional support. I would also like to thank Jim Cummins for his thoughtful scientific reasoning, Marcelle Huard for her talent with the cryostat sectioning, and Ryan Sauder for his excellent editorial assistance. Last but not least, I wish to thank our supportive administrators, Barbara Lipari and Melanie Predis for offering outstanding assistance and support behind the scenes. I would also like to thank Drs. Hairong Peng, Terry Partridge, and Paul Robbins for generously sharing NGF retroviral vector, dystrophin antibody, and NGF cDNA, respectively. Finally, I would like to acknowledge the funding support for the work presented here in part by grants to Dr. Johnny Huard from the Muscular Dystrophy Association, the National Institutes of Health (NIH, 1R01 AR49684-01), the Department of Defense (DOD, 03099002), the William F. and Jean W. Donaldson Chair at Children's Hospital of Pittsburgh, and the Henry J. Mankin Endowed Chair at the University of Pittsburgh.

1.0 BACKGROUND

1.1 ADULT SKELETAL MUSCLE CHARACTERISTICS

The muscle fibers are the basic contractile units of skeletal muscles, individually surrounded by a connective tissue layer and grouped into bundles called perimysium to form a skeletal muscle (Figure 1.1A). Myofibers are multinucleated syncytia with their postmitotic myonuclei located at the periphery, as seen in the muscle cross-section stained with hematoxylin and eosin (H&E) (Figure 1.1B, arrow). As well as being rich in connective tissue, skeletal muscles are highly vascularized to provide essential nutrients for muscle function (Figure 1.1B, black arrowhead). As the myofiber matures, it is contacted by a single motor neuron that branches throughout the muscle (Figure 1.1B, white arrowhead). The functional properties of skeletal muscle including its contractile ability depend on the maintenance of a complex framework of myofibers, motor neurons, blood vessels, and extracellular connective tissue matrix. Therefore, revascularization, reinnervation, and reconstitution of the extracellular matrix are all essential aspects of the muscle regeneration process.

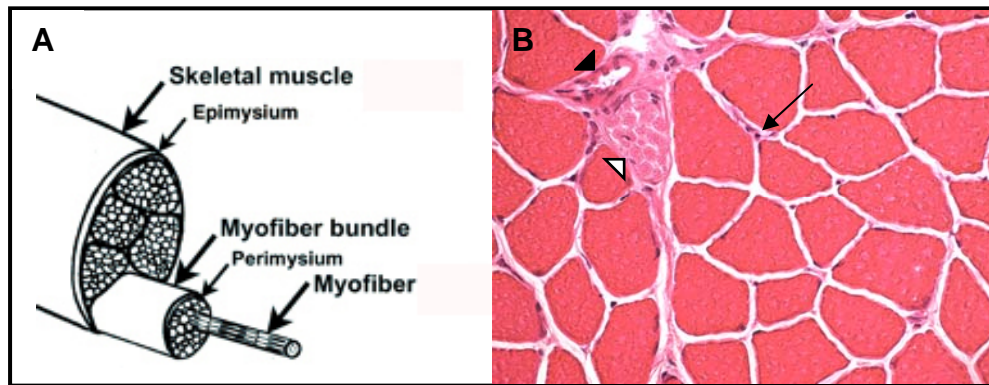


Figure 1.1 Morphological characteristics of adult mammalian skeletal muscle

1.2 MORPHOLOGICAL CHARACTERISTICS OF SKELETAL MUSCLE REGENERATION

Skeletal muscle is a heterogeneous tissue, containing vascular and neural cells in addition to the contractile myofibers. Adult mammalian skeletal muscle is a stable tissue with little turnover of nuclei [1, 2]. Minor lesions inflicted by day-to-day wear and tear elicit only a slow turnover of its constituent multinucleated muscle fibers. It is estimated that in a normal adult rat muscle, no more than 1–2% of myonuclei are replaced every week [2]. Nonetheless, mammalian skeletal muscle has the ability to complete a rapid and extensive regeneration in response to severe damage. Whether the muscle injury is inflicted by a direct trauma (i.e., extensive physical activity and especially resistance training) or innate genetic defects (i.e., DMD), muscle regeneration is characterized by two phases: a degenerative phase and a regenerative phase (Figure 1.2A).

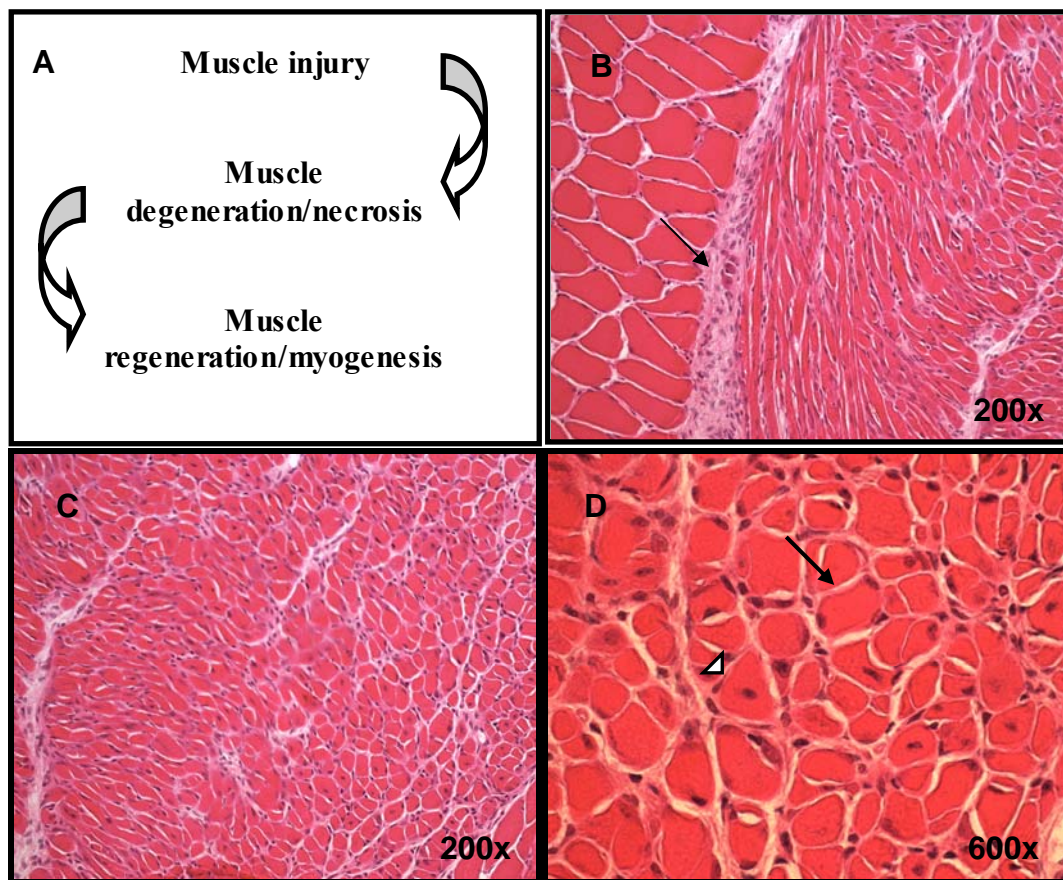


Figure 1.2 Skeletal muscle repair process

The initial event of muscle degeneration is necrosis of the muscle fibers. Figure 1.2B shows 10 μm cross sections of mice gastrocnemius muscle stained with H&E. Injury by cardiotoxin (CTX) injection in the muscle results in a rapid necrosis of myofibers and the activation of an inflammatory response leading to the loss of muscle architecture (compare Figure 1.2B with Figure 1.1B) including the formation of fibrosis (Figure 1.2B, arrow). This event is generally triggered by disruption of the myofiber sarcolemma resulting in increased myofiber permeability and disruption of the myofiber integrity. The early phase of muscle injury

is usually accompanied by the activation of mononucleated cells, principally inflammatory cells and myogenic cells. Present reports suggest that factors released by the injured muscle activate inflammatory cells residing within the muscle, which in turn provide the chemotactic signals to circulating inflammatory cells (reviewed in Refs. [3, 4]). Neutrophils are the first inflammatory cells to invade the injured muscle, with a significant increase in their number being observed as early as 1–6 hours after myotoxin or exercise-induced muscle damage [5, 6]. After neutrophil infiltration and ~ 48 hours post-injury, macrophages become the predominant inflammatory cell type within the site of injury [4, 6]. Macrophages infiltrate the injured site to phagocytose cellular debris and may affect other aspects of muscle regeneration by activating myogenic cells [7-10]. Thus muscle fiber necrosis and increased number of nonmuscle mononucleate cells within the damaged site are the main histopathological characteristics of the early event following muscle injury (Figure 1.2C).

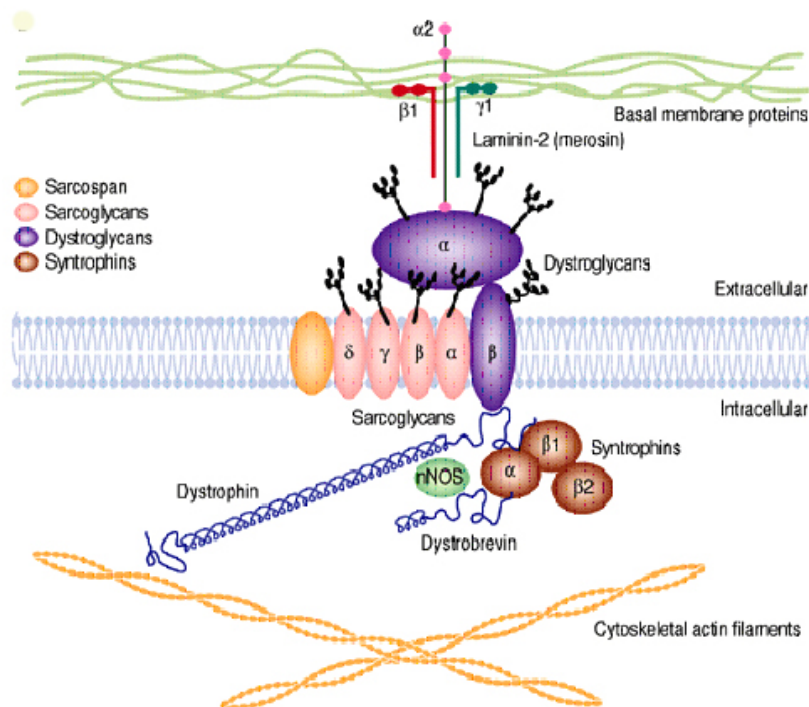
Myofiber regeneration is characterized by the activation of myogenic cells to proliferate, differentiate, and fuse to necrotic fibers for repair or to each other for new fiber formation. Notably, the expansion of myogenic cells provides a sufficient source of new myonuclei for muscle repair (reviewed in Refs. [11-13]). Numerous nuclear radiolabeling experiments have demonstrated the contribution of dividing myogenic cells to regenerate myofibers, by proliferation phase to form new muscle fibers followed by myogenic cells differentiation and fusion into mature muscle fibers [14-16]. Long-standing histological characteristics are still used to identify the mammalian skeletal muscle regeneration process. On muscle cross-sections, regenerating fibers are characterized by their small caliber and their centrally located myonuclei (Figure 1.2D, white arrowhead). Once fusion of myogenic cells is complete, newly formed myofibers increase in size, and myonuclei move to the periphery of the muscle fiber (Figure

1.2D, black arrow). Moreover, on muscle longitudinal sections and in isolated single muscle fibers, central myonuclei are observed in discrete portions of regenerating fibers or along the entire new fiber, suggesting that cell fusion is not diffuse during regeneration but rather focal to the site of injury [17]. In a time dependent manner after injury, the regenerated muscle fibers will become almost morphologically and functionally indistinguishable from undamaged muscle.

1.3 DUCHENNE MUSCULAR DYSTROPHY: A SKELETAL MUSCLE DISORDER

Duchenne muscular dystrophy (DMD) is a devastating muscle disease affecting about 1 in 3500 boys in all populations. It is an X-linked recessive disorder [18] where a mutation in the 2.5 million bp gene results in a failure to produce the 427 kDa protein called dystrophin at the sarcolemma of the muscle fibers [19-21]. Dystrophin and dystrophin associated protein complex (DAPC) form a link between the intracellular actin-based cytoskeleton and the extracellular matrix (ECM) which plays a major role in maintaining plasma membrane integrity and stability [22-24] (Figure 1.3). Disruption of this complex leads to increased susceptibility to contraction-induced injury and sarcolemmal damage leading to myofiber necrosis [(Figure 1.4, compare normal human skeletal muscle (A) with dystrophic muscle (B)]. Indeed, upon muscle injury, a finely orchestrated set of cellular responses is activated, resulting in the regeneration of a well-innervated, fully vascularized, and contractile muscle apparatus. This repair process is present in DMD, but is not efficient enough to compensate for the necrotic process and fibrosis. Thus, in DMD patients, repeated cycles of degeneration-regeneration would exhaust the regenerating potential of myogenic precursor cells leading to massive activation of connective tissue that

results in muscle fibrosis [18] causing the muscle to undergo progressive weakness and wasting [25] which eventually leads to congestive cardiac and respiratory failure before adulthood. Despite extensive research in developing an effective approach of dystrophin delivery in dystrophic muscle (e.g., cell and gene therapy), there is no therapy capable of substantially slowing the course of the disorder and rescuing the diseased muscle tissue.



Dystrophin protein structure and interactions

Expert Reviews in Molecular Medicine ©2002 Cambridge University Press

Figure 1.3 Membrane stabilization by dystrophin protein interaction with intracellular cytoskeleton, actin filaments, and the extracellular matrix (Adapted from Expert Reviews in Molecular Medicine 2002, Cambridge University Press)

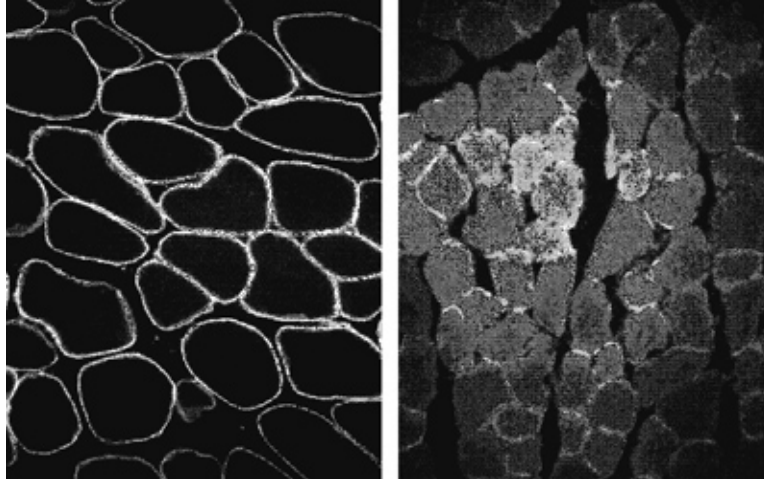


Figure 1.4 Immunohistochemical dystrophin labeling of skeletal muscle biopsies, taken from a normal individual versus a patient with Duchenne's muscular dystrophy (Courtesy of Johnny Huard, PhD, Pittsburgh, PA)

1.3.1 Animal Model of DMD

The biochemical and genetic animal homologue to human DMD is the *mdx* mouse. It is a spontaneously occurring mouse line deficient for dystrophin due to a point mutation in exon 23 of the dystrophin gene, which forms a premature stop codon [26]. The *mdx* mouse with less than 10% of the normal amount of dystrophin, and less than 0.1-0.01% of muscle fibers staining positively for dystrophin, is considered a true genetic homologue of DMD [27]. Although *mdx* mice are normal at birth, skeletal muscles show extensive signs of muscle degeneration by 3–5wk of age [28-30]. This acute muscle degeneration phase is accompanied by an effective regeneration process leading to a transient muscle hypertrophy [28, 29]. After this period, the degeneration/regeneration activity continues at lower and relatively constant levels throughout the life span of the animal. In fact, muscle of *mdx* mice differs from DMD patients in that it exhibits a greater degree of compensatory muscle regeneration and a scar fibrotic replacement

[28]. However, for reasons that remain unclear, in the older animals (~15 months), the muscle regeneration process is defective and the mice become extremely weak and die before wild-type littermates [31-33]. Such a milder histopathological modification is reflected by a slower progression of the disease.

1.4 CURRENT TREATMENTS AND THEIR LIMITATIONS

Two different therapeutic approaches have been explored in an effort to deliver normal dystrophin to murine and human dystrophic muscle: cell therapy based on myoblast transplantation (MT) and *ex vivo* gene therapy based on viral and non-viral vectors.

MT involves transplantation of primary myoblasts into defected muscle which contribute to the formation of new muscle fibers during repair and regeneration, and help in delivery of dystrophin [34-42]. The initial animal experiments and clinical trials, however, have suggested that although myoblast transplantation is feasible and introduced donor cells have fused with host myofibers around the site of injection and produced normal dystrophin [43-45], the amount of muscle fiber expressing dystrophin was not therapeutically significant and rather inefficient [39, 41, 42, 45, 46]. Donor cells may have also suffered from poor spread from the injection site, a low survival rate, and immune rejection by the host system [47-54]. In animal experiments, immunodeficient animals and/or immune-suppressive regimens [40, 44, 48, 55, 56], preirradiation of the injected muscle [44], and myonecrotic agents [35, 48] have been used extensively to improve the success of this technique. Although these approaches may be used to improve the restoration of dystrophin in *mdx* mice, the success of this technique remains rather

limited and for the most part, clinically impractical. To minimize the problem of immune rejection in human, autologous myoblast transfer has been employed, where primary myoblasts are removed from a patient via biopsy, expanded in cell culture, genetically manipulated with therapeutic genes, and re-introduced to the same patient. This technique therefore permits the introduction of myoblasts capable of expressing the transgene into defected muscle.

Virus-mediated delivery of the dystrophin gene to alleviate the biochemical deficiency in skeletal muscle became more of the research focus as a novel and attractive alternative. Viral and non-viral vectors have evolved rapidly. Plasmid, DNA, liposomes, viral vectors (e.g., adenovirus, adeno-associated virus, retrovirus, and herpes simplex virus) have already been used in the approach for gene delivery to muscles [57-64]. Two basic approaches for local gene therapy in the musculoskeletal system have been extensively investigated. Either the vectors are injected directly into the host tissue (*in vivo*) or the cells harvested via biopsy from different tissues (e.g., mesenchymal stem cells, muscle-derived cells, or dermal fibroblasts) are expanded *in vitro*, genetically engineered (transduced/transfected) *in vitro*, and re-introduced to the same patient (autologous) where they either replace degenerated fibers (as in the case of DMD) or form additional fibers expressing the desired gene (*ex vivo*) [65-67].

The advantage of direct (non-cell-based) approaches are low toxicity and immunogenicity [68], but the inability of most viral vectors to efficiently transduce or infect non-dividing muscle fibers is one of the major limitations [61, 69, 70]. In addition, the choice of the target cell is limited by the location of the defect, and insertion of genetic material into a specific type of cell is difficult to control. One way to overcome the difficulties of the direct approach and to help maximize the gene transfer efficiency and stabilize the expression was to develop an *ex vivo* method of gene transfer [71-80]. The *ex vivo* method has been

successfully used to deliver dystrophin in dystrophic muscle of *mdx* mice [81]. In humans, this method was used in the clinical setting to deliver and express factor IX for hemophilia B [80], interleukin 1 receptor antagonist protein for arthritis [82], human pro-insulin for diabetes [83], tyrosine hydroxylase for Parkinson's disease [84], and human growth factor for growth retardation [77]. The advantage of this method is multifaceted. First, the gene manipulation takes place outside the body (*in vitro*), thereby bypassing the need to inject massive amounts of virus into the patient. Also, we can select cells after transduction by special markers (e.g., neomycin) to increase the transduction efficiency and expression of the desired protein. In addition, this method give us enormous flexibility because we can choose the ideal cells for specific deficiency, For example, in case the of muscular dystrophies, muscle-derived stem cells would be an ideal choice for *ex vivo* gene therapy, with the reasons for this being discussed in detail in next the section.

It is important to realize that *ex vivo* gene therapy is not without limitations. It is clear that immunological problems associated with virally transduced cells still limit this technique. The efficiency of retroviral vector-mediated gene transfer is highly variable depending upon the vector design, the titer of the package virus, the type and species of the target cell, and is strictly dependent upon cell replication [85]. The integration of viral vectors into the genome of cells bears the risk of mutagenesis and the development of a potential malignancy. Consequently, all gene therapy techniques should be regarded with extreme caution. However, with viral vectors continuously being engineered to be less immunogenic, major advances can be expected in the near future.

1.5 MUSCLE-DERIVED STEM CELLS: POTENTIAL FOR MUSCLE REGENERATION

Stem cells are undifferentiated cells with unique features including i) appearance in early development and persistence throughout life; ii) self-renewal ability resulting in a large number of progeny; iii) long term proliferation potential while maintaining transient quiescent state; and iv) multilineage potential to enhance the new cell's incorporation into injured or diseased tissues. The stem cells' definition primarily emerged through extensive research on marker profiles, self-renewal, and the multi-potential behavior of hematopoietic stem cells (HSCs). On that note, the different populations of muscle-derived progenitor cells also appear to exhibit varied degrees of pluripotency. The most well-characterized muscle progenitor cells are satellite cells [86], usually referred to as "muscle stem cells." These unique undifferentiated myogenic cells have a committed fate and can regenerate injured skeletal muscle very efficiently [87, 88]. In addition to participating in the formation of myofibers, satellite cells can also differentiate into other lineages, such as adipocytic, osteoblastic, and chondrogenic [89, 90]. Satellite cells are integral to the development of skeletal muscle during embryogenesis and the regeneration of muscle fibers during postnatal life. During postnatal life, these cells are mitotically quiescent and reside between the basal lamina and the sarcolemma of myofibers. During the need for perceived growth or during post-natal reparative responses to stress or damage, satellite cells become activated, migrate, re-enter the cell cycle, differentiate, and fuse to form new regenerating myofibers [87, 88, 91]. Researchers have investigated the injection of satellite cells/myoblasts as a means to promote muscle repair in both animals and humans [88, 89]. The results suggest that, although the injected cells can improve muscle regeneration, various limitations such as poor

survival, limited dissemination of the injected cells, and immune rejection limit the success of this technique [47-54]. The development of using stem cells for transplantation may enable scientists to overcome these limitations because stem cells in theory are capable of long term proliferation, efficient self-renewal, and multilineage differentiation, all of which can improve the long-term survival of the cells post-transplantation [37, 92-94]. Investigators in our lab have obtained early myogenic progenitor cells highly proliferative, late-adhering, and Sca-1[+]/CD34[+]/CD45[-]/c-Kit[-] called muscle-derived stem cells (MDSCs) using a preplating enrichment technique [95] (for details refer to Appendix A). This technique separates myogenic cells based on their adhesion to collagen-coated flasks. The fraction of more committed myogenic cells that were attached to bottom of flask at early time points [early preplate (EP)] exhibit in vitro marker profiles, as well as proliferation and fusion behavior comparable to that of satellite cells (Table 1.1). The cell population from the late preplate (LP) were called long-term proliferation (LTP) or muscle-derived stem cells (MDSCs).

Table 1.1 The Marker profile comparison between myogenic, stem, and blood cells, adapted from [96, 97]

Cell Types	Cell Markers *	EP	LTP (MDSCs)
Myogenic cells	Desmin	+	-/+
	M-cad	+	-
	Pax7	+	-
Stem cells	CD34	-/+	+(+)
	Sca-1	-(N)	+(+)
	Bcl-2	-(N)	+(+)
	Flk-1	N	+(N)
Blood Cells	c-Kit	-	-
	CD45	-	-

+: >90%, -: <5%, -/+: 5-30%, +/-: 40-80%, N: Not determined

*(refer to nomenclature for marker profiles name and description)

MDSCs have unique characteristics usually associated with non-committed progenitor cells such as i) long term proliferation ability *in vitro* and *in vivo*, ii) high self-renewal, iii) multipotent differentiation capability (particularly into blood vessel and nerve); and iv) immune-privileged behavior [96, 98]. In addition, MDSC are c-Kit[-]/CD45[-], eliminating their potential

hematopoietic origin. Moreover, they spontaneously express myogenic markers, MyoD and desmin (Table 1). Finally, the MDSCs have a high potential for myogenic differentiation *in vitro* and *in vivo*, when compared with satellite cells, and they display a significant improved transplantation capacity (higher number of dystrophin (+) myofibers) starting at 10 days up to 30 and 90 days post-transplantation in gastrocnemius of *mdx* mice [96].

Until recently, the satellite cells were presumed to be the sole source of myonuclei in muscle repair. However, recent findings have demonstrated the presence of multi-potential stem cells in various adult tissues, thereby challenging the widely held view that tissue-specific stem cells are predetermined to a specific tissue lineage. In fact, adult stem cells isolated from various tissues appear to differentiate *in vitro* and *in vivo* into multiple lineages depending on environmental cues. Progenitor cells isolated from bone marrow (BM) [37, 99-101], the adult musculature [37, 96, 102-104], the neuronal compartment [105, 106], and various mesenchymal tissues [107, 108] can differentiate into the myogenic lineage. In particular, BM and muscle adult stem cells have been shown to differentiate into muscle cells *in vitro* and to contribute to muscle regeneration *in vivo* (for review, see Refs. [12, 109, 110]). Although these various types of cells appear to be able to differentiate toward myogenic lineage their regeneration capacity in skeletal muscle is limited. Therefore, MDSCs compared to many other cell types are better candidates for skeletal muscle transplantations, particularly because these cells can highly regenerate skeletal muscle, be obtained easily from a superficial muscle biopsy (non-invasive manner) from patients, be expanded to the desire number, and most importantly, through multi-potential differentiation into endothelial and neural lineages, they may enhance the neural and vascular supply during muscle regeneration [96].

1.6 ROLE OF GROWTH FACTORS IN MUSCLE REGENERATION

General terms such as hormone, cytokine, and growth factor are principally of historical interest. Specific terms such as nerve growth factor were derived from early descriptions of a factor's action or source, consequently, such terms do not necessarily provide meaningful descriptions of their function but rather they exist as identifiers accepted by tradition. There are small proteins that serve as signaling agents for cells. Despite being present in plasma or tissue at concentrations that are generally measured in picomolar (ng/ml) range, growth factors are the principal effectors of such critical functions as cell division, matrix synthesis, and tissue differentiation in virtually every organ system [111].

Figure 1.5 shows a schematic of the mechanism by which growth factors regulate cell behavior in general. Growth factors elicit their cellular actions by binding to specific transmembrane receptor molecules (Receptor-binding domain) on their target cells membrane. These receptors serve as information transducers, converting information carried by a growth factor into a form that is usable by the cell. This ligand-receptor interaction activates the intracellular domain of the receptor (kinase domain) which possesses the enzymatic ability to transfer phosphate groups to proteins (kinase activity). This acts as an intracellular communication step. The presence or absence of the receptor defines whether or not a cell can respond to information in its external environment. Growth factor receptors are linked by a cascade of chemical reactions in the cytoplasm to various genes in the nucleus with the binding of transcription factors (proteins that bind to specific regulatory sequences of DNA) to activate gene transcription into messenger RNA (mRNA). The mRNA is then transcribed into protein to

be used within the cell. Often this cascade activates several genes at once. As a result, when use of a growth factor is considered to treat a specific cell defect, one must be aware that the factor may generate multiple effectors, even within a single cell type. While these results may be advantageous (as when both cell division and matrix synthesis are desired for a repair response), it is a theoretical disadvantage if so-called mismatched effects (for example, cell division and matrix degradation) are stimulated simultaneously. Each family of growth factors has its own corresponding family of receptors. Despite marked differences in structure among receptor families, many of the key links in the gene-activating chain of reactions are shared by these families. Thus, binding of different growth factors to their respective receptors may lead to the same cellular response (such as cell division). Much more impressive than the similarities among post-receptor pathways, and much less well understood, are the differences. Many growth factors display pleiotrophic activity, eliciting a variety of effects in different stages of development. Although it is not yet clear how this remarkable versatility is achieved, these specific mechanisms probably will be important in the design of growth factor therapies that will be capable of activating only certain genes and not others. Knowledge about receptors is crucial to the successful application of growth factors as therapeutic agents. Clearly, treatment with growth factors will not help a problem caused by abnormalities in the receptor for that factor. In addition, the growth factors must be regulated, so as not to extend treatment beyond the therapeutic level and to prevent overgrowth of various tissues in the target area.

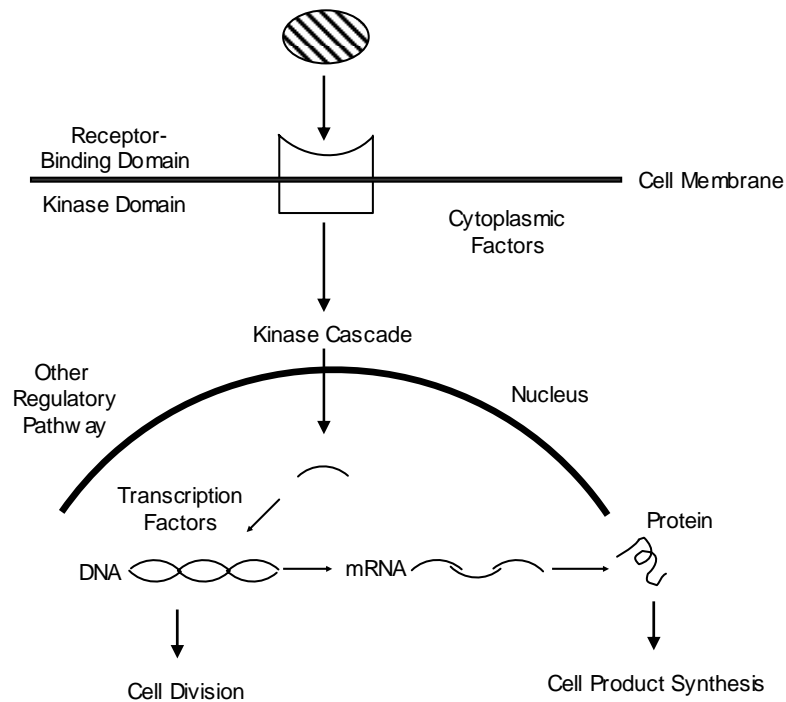


Figure 1.5 Schematic of the mechanism by which growth factors regulate cell behavior, adapted from [111]

It is well documented that growth factors can regulate skeletal myoblast proliferation and differentiation *in vitro* [112, 113] and act as stimulators or inhibitors (Table 1.2). Various growth factors are thought to play a role in different stages of muscle generation [114, 115] by stimulating satellite cells to release, proliferate, and terminally differentiate [116-119]. These factors that regulate muscle regeneration *in vivo* must act to maintain a balance between growth and differentiation in order for restoration of normal tissue architecture to occur. It is likely that a combination of many growth factors is involved in the regulation of myogenesis during muscle development and regeneration. The insulin-like growth factor (IGFs), basic fibroblast growth

factor (bFGF), platelet-derived growth factor (PDGF), leukemia inhibitory factor (LIF), and transforming growth factor beta (TGF- β) have been localized to muscle cells or other cell types present in muscle tissue [113, 120-123]. Expression of bFGF and the IGFs have been examined in regenerating skeletal muscles by immunocytochemistry and in situ hybridization, and they have been found to be up-regulated compared to non-injured muscles [121, 124, 125]. The pre-treatment of myogenic cells in culture with bFGF has shown to promote cell proliferation, resulting in an up to four-fold increase in myofiber regeneration [126]. In the mouse model, the IGF-1, bFGF, and to a lesser extent, nerve growth factor (NGF), directly injected post-injury have enhanced muscle regeneration in lacerated, contused, and strain-injured muscle [127-138].

Table 1.2 Effect of growth factors on the proliferation and fusion of myoblasts *in vitro*, adapted from [130]

Growth Factor*	Proliferation	Fusion
bFGF	Stimulates	Stimulates
IGF-1	Stimulates	Stimulates
NGF	Stimulates	Stimulates
α -FGF	Inhibits	Inhibits
PDGF	Inhibits	Inhibits
EGF	Inhibits	Inhibits
TGF- α	Inhibits	Inhibits
TGF- β	Inhibits	Inhibits

*(refer to nomenclature for the list of growth factors name)

While, in the past few years, much has been learned about the effects of these factors on musculoskeletal tissues, and a few notable therapeutic successes have been achieved, the understanding of their role in muscle diseases remains rudimentary. With continued progress in the basic science and clinical investigation of these factors, it is probable that they will become the method of choice for the prevention and treatment of a variety of current unsolved problems.

1.6.1 Nerve Growth Factor— NGF

The term “NGF” was introduced 50 years ago as a target-derived neurotrophic factor that is essential for the development, survival, and differentiation of developing neurons in the peripheral sympathetic and sensory neurons [139, 140]. NGF belongs to the neurotrophin family of growth factors that are synthesized as precursors (pro-neurotrophins) that are proteolytically cleaved to mature and biologically active form [141]. Because neurotrophins are normally expressed at low levels, little is known about their processing and secretion by neurons and non-neuronal cells *in vivo*.

The ideas about the biological role of NGF have been dominated by concepts that arose from studies on the differentiation and survival of young neurons. Until recently, the expectation was that the biology of NGF would center on the classical target-derived neurotrophic factor paradigm in which NGF released by postsynaptic targets acts on presynaptic neurons to build or maintain functional contacts and enhance the function of well-defined neural circuits. Although this paradigm undoubtedly plays a critical role in both the peripheral nervous system (PNS) and central nervous system (CNS), it does not appear to be the sole role for NGF actions suggesting this molecule may have broader physiological effects. For example, NGF has been reported to be

expressed by the luminal epithelium of the epididymis and the germ cells of the rat and mouse testes [142], and the circulation levels of NGF change not only with age, but also during neuroendocrine disregulation, after neurological insults, and during autoimmune and allergic diseases [143-149]. More relevant to the work being presented here, NGF has been shown to promote the differentiation of muscle cells in culture [150]. Furthermore, Rende et al. in 2000 showed that NGF expression in skeletal muscle is not only associated with a classical target-derived neurotrophic function for peripheral nervous system neurons, but also with an autocrine action (locally binding to cell-surface receptors on the same cells that produced it) which affects the proliferation, fusion into myotubes, and cell morphology of developing myoblasts, thereby suggesting that among other roles, endogenous NGF signaling through both neurons and non-neuronal cells subserves neuroprotective functions and facilitates muscle repair. The regulated expression of NGF throughout adult life suggests multiple functions for NGF signaling, many of which are poorly understood.

1.6.2 NGF Receptors: TrkA and p75^{NTR}

The NGF functions as a dimer of identical subunits linked together by noncovalent bonds and with molecular mass of about 26 kDa [151]. The functional activity of NGF is mediated by two classes of receptors: high-affinity receptor, TrkA ($K_d = 10^{-11}$ M), and low-affinity receptor, p75^{NTR} ($K_d = 10^{-9}$ M) [152-156].

A schematic drawing of the structural features of Trk and p75^{NTR} is displayed in Figure 1.6. TrkA is a 140 kDa single-pass transmembrane protein with a single transmembrane domain and a single cytoplasmic tyrosine kinase domain that serves as a receptor tyrosine kinase (RTK)

for NGF. Neurotrophin-mediated activation of TrkA receptor leads to a variety of biological responses and elicits many of the classical neurotrophic actions ascribed to NGF, including proliferation and survival, axonal growth and remodeling, assembly and remodeling of cytoskeleton [157-159]. p75^{NTR} is a 75-kDs transmembrane glycoprotein that belongs to a superfamily of cytokine receptors which includes TNF receptors (TNFR), Fas, CD27, CD40, and CD30. p75^{NTR} binds all members of the neurotrophin family with approximately equal nanomolar affinity, and is therefore referred to as a neurotrophin receptor, and not as an NGF receptor. p75^{NTR} has a distinctive extracellular-domain sequence that differs with TrkA, with four distinct cytosine-rich domains that are responsible for ligand-binding. The precise role of p75^{NTR} in NGF signal transduction has not been fully elucidated. Several studies have indicated that stimulation of TrkA is necessary and sufficient to elicit a full biologic response and is required for cell survival, while other reports have highlighted the crucial role of the association of TrkA and p75^{NTR} in regulating NGF biological activities on NGF-responsive cells [155]. These studies shed light on the often conflicting roles for p75^{NTR} in mediating apoptosis and in augmenting Trk-induced survival and differentiation. The selectivity of proNGF for p75^{NTR} suggests that its local secretion may determine whether apoptotic or survival actions predominate.

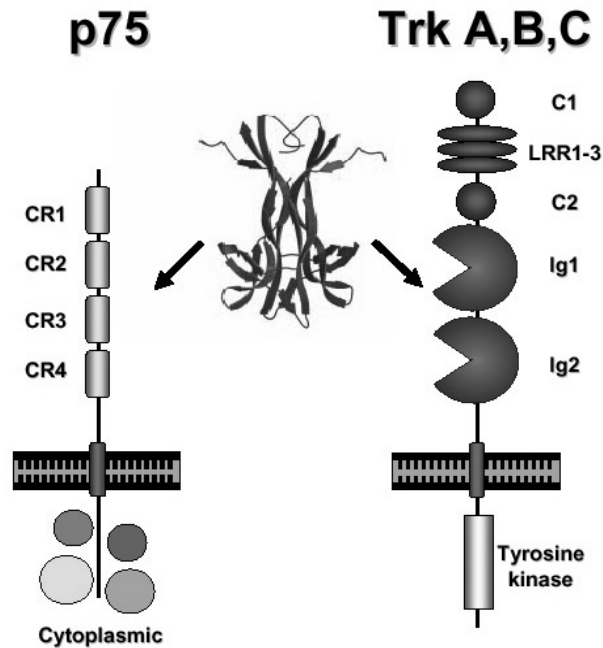


Figure 1.6 A schematic drawing of the structural features of Trk and p75 receptor, adapted from www.izn.uni-heidelberg.de/download/LFB2004/Tucker.pdf

1.7 MDSCs & NGF AS A REMEDY FOR TISSUE ENGINEERING

Tissue Engineering has been defined as the application of the principles and methods of engineering and life sciences towards the development of biological substitutes to restore, maintain, or improve functions. It is our expectation that a cell-based therapy can help to provide a solution to the growing problem of tissue and organ failure. Therefore, there has been growing enthusiasm for a tissue-engineering approach that aims at utilizing stem cells to deliver genes of interest to improve healing of the musculoskeletal system. The feasibility of direct injection of

human recombinant growth factors for treatment of muscle injuries due to its safety and ease is practically hindered because high concentrations of the growth factor are often required to produce the beneficial effect. Indeed, studies have shown that growth factors exhibit a dose-dependent effect on myoblasts proliferation and differentiation *in vitro*, while *in vivo*, three consecutive injections of high concentration (100 ng) NGF, IGF-1, and bFGF are required to improve muscle healing in the mice model [127-138]. The relatively short biological half-life, the bloodstream's rapid clearance, and the limited adequate duration of growth factor delivery are the main reasons why large concentrations of growth factors are typically required.

In this regard, isolated muscle-derived stem cells obtained through the preplate technique would be the perfect candidate for cell-mediated therapy and the perfect choice for *ex vivo* gene delivery since these cells show i) long-term proliferation and self-renewal capacity ii) multilineage differentiation ability (e.g., myogenic, neurogenic, osteogenic, adipogenic, hematopoietic, and chondrogenic), and iii) potential immune-privileged behavior (i.e., the failure to trigger the immune response). While the direct *in vivo* injection of growth factors or stem cells is technically less complex, the indirect, *ex vivo*, gene delivery technique is safer because the gene manipulation (i.e. genetically engineering using viral vectors) takes place under controlled conditions outside the body. With the *ex vivo* approach, growth factors can be delivered using endogenous cells. These cells are capable of responding to stimuli created by injured tissue and can participate in healing process more effectively by delaying, ameliorating, or arresting the further degeneration.

2.0 PROJECT OBJECTIVES

The overall goal of this project is to evaluate a novel tissue engineering method for skeletal muscle repair. Both muscle-derived stem cell transplantation and *ex vivo* gene therapy are excellent candidates for growth factor delivery. We propose that direct stimulation of MDSCs with nerve growth factor (NGF) protein and genetically engineering MDSCs with retroviral transduction used for sustained delivery of NGF can hold great promise as the basis for tissue engineering and gene therapy applications to acquire muscle healing. The development of such a novel therapeutic strategy hold tremendous potential for the treatment of pathological conditions associated with poor muscle regenerative capacity, such as those observed during injuries and muscular dystrophies.

2.1 OBJECTIVE 1: EXAMINE THE PHENOTYPIC EFFECT OF NGF STIMULATION ON MDSCS *IN VITRO*.

A variety of growth factors epidermal growth factor (EGF), fibroblast growth factor-2 (FGF-2), insulin-like growth factor-1 (IGF-1), and stem cell factor (SCF) have been shown to be potent stimulators of the proliferation and myogenic differentiation of MDSCs *in vitro* [160]. The current study aims to address the phenotypic behavior (proliferation and fusion) of MDSCs

under the influence of NGF. Two stem cell markers: Sca-1 and CD34 and two myogenic markers: desmin and Pax7 will be examined before and after NGF stimulation. The proliferation kinetics and myogenic cell behavior of the control and stimulated MDSCs will be monitored using a novel bioinformatic cell culture imaging system, allowing time-lapse image analysis, including cell division time and fusion behavior. The myogenic differentiation capacity of these cells will be investigated by the ability of cells to differentiate in vitro and to fuse and form myotubes. We hypothesize that MDSCs' marker profiles will remain the same while the myogenic marker expression, proliferation kinetics, and myogenic differentiation will change following NGF stimulation.

2.2 OBJECTIVE 2: EVALUATE THE EFFECT OF NGF STIMULATION ON MDSCS' REGENERATION CAPACITY.

Our preliminary studies indicate that growth factors promote the multipotent differentiation of MDSCs into muscle fibers, blood vessels, and peripheral nerve. They may also contribute to the formation of functional skeletal muscle tissue with adequate vascular and neural supplies. We hypothesize that NGF stimulation will promote multilineage differentiation, which in turn enhances engraftment efficiency (higher number of dystrophin-positive myofibers) and improves the regeneration capacity of MDSCs in *mdx* skeletal muscle.

3.0 INTRODUCTION

Duchenne muscular dystrophy (DMD) is a progressive muscle disorder characterized by dystrophin deficiency that results in initial necrosis of muscle fibers, which in turn leads to progressive muscle weakness and, ultimately, death before or shortly after patients reach the second decade of life [19, 161]. Dystrophic muscle has a heightened susceptibility to structural damage and a decreased capacity to undergo self-repair.

Researchers have localized dystrophin in the sarcolemma of myofiber [162-164], where it is thought to play a role in maintaining plasma membrane integrity and stability [22-24]. Like the muscles of humans with DMD, the muscles of *mdx* mice are dystrophin deficient [165], which makes the *mdx* mouse an excellent genetic and biochemical model for DMD. Unlike the muscles of humans with DMD, however, the muscles of *mdx* mice show no progressive weakness or progressive fibrosis; instead, they exhibit muscle hypertrophy and maintain their regeneration capacity [166].

Although lack of dystrophin leads to progressive muscle degeneration, the evolution of DMD is likely to be dependent upon other factors, such as insufficient expression of growth-associated proteins. After skeletal muscle damage, quiescent myogenic stem cells, which are normally embedded in the basal lamina of the muscle fibers, are activated and migrate toward the damaged area, where they undergo a cycle of proliferation, fusion, and differentiation that culminates in the generation of myofibers that replace the damaged ones [167]. In most cases,

myogenic differentiation is measured as increased expression of muscle cells functions such as creatine kinase activity, fusion of single cells to form myotubes, or elevation of myosin heavy or light chain expression, or other proteins associated with the contractile apparatus. Various growth factors can regulate skeletal myoblast proliferation and differentiation and are known to play a role in different stages of new muscle regeneration, therefore enhancing the healing process [111, 114, 115]. In addition to stimulating cell proliferation, growth factors can maintain cell survival and regulate critical intracellular signal transduction pathways [168] under conditions that otherwise lead to apoptotic death.

To date, the list of growth factors known to affect the behavior of skeletal muscle cells or to be expressed in skeletal muscle tissue is extensive. However, few studies have investigated the role of NGF during skeletal muscle regeneration, and its exact mechanism of activity is poorly understood. In addition to acting as a target-derived factor for developing neurons, NGF has an autocrine effect on myoblast proliferation and fusion [169-171]. Moreover, adult knockout mice expressing a neutralizing antibody against NGF display a severe dystrophy and reduced muscle mass [172, 173]. Recent evidence suggests that NGF acts by binding to the high-affinity tyrosine-kinase receptor (TrkA) and the low-affinity p75-neurotrophin receptor (p75^{NTR}). TrkA is found in developing adult rat myoblasts [174] and during differentiation of muscle cells [170]. NGF and p75^{NTR} are widely expressed in myoblasts, human myocyte cultures, and regenerating myofibers in the muscle of DMD patients [175, 176].

Previous studies in our laboratory have revealed that the delivery of human recombinant NGF protein via direct intramuscular injection improves both muscle recovery [130] and muscle force (fast-twitch strength) after strain injury [129]. However, the efficiency of direct intramuscular injection of growth factors varies according to the type of injury encountered and

is limited by the need to maintain high enough concentrations to achieve a therapeutic effect. In addition, the use of growth factor proteins to promote healing is severely hindered by the difficulty of ensuring their delivery to the injured site [177], their short biological half-lives [66, 177], and the bloodstream's rapid clearance of these molecules. For the study reported here, we used a combination of MDSC-based gene therapy and direct stimulation with NGF protein to examine the effects of NGF on the proliferation and differentiation capacity of MDSCs *in vitro* and their regeneration efficiency in *mdx* muscle *in vivo*.

4.0 MATERIALS AND METHODS

4.1 ANIMALS

Mdx mice (C57BL/10SCsn DMD^{mdx}/J) were purchased from the Jackson Laboratory (Bar Harbor, ME). All animal protocols used for these experiments were approved by the Children's Hospital of Pittsburgh's IACUC committee (protocol # 3/02).

4.2 CELL ISOLATION AND CULTURING

A previously described modified preplate technique [96] was used to obtain MDSCs from normal (C57BL/6J) 3-week-old female mice. Cells were cultured at an initial density of 450 cells/cm² in flasks coated with collagen type I (Sigma-Aldrich Corp., St. Louis, MO) and maintained in proliferation medium (Dulbecco's modified Eagle's medium (DMEM) supplemented with 10% horse serum, 10% fetal bovine serum (FBS), and 1% penicillin-streptomycin; all reagents from Gibco, Inc., Carlsbad, CA) containing 0.5% chick embryo extract (Accurate Chemical, Westbury, NY). After 2 days of growth (confluency < 50%), the

cells were trypsinized, counted, and replated to generate the quantity of cells needed for each experiment. The preplating technique was used to purify slowly adhering MDSCs if necessary.

4.3 GENERATION OF RETROVIRAL VECTOR EXPRESSING NGF

NGF cDNA was amplified from plasmid pSP72NGFpA (provided by Dr. Paul Robbins) using primers NGF1 (agg cgg ccg ccc acc atg ctg tgc ctc aag cca gtg aaa) and NGF2 (tca aga tct tca gcc tct tct tgt agc ctt cct) and Pfu DNA polymerase (Stratagene, CA). The PCR product was cut with restriction enzymes Not I and Bg III and cloned into the same 2 sites of retroviral vector pCLX [178]. The vector DNA was converted into a replication-defective retrovirus by co-transfection (with calcium-phosphate precipitation) into packaging cell line GP-293 (Clontech, Palo Alto, CA) with a plasmid, pVSVG, which expressed vascular stomatitis virus glycoprotein as the viral envelope. Conditioned medium containing retroviral vector was stored at -80 °C until use.

4.4 STIMULATION OR RETROVIRAL TRANSDUCTION OF MDSCS WITH NGF

MDSCs were plated at 20%–30% initial confluency and either stimulated with 100 ng/ml of NGF (Sigma-Aldrich) for 7 days (S-MDSCs) or retrovirally transduced with the CLNGF vector to express NGF (E-MDSCs) at a multiplicity of infection of 5 in the presence of polybrene (8 µg/ml). Normal MDSCs neither stimulated nor transduced served as the control group (C-MDSCs). E-, S-, and C-MDSCs were expanded for one week in proliferation medium (20%

serum) at an initial density of 8×10^4 cells/well on collagen type I-coated 6-well plates, where they remained for 48 hours; proliferation medium was then replaced with low-serum medium (2% FBS) in which cells were cultured for an additional 24 hours. Tissue culture supernatant was collected and spun at 1200 rpm for 5 minutes at 4 °C, and the level of functional NGF secreted by the cells in the tissue culture supernatant was measured by enzyme-linked immunosorbant assay (ELISA) (NGF Emax® Immunoassay System kit, Promega, WI) performed as detailed in the manufacturer's instructions.

4.5 CELL CHARACTERIZATION BY FLOW CYTOMETRY

Flow cytometry was used to analyze the expression of the cell surface markers cluster differentiation (CD34) and stem cell antigen-1 (Sca-1). Cultured cells were trypsinized, spun, washed in a buffer made of phosphate buffered saline (PBS) (Dulbecco phosphate-buffer salt solution 1X; Mediatech, Inc., Herndon, VA) containing 0.5% bovine serum albumin (BSA) (ICN Biomedicals) and 0.1% sodium azide (Sigma-Aldrich), and then counted. After trypsinization, the cells were maintained on ice for the remainder of the procedure. The cells were then divided into equal aliquots and spun into a pellet. A 1:10 mouse serum (Sigma-Aldrich) was used to resuspend each pellet, and the suspensions were incubated for 10 minutes on ice. Predetermined, optimal amounts of both direct and biotin-conjugated rat anti-mouse monoclonal antibodies (CD34 and Sca-1) were placed in each tube for 30 minutes. Each experimental tube received FITC-conjugate for CD34 and biotin-conjugated Sca-1. A separate cell portion received equivalent amounts of isotype control antibodies. After several rinses, all fractions (including the

controls) were labeled with streptavidin-allophycocyanine (APC) for 20 minutes. Just before the analysis, 7-amino-actinomycin D (7-AAD) was added to each tube to exclude non-viable cells from the analysis. All antibodies, including APC and 7-AAD, were purchased from BD PharMingen (San Diego, CA). At least 10,000 live cell events were analyzed via flow cytometry (FACS Aria cytometer using FACS Diva software, Becton Dickinson, San Diego, CA).

4.6 MYOGENIC MARKER EXPRESSION BY IMMUNOCYTOCHEMISTRY

A fraction of each group was evaluated by immunofluorescent staining for expression of the myogenic proteins desmin and Pax-7. Analysis was performed on methanol-fixed cells that were blocked with 5% goat serum in PBS for 1 hour. The cells were incubated for 1 hour with the following primary antibodies: mouse IgG anti-desmin (1:250; Sigma-Aldrich) and mouse anti-Pax-7 (1:50; R&D Systems, Minneapolis, MN). After being rinsed thoroughly with PBS, the cells were incubated for 30 minutes with the secondary antibody biotinylated goat anti-mouse IgG (1:250; Vector, Burlingame, CA). To fluorescently label the antigenic binding, the cells were washed and incubated with Streptavidin-Cy3 (1:500; Sigma-Aldrich) for 10 minutes; nuclei were then counterstained with DAPI (1:100; Sigma-Aldrich) in PBS. All dilutions were in 5% goat serum in PBS at room temperature. Negative control staining was performed using an identical procedure, with omission of the primary antibody. Northern Eclipse software (v.6.0, Empix Imaging, Mississauga, ON, Canada) was used to quantify the percentage of myogenic cells as the ratio of cells that strongly expressed desmin or Pax-7 to the total number of nuclei in 10 randomly chosen fields at 200x magnification.

4.7 CELL DIVISION ANALYSIS

The time lapse between cytokinesis events were recorded as the length of the cell division cycle from the time-lapsed video images from a novel microscope imaging system described below. For each population, 100 cells were selected and tracked. The division time (DT) of each cell was determined by direct observation of the cells from the time-lapsed video record. The initiation of cell division was marked at the time when two daughter cells were formed, and these cells were followed until their respective division. The lapse time between those two division events was recorded as the length of the cell division cycle. The average population doubling time (PDT) was calculated by fitting an exponential trend line to several measured data points. PDT was estimated by using the software package SigmaStat 2.0 (Jandel Scientific, San Rafael, CA) to perform nonlinear regression in order to generate the best fit to the curve. The fraction of daughter cells that were actively entering the mitotic cell cycle (α) was calculated from experimental data using PDT and DT and solving the re-arranged Sherley model to obtain the correlation coefficient (R^2) for the nonlinear regression [179, 180], a value that indicates how well the data actually fit the model (such that $0 < R^2 < 1.0$).

4.7.1 Experimental Settings

Various cell culture and imaging settings such as cell plating densities, image acquisition intervals, duration of cell growth, viewfield limits, and optimized phase contrast have already

been tested [181]. These settings are important in determining the best densities at which the cells are able to interact with each other, while remaining visible. This way, the events can be captured accurately without the cells being lost to follow-up.

MDSCs from each group were plated at an initial density of 450-500 cells/well in a collagen type I-coated 12-well plate in 20% serum medium, as described in section 4.2. Cells were allowed to adhere for 6-12 hours. Using the microscopic imaging system, time-lapsed visible imaging was obtained for individual cells and subsequently, for growing colonies [182]. In these experiments, groups of 4 to 6 cells were selected for imaging. Coordinate positions of these view fields were recorded by the CytoWorks software program that subsequently controls the time and position of stage movement. Images of each view field were acquired at 10-minute intervals for 4 days. For each cell type and treatment condition, 15 view fields were selected from 6 wells. Cell population growth was monitored by counting the total number of cells, N , in the view field at 12-hour intervals.

4.7.2 Imaging System

Our imaging system showing in Figure 4.1 consists of a customized mechanical stage containing a cell culture system and microscopy (Nikon Eclipse TE-2000-U microscope) specifically designed for time-lapsed imaging over long periods of time. In the system, an environmentally-controlled biobox incubator is mounted to the stage of the microscope, which is in turn linked to a CCD camera (Automated Cell Technologies, Inc., Pittsburgh, PA). The x-y position of the stage is under the control of the user such that any position on a culture plate can be selected for viewing. The system accommodates any sized multi-well plates from 6-well to 384-well.

Multiple viewfields can be selected in each well. Each view field or x-y position that is selected becomes the location for time-lapsed imaging. Individual images are directly recorded in jpeg from the continuous images. Automated measures of the total numbers of cells can be made at any time point and the division times can accurately be determined by direct observation of cytokinesis.

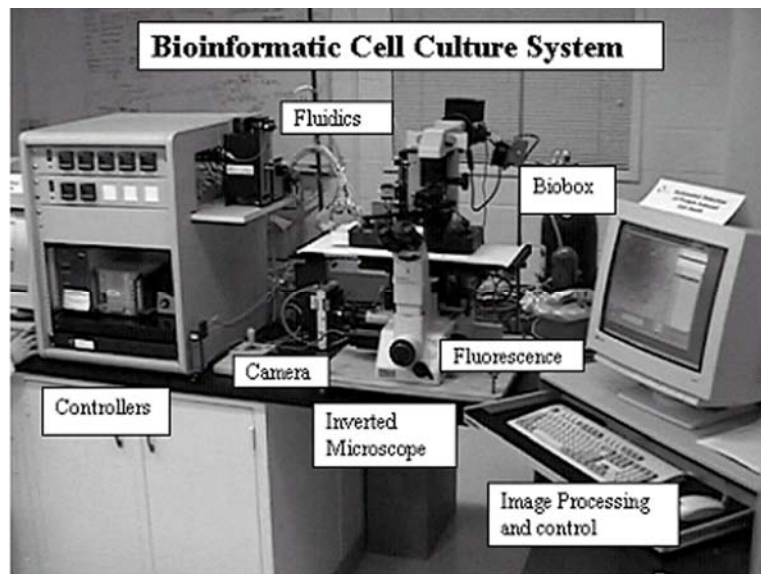


Figure 4.1 Bioinformatic Cell Culture and Imaging System (Courtesy of Bridget Deasy, PhD, Pittsburgh, PA)

4.7.3 Non-exponential Growth Model

This model was proposed by Sherley [180] and is particularly well-suited for studying the expansion of all cell populations and estimation of division time, mitotic fraction or population doubling time. Consequently, this model enables researchers to assess the behavior of a particular cell population under various culture conditions. The model is based on the Sherley

equation that is easy to use and offers a simple way of modeling cell growth for stem cell biologists based on the fraction of daughter cells that are dividing, α , while accounting for the presence of non-dividing cells:

$$N = N_0 \left[0.5 + \frac{1 - (2\alpha)^{(t/DT)+1}}{2(1 - 2\alpha)} \right]$$

where N is the number of cells at any time t , N_0 is the initial number of cells, and both DT and cell number at each time point are determined by image analysis directly through individual observations of cytokinesis. A brief derivation of this model, including assumptions inherent to its use, is provided in Appendix B.

4.8 MYOGENIC DIFFERENTIATION

Myogenic differentiation was evaluated by immunocytochemical staining for fast myosin heavy chain (MHC) expression. E-, S-, and C-MDSCs were plated at an initial density of 1000 cells/cm² in multi-well collagen type I-coated 12-well plates in high-serum DMEM (details above) for 2 days. To induce fusion, proliferation medium was replaced with differentiation medium (low serum: DMEM supplemented with 2% FBS and 1% penicillin-streptomycin) for an additional 3 to 4 days. Immunocytochemistry staining was performed as described above with the monoclonal mouse anti-MHC (1:250; Sigma-Aldrich) as the primary antibody to reveal fast MHC expression. Nuclei were visualized by DAPI (1:100; Sigma-Aldrich). Representative fields

were evaluated to determine the degree of differentiation (percent ratio of MHC-expressing nuclei to total number of nuclei), an indicator of differentiation efficiency.

4.9 MYOFIBER REGENERATION *IN VIVO*

A total of $2\text{--}3 \times 10^5$ C-, E-, or S-MDSCs were injected into the gastrocnemius muscle of 6–8 week-old male *mdx* mice. Mice in the E-MDSC group and their controls were immunosuppressed by subcutaneous injection of FK506 (2.5 mg/kg mouse body weight/day) beginning on the day of cell transplantation and continuing until the day of sacrifice [183]. Ten to fourteen days after transplantation, the gastrocnemius muscles were harvested, flash frozen in liquid nitrogen-cooled 2-methylbutane, and serially sectioned (10 μm). Dystrophin staining of cryopreserved tissue was performed on acetone-fixed, horse serum-blocked sections using a rabbit anti-dystrophin antibody (1:1000; provided by Dr. Terry Partridge) for 3 hours. Sections were then washed in PBS and incubated with biotinylated anti-rabbit IgG antibody for 1 hour. Next the sections were washed again and incubated with Streptavidin-Cy3 (1:300; Sigma-Aldrich) for 20 minutes. All incubations were at room temperature. Fluorescence microscopy was performed and digital images were acquired. Muscle regeneration was assessed by counting the number of dystrophin-positive myofibers in an area containing the largest graft and calculating the regeneration efficiency index (RI: the number of dystrophin-positive fibers in the host muscle per 10^5 donor cells) for ease of comparison and graphical display [103].

4.10 QUANTIFICATION OF DYSTROPHIN-POSITIVE MYOFIBERS USING NORTHERN ECLIPSE

The digital images of regenerated dystrophin-positive myofibers from gastrocnemius muscle sections immunostained against dystrophin were acquired using a Nikon Eclipse E800 microscope equipped with a Spot digital camera (Figure 4.2A). Northern Eclipse software package (v6.0, Epix Imaging, Inc.) was used to perform dimensional analysis of dystrophin-positive myofibers both manually and automatically. For manual count, each myofiber was numbered and counted using the manual counter provided by the software. For the automatic count, the images were converted into binary, black and white (8-bit grayscale) (Figure 4.2B). Using a manually-set threshold to delineate the immunofluorescence signal from the background, the Northern Eclipse software identifies myofibers that meet the chosen criteria by the user and places a circle or a number inside each individual myofiber. The pixel intensities were chosen as a set point so that any pixel darker than the set point is turned red/white while pixels lighter than the set point are turned cyan/black. The correct set point was determined manually by the user. This procedure is called thresholding (Figure 4.2C). During the thresholding, the user should maximize the number of connected components so that the myofibers remain distinct enough so that the software will be able to count each myofiber separately (Figure 4.3A). If the threshold point is at low pixel intensity, the red/white will flood the myofibers (Figure 4.3B), while with high pixel intensity, only a few fibers will be distinguished (Figure 4.3C), thereby resulting in a low count of myofibers and an under estimation of the data. Increasing the threshold will maximize the number of connected components (boundaries around each fiber), and the correct number of myofibers will be measured. The software determines the actual myofiber cross-sectional area of each fiber and provides quantitative measurements of the number of pixels

occupied by each individual fiber. The fiber area distribution (FAD) of 4000 individual myofibers per group was measured by determining the total number of pixels occupied by each fiber— a number that was easy to convert to μm^2 with analysis software. H&E staining of non-injected regions of the same grafts was used to detect the boundaries of the host *mdx* myofibers. The parameters such as cross-sectional area, diameter (maximal myofiber length in microns), minor axis diameter (the longest line through myofiber that is perpendicular to its orientation) and myofiber elongation (ratio of major axis to minor axis) were also calculated as median, 10th, 25th, 75th, and 90th percentiles (for detailed descriptions of each parameter refer to Appendix C). This data was compared with control or between groups, using non-parametric one-way ANOVA on ranks with a Dunn's method for multiple comparisons with an unequal sample size.

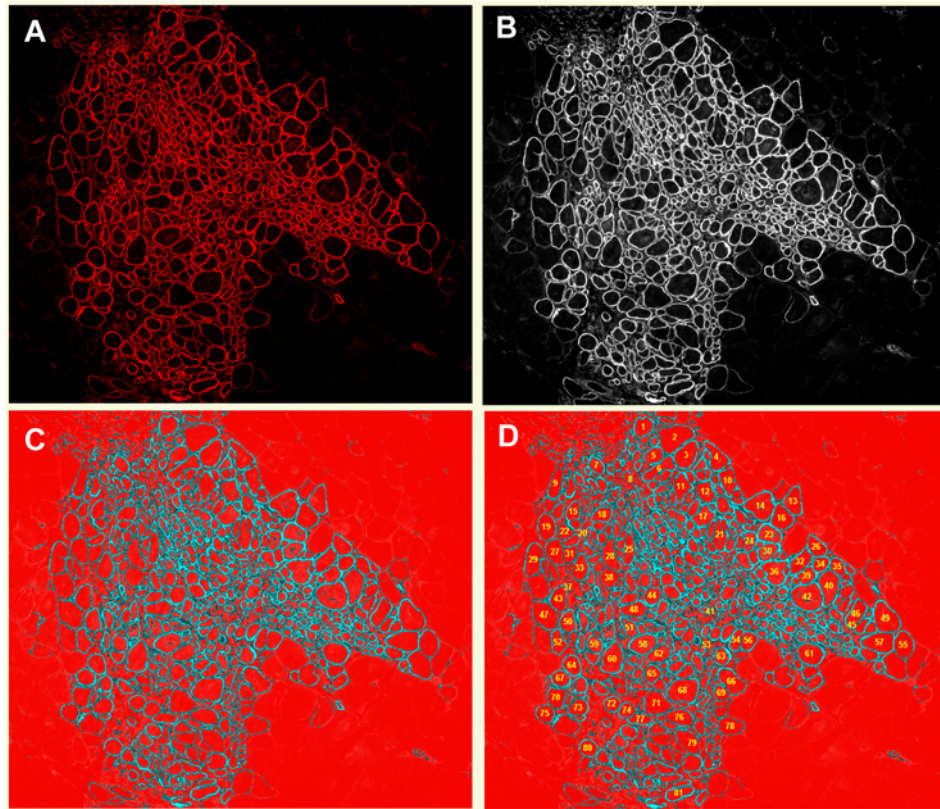


Figure 4.2 Dimensional analyses of immunohistochemically-labeled dystrophin-positive myofibers

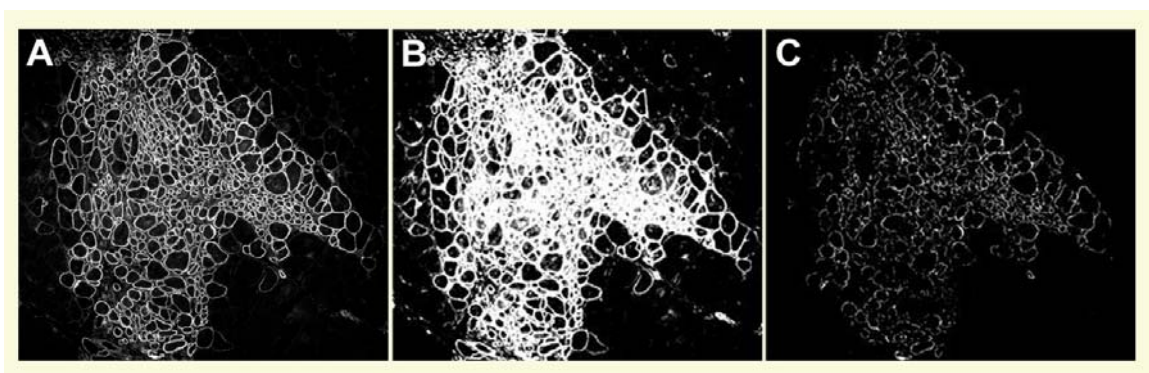


Figure 4.3 Challenges encountered during thresholding an image

4.11 STATISTICAL ANALYSIS

Differences with $p < 0.05$ were considered statistically significant. All values are given as the mean \pm standard deviation of the mean (SD). Direct comparisons between treatment and control groups were made by using Student's t test or the Mann-Whitney Rank Sum test (where appropriate). Multiple group comparisons were made by using one-way analysis of variance (ANOVA). In cases where the data failed this test and indicated that the data varied significantly from a population with a normal distribution, nonparametric tests, the Kruskal-Wallis One Way Analysis of Variance on Ranks, were used ($p < 0.05$ significance level). Nonparametric distributions were also detected and comparisons were made using Kruskal-Wallis one-way ANOVA on ranks with Dunnett's test for comparing treatment groups with a single control group or comparing between groups with an equal number of sample size; or Dunn's test for comparing treatments groups with unequal number of sample size. All statistical testing and regression analyses were performed using SigmaStat for Windows Version 2.0 (Copyright 1992-1995 Jandel Corporation).

5.0 RESULTS

5.1 QUANTITATIVE DETECTION OF NGF

Two different methods of NGF stimulation were used in this study: retroviral transduction of MDSCs with the CL-NGF vector to induce expression of human NGF (E-MDSCs) and direct stimulation of MDSCs with NGF protein (100 ng/ml) for 7 days (S-MDSCs). For both groups, normal MDSCs that were neither stimulated nor transduced served as controls (C-MDSCs). We used ELISA to measure the levels of NGF secreted by MDSCs *in vitro*. After transduction with CL-NGF that carries a 3' long-terminal repeat (LTR), virus packing signal (ψ), and human NGF cDNA driven by the cytomegalovirus promoter (CMV-P), genetically engineered MDSCs (E-MDSCs) were able to synthesize, process, and secrete active human NGF (Figure 5.1).

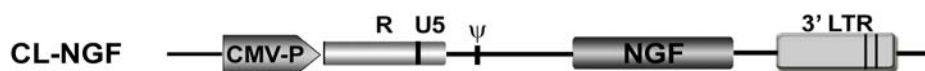


Figure 5.1 Schematic representation of the retroviral vector expressing NGF

Quantitative detection by ELISA of NGF protein within the cell supernatant revealed that the level of NGF secreted by E-MDSCs reached 307.4 ± 42.5 ng/ 10^6 cells/24 hours 3 days after transduction and continued to be high 6 and 9 days after transduction (173.2 ± 11.1 ng/ 10^6 cells/24 hours and 164.9 ± 28.2 ng/ 10^6 cells/24 hours, respectively, $*p < 0.05$). In contrast, NGF-stimulated MDSCs (S-MDSCs) and control (non-treated) MDSCs (C-MDSCs) on average secreted NGF at barely detectable levels at the three time points (0.09 ± 0.17 ng/ 10^6 cells/24 hours and 0.02 ± 0.37 ng/ 10^6 cells/24 hours, averages for S-MDSCs and C-MDSCs, respectively, Figure 15).

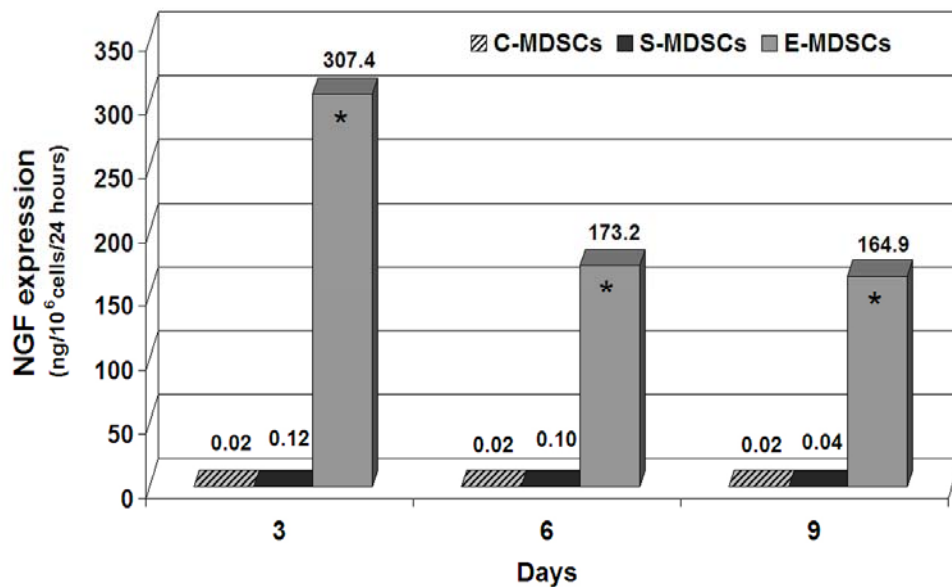


Figure 5.2 Quantitative detection by ELISA of the NGF protein in the cell supernatant

5.2 PROLIFERATION KINETICS

Growth factors stimulate the proliferation of myogenic precursor cells. To investigate the cellular response of MDSCs to NGF, we examined cellular division time (DT), and population doubling time (PDT). We fit experimental data sets for C-, E-, and S-MDSCs to the Sherley model equations by using nonlinear regression with the correlation coefficient $R^2 > 0.90$ to estimate mitotic fraction (α) (i.e., the fraction of daughter cells that are actively dividing). Our data suggest that the average DTs (C-MDSCs = 11.9 hours, E-MDSCs = 11.5 hours, and S-MDSCs = 12.1 hours) were not significantly different in the various groups ($p = 0.053$, Kruskal-Wallis analysis on ranks) and that the PDTs of the different cell groups were also quite similar (11–13 hours). Moreover, we observed a strong association (as indicated by the high correlation coefficient) for all of the groups ($R^2 = 0.99$), but no difference in the estimated α for the 3 groups (C-MDSCs = 0.94, E-MDSCs = 0.92, and S-MDSCs = 0.94). The mean mitotic fraction remained relatively constant among the groups (~ 0.94) (Figure 5.3). These results indicate that neither NGF transduction nor stimulation significantly alters the proliferation kinetics of MDSCs.

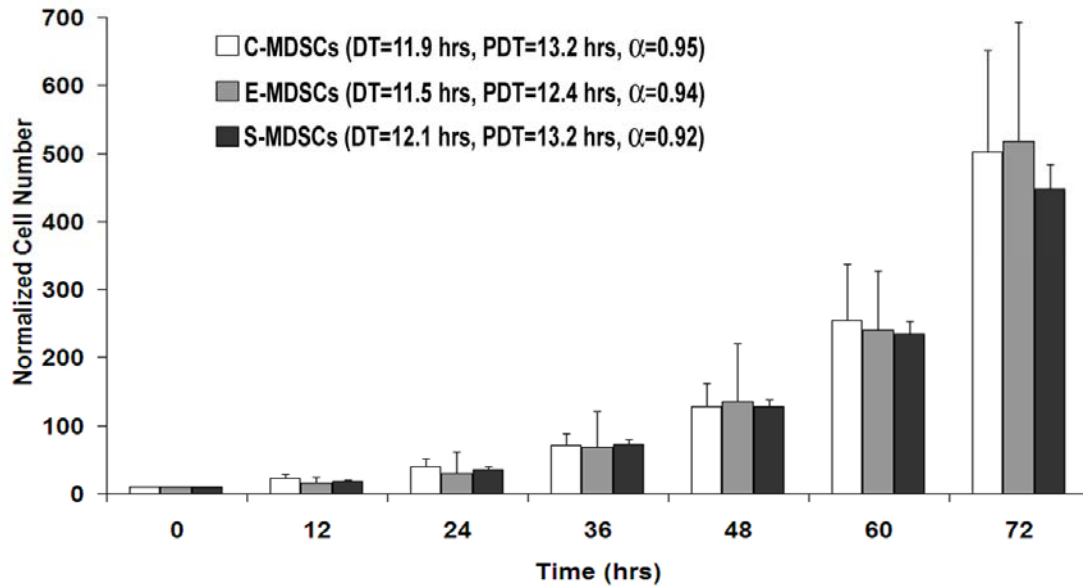


Figure 5.3 Proliferation kinetics of MDSCs

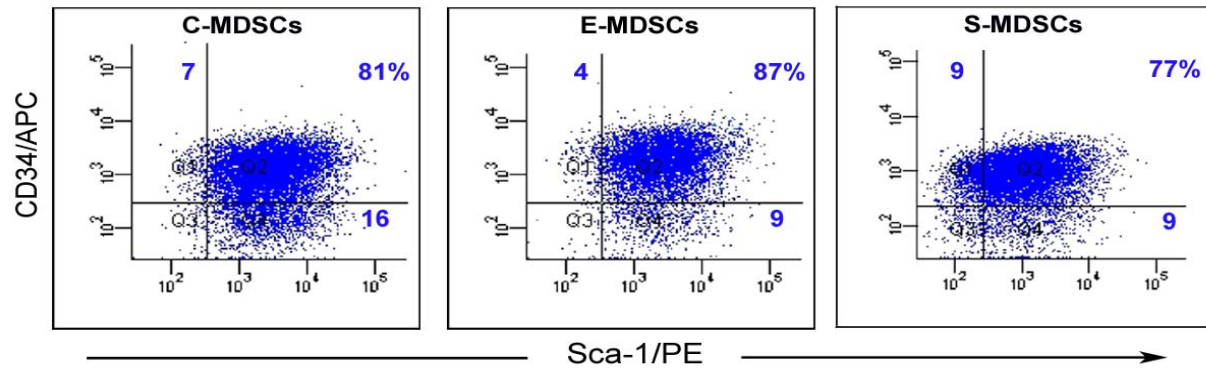
5.3 IN VITRO STEM CELL AND MYOGENIC MARKER PROFILES

We investigated the expression levels of the stem cell markers CD34 and Sca-1 by flow cytometry. Data were collected by performing logarithmic amplification on 5000 cells, excluding cell debris by combining forward and side scatters. This data is presented as dot plots in Figure 5.4A (the percentage of cells in each quadrant is indicated in the upper right-hand corner). Our results indicate high expression levels of the stem cell markers CD34 and Sca-1 (> 70%) by the

control group (C-MDSCs), 7 days after either retroviral transduction of the cells with the CL-NGF vector (E-MDSCs) or stimulation with 100 ng/ml NGF (S-MDSCs). We observed no significant difference between the groups (in terms of stem cell marker expression) after 2 weeks of *in vitro* expansion ($p = 0.655$). This marker stability suggests that NGF does not affect the stem cell marker expression of MDSCs *in vitro*.

We also used immunofluorescent staining to assess the cells' expression of two myogenic proteins: Pax-7 and desmin. Myogenic differentiation assay revealed low levels of Pax-7 and desmin expression. We quantified the expression of Pax-7 and desmin as the ratio of nuclei positive for Pax-7 or desmin to the total nuclei in 10 randomly chosen fields. As shown in Figure 5.4B, there were no significant differences in Pax-7 expression by the different groups of treated and untreated MDSCs ($p = 0.148$, $n=6$). Whereas E- and C-MDSCs expressed similar levels of desmin, we observed significantly more desmin-expressing cells in the S-MDSC group ($p < 0.05$, $n=6$).

A.



B.

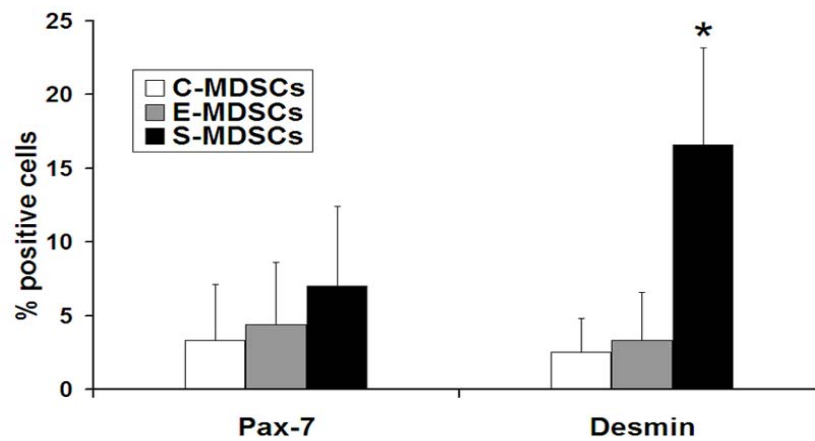


Figure 5.4 Marker profile analysis of MDSCs

5.4 IN VITRO MYOGENIC DIFFERENTIATION

After cultivating the cells under low-serum and high density conditions, we assessed myogenic differentiation in the 3 groups by performing immunohistochemical staining for fast myosin

heavy chain (MHC) expression to analyze myotube formation. Representative images of MHC-positive C-, E-, and S-MDSCs (Cy3; red) overlaid on nuclear counterstain (DAPI; blue) are shown in Figures 5.5A–C. We defined differentiation efficiency as the percentage ratio of MHC-expressing nuclei to total number of nuclei. C-MDSCs consistently showed a differentiation efficiency of 35%, and E-MDSCs showed 30% differentiation efficiency. In contrast, the differentiation efficiency of S-MDSCs, 26%, was significantly lower than that of C-MDSCs, which indicates that S-MDSCs have a decreased ability to fuse and form multinucleated myotubes ($*p < 0.05$, $n=3$, Figure 5.5D). Scale bar represents 100 μm .

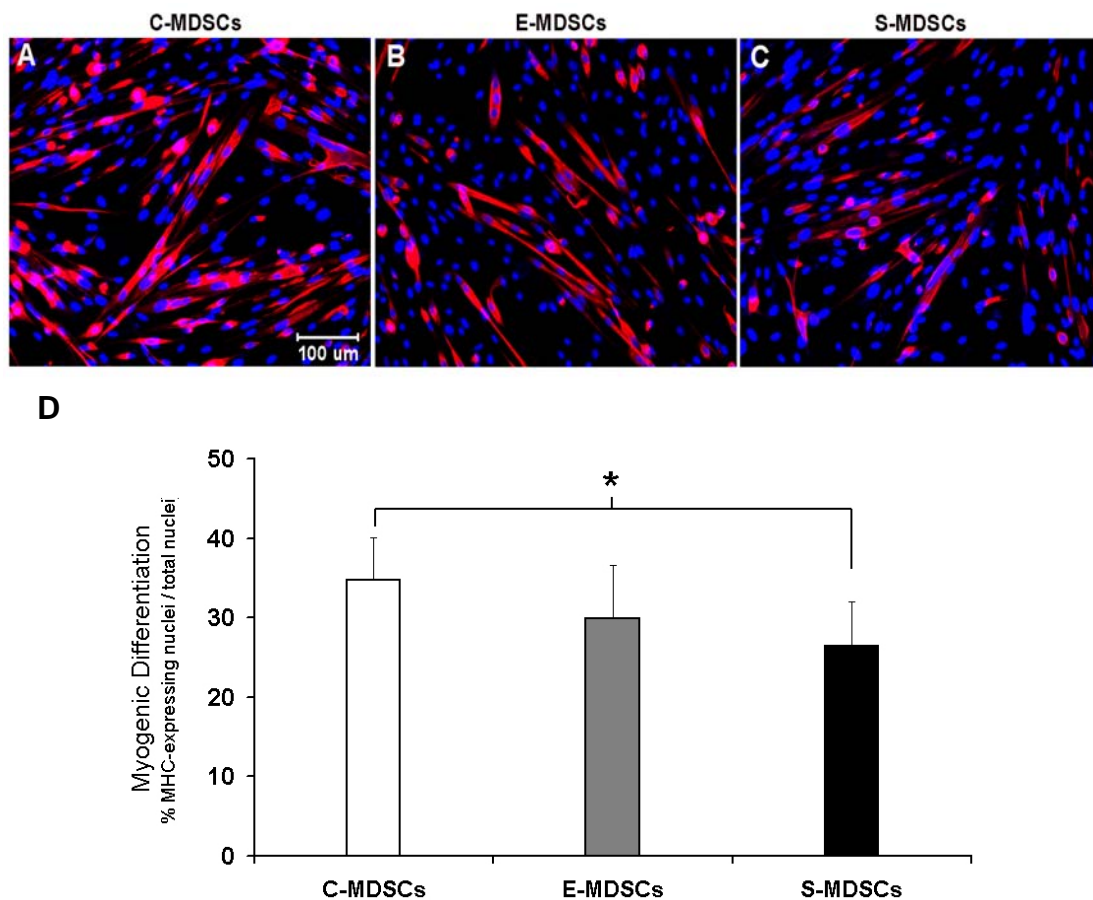


Figure 5.5 Myogenic differentiation *in vitro*

5.5 MUSCLE REGENERATION

We evaluated the ability of the 3 groups of cells (E-, S-, and C-MDSCs) to regenerate dystrophic skeletal muscle by transplanting 3×10^5 cells from each cell group into the gastrocnemius muscles of 8-week-old male *mdx* mice. Fourteen days after transplantation, we sacrificed the animals; we harvested the injected gastrocnemius muscles, snap froze them, and sectioned them using a cryostat. Using immunohistochemical staining, we assessed the number of dystrophin-positive myofibers with manual count and quantitated muscle regeneration in terms of the regeneration index (RI: the number of dystrophin-positive fibers in the host muscle per 10^5 donor cells). The dystrophin-positive grafts of E- and C-MDSCs are shown in Figures 5.6A and 5.6B. The average RI of E-MDSCs was significantly larger than that of C-MDSC's (435.6 ± 85.5 vs. 197.5 ± 53.8 , $*p < 0.001$, $n=8$, Figure 5.6C). Scale bar represents 250 μm .

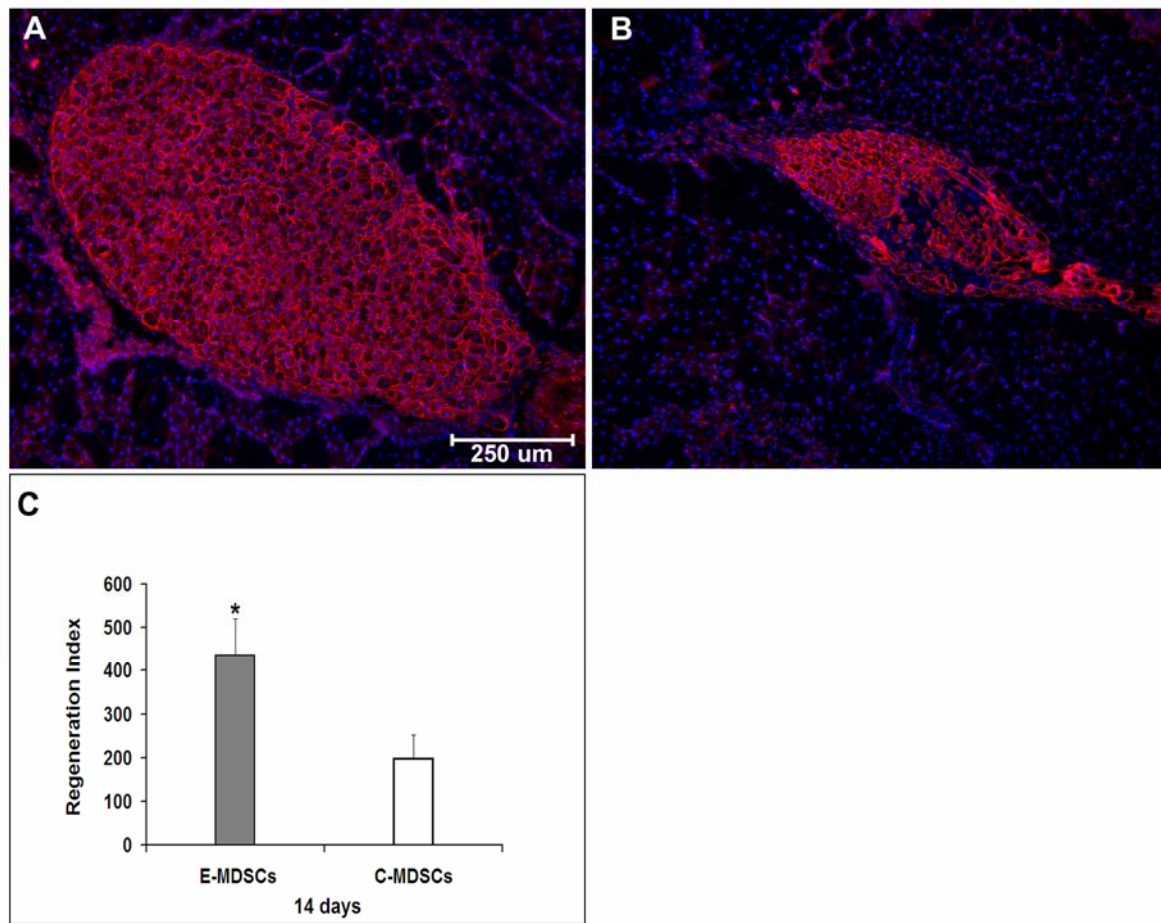


Figure 5.6 Dystrophin-positive myofiber regeneration elicited by MDSCs transduced with CL-NGF

Differences in the size of the dystrophin-positive grafts generated by S-MDSCs vs. C-MDSCs were even more dramatic, as shown in Figures 5.7A and 5.7B, respectively. Our analysis revealed that the average RI of S-MDSCs was 3-fold higher than that of C-MDSCs (852 ± 203.3 vs. 266.8 ± 137.4 , < 0.001 , $n=11$, Figure 5.7C). In addition, the RI of S-MDSCs was statistically higher than that of E-MDSCs ($*p < 0.001$). Scale bar represents 250 μm .

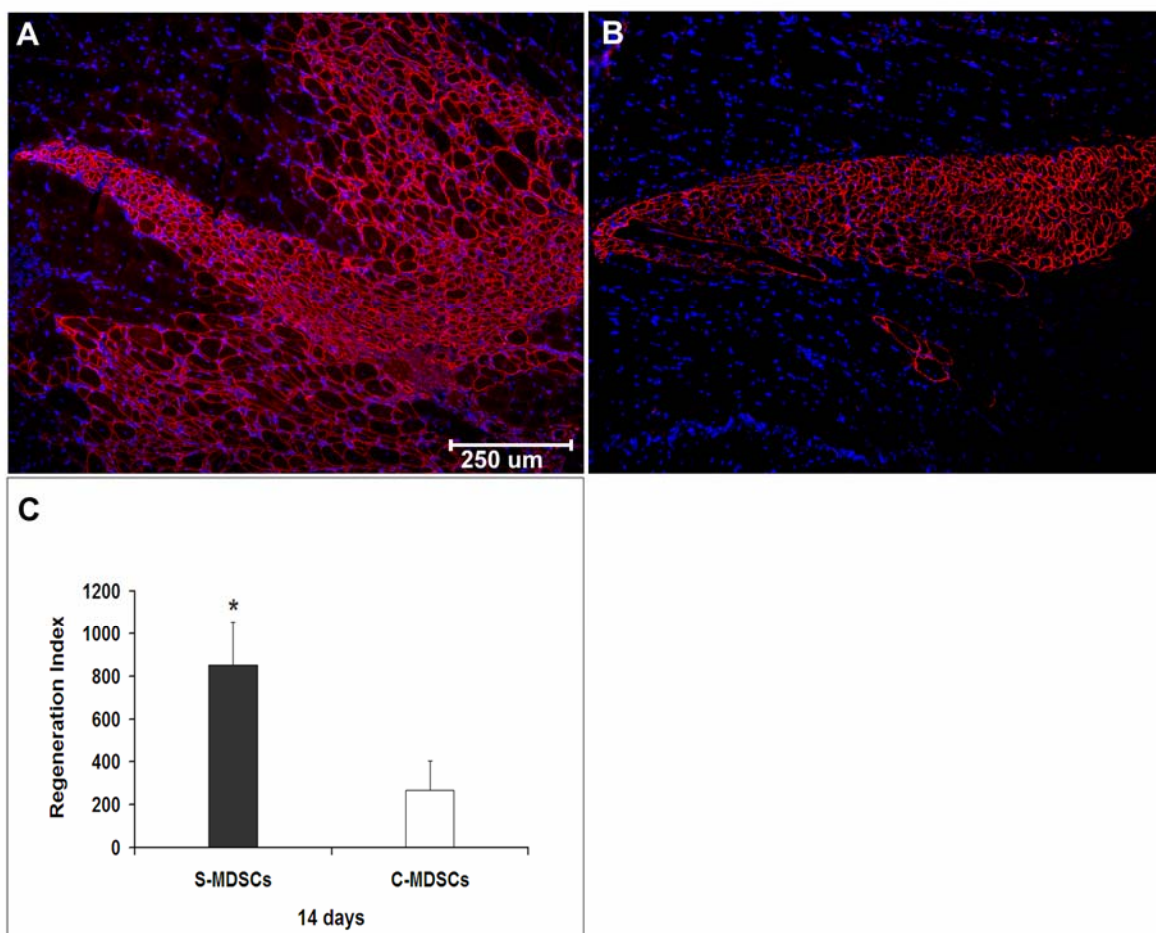


Figure 5.7 Dystrophin-positive myofiber regeneration elicited by MDSCs stimulated with NGF protein

5.6 MORPHOLOGICAL ANALYSIS

Cell morphology was qualitatively examined from the time-lapsed images obtained from the bioinformatic cell culture system (200x magnification) during expansion. An example of such

images at 0-96 hour's intervals is shown in Figure 5.8. It is apparent that the morphology of the cell population in all three groups is heterogeneous, containing mainly small round shape, with some well-defined spindle-shaped cells also being observed.

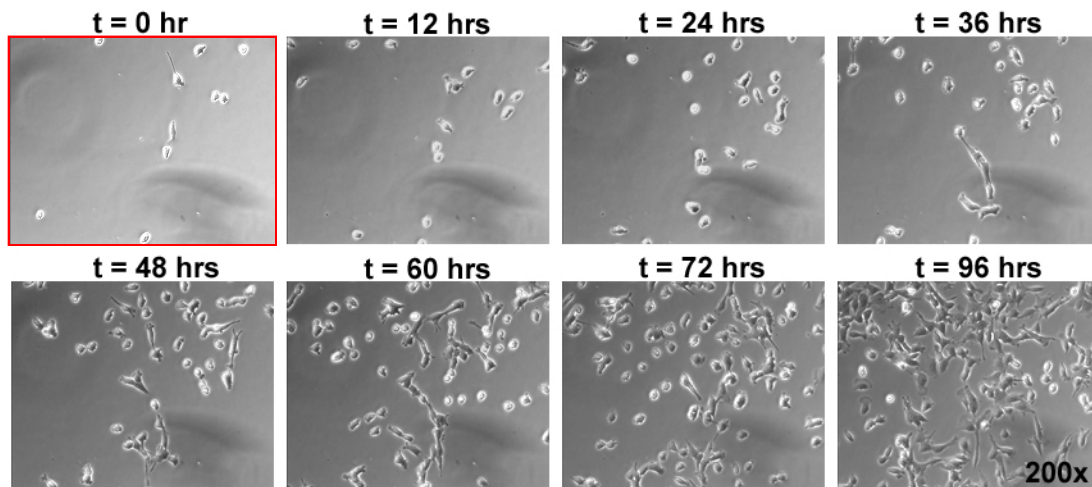


Figure 5.8 Representative time-lapsed images of C-MDSCs population demonstrating visualization and morphological recognition of cell morphology in culture (refer to attached video clip by double clicking on first image)

Quantitative analysis of fiber area distribution (FAD) was evaluated using the same immunohistochemical engraftment that was used to calculate the RI. FAD analysis of grafts generated by the 3 groups of MDSCs revealed that more than 50% of the total number of dystrophin-positive myofibers in each group had areas of 0–100 μm^2 . In this range, no statistically significant differences existed among the treatment groups compared to C-MDSCs ($p = 0.678$; Figure. 5.9). We also analyzed non-injected areas of *mdx* muscle and found that most of the myofibers had areas $> 1000 \mu\text{m}^2$. A non-parametric distribution weighted toward smaller

myofiber sizes was apparent. These findings indicate that C-, E-, and S-MDSCs all generated new dystrophin-positive myofibers, as indicated by their small size and centronucleation (Figure. 5.10, arrow). Scale bar represents 50 μm .

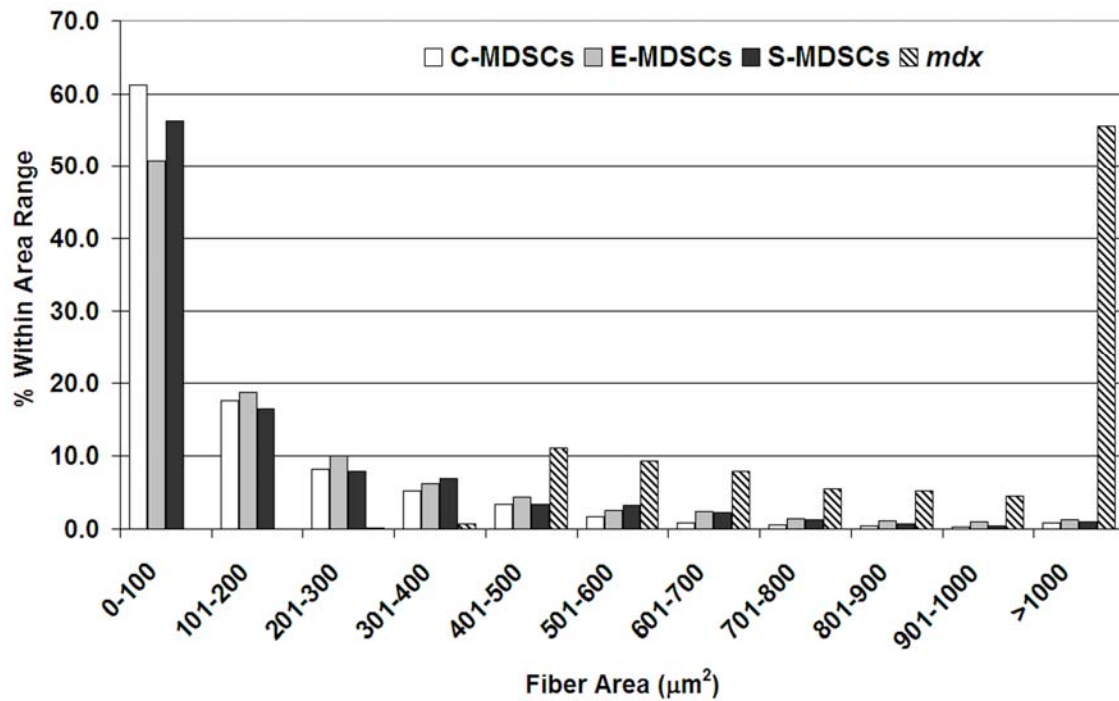


Figure 5.9 Fiber area distribution (FAD) of newly generated (dystrophin-positive) and host myofibers

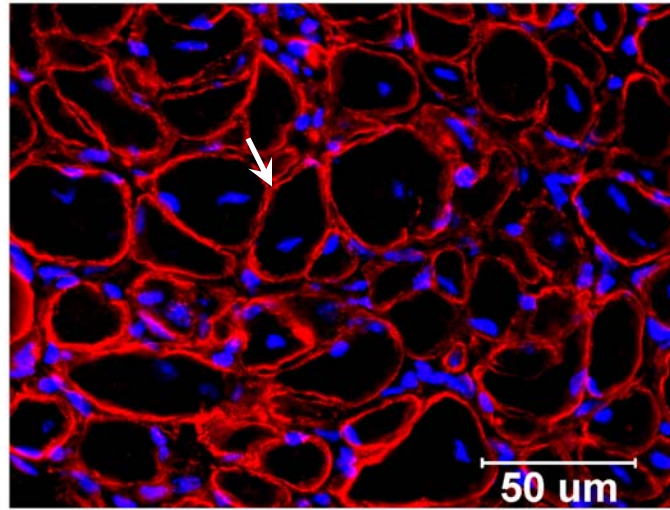


Figure 5.10 A high magnification image of a small portion of an E-MDSC graft shows a large number of centronucleated myofibers

Quantitative measurement of other morphometric parameters such as cross-sectional area, diameter, minor axis diameter, and myofiber elongation were also measured and compared based on the same images used to calculate RI. Figure 5.11 illustrate the myofiber measurement using box plots with median, 10th, 25th, 75th, and 90th percentiles as vertical boxes for each parameter mentioned above. Dystrophin-positive myofibers generated by E-, S-MDSCs groups showed a statistically greater median values for area, diameter, perimeter, minor axis diameter when compared to C-MDSCs ($p < 0.05$) indicating accelerated muscle fiber regeneration. Median cross-sectional area: C-MDSCs ($63.2 \mu\text{m}^2$), E-MDSCs ($112.8 \mu\text{m}^2$), S-MDSCs ($95.3 \mu\text{m}^2$). Median diameter: C-MDSCs ($14.4 \mu\text{m}$), E-MDSCs ($19.7 \mu\text{m}$), and S-MDSCs ($17.3 \mu\text{m}$). Median minor axis diameter: C-MDSCs ($7.7 \mu\text{m}$), E-MDSCs ($11.5 \mu\text{m}$), and S-MDSCs ($9.6 \mu\text{m}$). Elongation: C-MDSCs (1.7), E-MDSCs (1.7), and S-MDSCs (1.7). The elongation

parameter (the ratio of the major axis of the myofiber to of its minor axis) between the groups did not differ, thereby showing the same physical morphology of myofibers in all the groups (Table 5.1).

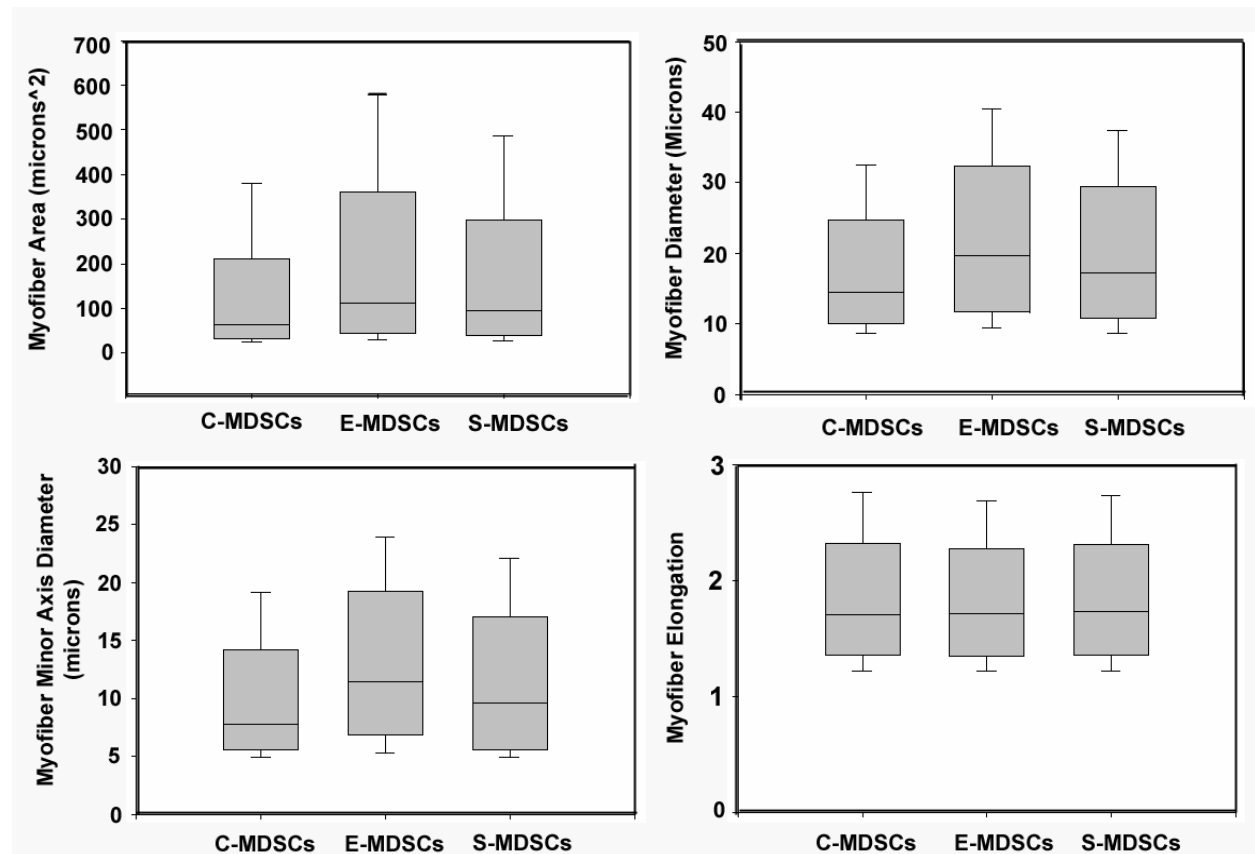


Figure 5.11 Morphological features of dystrophin-positive myofiber

Table 5.1 Dimensional characteristics of dystrophin-expressing myofibers

	Area (μm^2)		Elongation	
	Median	Percentiles 25%-75%	Median	Percentiles 25%-75%
<i>Mdx</i> (non-injected)	2390.3	1481 – 3724.8	1.7	1.4 – 2.2
C-MDSCs	63.2	33.9 – 155.8	1.7	1.4– 2.1
E-MDSCs	112.8	48.9 – 288	1.7	1.4 – 2.2
S-MDSCs	95.3	44.9 – 234.5	1.5	1.3 – 1.7

	Diameter (μm)		Minor Axis Diameter (μm)	
	Median	Percentiles 25%-75%	Median	Percentiles 25%-75%
<i>Mdx</i> (non-injected)	14.4	10.6 – 22	7.7	5.8– 12.5
C-MDSCs	19.7	12.5 – 29.7	11.5	7.3 – 17.7
E-MDSCs	17.3	11.5 – 26.8	9.6	5.8 – 15.3
S-MDSCs	71.8	57.4 – 92.9	48.8	38.3 – 62.2

At last, the method of manual and automatic count of dystrophin-positive myofibers were compared between engraftments obtained from all the groups. While small engraftments were easily analyzed with the automatic count, the larger engraftments were challenging. The percent

difference between the manual and automatic count were on average 12.4% for small engraftments (C-MDSCs) and increased to 23.6-44% for larger engraftments (E-MDSCS and S-MDSCs, respectively) showing an underestimation of myofiber counts by automatic analysis. This is more likely due to loss of resolution in larger engraftments at the edges where the images are merged (Figure A.2, Appendix C), and also higher numbers of small, newly generated myofibers that are difficult for the software to detect.

6.0 DISCUSSION

Although the precise role that NGF plays in the different steps of muscle regeneration remains largely unknown, our observations indicate that NGF can improve the regeneration ability of MDSCs in skeletal muscle of *mdx* mice. Whereas the results of our *in vitro* experiments demonstrate that neither retroNGF transduction nor direct stimulation with NGF protein changes the marker profile of MDSCs or their proliferation dynamics, direct stimulation with NGF protein appears to delay the myogenic differentiation of MDSCs.

It is well documented that the process of muscle regeneration in normal and dystrophic muscle depends on locally produced cytokines and growth factors [111, 121, 125, 184]. Skeletal muscle injuries induce a well-established sequence of cellular events that result in the release of growth factors that stimulate quiescent satellite cells and other muscle precursor cells to enter the cell cycle, proliferate, and eventually fuse to form newly regenerated myofibers and restore muscle architecture [167, 185]. Some studies suggest that NGF, the best characterized neurotrophic factor, plays an important role in restoring innervation in many tissues after injury. For example, NGF is integral to the survival of sensory and peripheral neurons that control contraction of smooth muscle [186-188] and axonal regeneration in skeletal muscle [189].

A prior study in our lab has shown that MDSCs stimulated with NGF or vascular endothelial growth factor (VEGF) differentiated toward nerve and endothelial lineages, respectively, in a more effective manner when compared with non-stimulated cells. This was

evident by a greater number of cells expressing 2',3'-cyclic-nucleotide 3'-phosphodiesterase (CNPase), a myelin-associated enzyme, and von Willebrand Factor (vWF), an endothelial cell marker [96]. These findings suggest that the release of local environmental cues (i) can trigger the differentiation of muscle stem cells toward non-myogenic lineages after transplantation of the cells into dystrophic muscle and (ii) may contribute to the regeneration of functional muscle tissue by enhancing vascular and neuronal supplies.

Here, we investigated whether MDSCs retrovirally transduced to express NGF display different proliferation behavior or altered myogenic differentiation *in vitro* and improved muscle regeneration of dystrophic muscle *in vivo*. We used MDSCs rather than satellite cells because the former exhibit a superior transplantation capacity and the ability to undergo multilineage differentiation [96, 103]. The *ex vivo* gene transfer approach enables constant delivery of lower, more physiological doses of proteins that, if delivered by direct injection, would be quickly degraded by natural processes. Retroviral vectors transduce dividing cells with high efficiency [190] and elicit long-term, stable expression of the gene of interest by integrating into the host cell genome; such vectors are already being used in clinical settings [191, 192]. Our results indicate that MDSCs transduced with a retrovirus vector continuously delivered high levels of NGF for up to 9 days in culture, while maintaining their typical stem cell marker profile (CD34 positive and Sca-1 positive). After injection into the skeletal muscle of *mdx* mice, E-MDSCs proliferated and differentiated to generate new muscle fibers that formed large grafts by as early as 14 days. These data suggest that the expression of NGF by retrovirally transduced MDSCs is relatively stable *in vivo* and may enhance MDSCs' survival at the muscle regeneration site.

In spite of what we have hypothesized in our specific aim 1, the proliferation dynamics of the treated MDSCs, including PDT, DT, and α , were similar regardless of the treatment method

(i.e., stimulation or transduction). However, S-MDSCs exhibited higher regeneration efficiency *in vivo* than E-MDSCs or C-MDSCs, perhaps due to the delayed differentiation of S-MDSCs caused by NGF stimulation *in vitro*. Some research suggests that cells with delayed fusion characteristics have increased regeneration capacities [103]. This could explain our observation that S-MDSCs differentiated into myotubes more slowly than did C- and E-MDSCs *in vitro* and exhibited the greatest regeneration efficiency *in vivo*. It is feasible that the higher proliferation ability of S-MDSCs before fusion *in vivo* allowed them to remain in an undifferentiated state longer, thereby resulting in enhanced regeneration. It should be noted that NGF in target tissues is in the subpico-molar range [193, 194]. Consequently, it is likely that high levels of NGF expression such as in the E-MDSCs, reflect changes such as down regulation of TrkA and p75^{NTR} receptors that can diminish the overall binding affinities for NGF.

Our currently-used methodology measures the dystrophin expression of transplanted cells participating in the regeneration process as a whole, including both the conversion of already existing myofibers, through donor-host fusion, as well as the formation of new myofibers from donor-host and donor-donor cell fusion. One indirect way to assess these differences of the probable route taken by the injected cells (i.e. new myofiber formation), is the fiber area distribution (FAD) of dystrophin myofibers relative to those of the control non-injected muscle. The FAD showed that most of the individual dystrophin-positive myofibers in all of the MDSC groups had areas of 0–100 μm^2 , whereas most of the host *mdx* myofibers had areas of > 1000 μm^2 . Furthermore, nuclear staining with DAPI revealed that most of the small myofibers observed in the MDSC grafts were centronucleated. In combination, these results suggest that injection of C-, E-, or S-MDSCs led to the formation of new dystrophin-positive myofibers via the fusion of the donor cells with one another rather than the fusion of donor cells with host

muscle fibers. Recent studies conducted by Toti et al. 2003 [195] show that only regenerated myofibers in the muscles of DMD patients consistently express NGF; dystrophic myofibers or healthy myofibers do not show NGF immunoreactivity. In addition, the authors report that regenerated myofibers in muscle biopsies from DMD patients are small, round, and occur mostly in clusters. These observations led them to hypothesize that in addition to its autocrine function, NGF exhibits a paracrine effect on neighboring regenerated myofibers. Our observations of myofibers generated by MDSCs transplanted in the skeletal muscle of *mdx* mice, particularly E-MDSCs, suggest a similar phenomenon.

It is worth mentioning that the method of evaluating muscle regenerative efficiency was assigned through manually counting dystrophin-positive myofibers on only sections of muscle with the largest engraftment as opposed to accounting for the area occupied by the myofibers and thus providing only a two-dimensional view of the regenerative process. This current method of quantifying dystrophin expression measures only local dystrophin expression, while ignoring the distribution of dystrophin-positive myofibers across the entire gastrocnemius muscle. It would be extremely difficult and time consuming to quantify the dystrophin-positive myofibers in the entire length of the muscle. Therefore, sophisticated image analysis software is needed with three-dimensional reconstruction to account for dystrophin-positive expression across the entire muscle. This would be practical for larger-scale studies with multiple group comparisons such as those being performed here.

7.0 FUTURE STUDIES

Aside from those studies already mentioned within previous sections, further experimentation is necessary in order to confirm the evidence presented here. In addition, more specific studies to address the underlying mechanisms of NGF action in muscle regeneration that would build upon and presumably strengthen the work herein presented are also needed. As a follow-up to the work described here, experiments will be conducted to further investigate the role of NGF stimulation mediating MDSCs' survival or promotion of cell death to explain the myogenic differentiation status and regeneration capacity. When placed *in vitro*, expansion and/or activation of quiescent progenitor populations may likely occur due to growth factors' effect. This may have important implications in terms of regeneration due to direct participation or the cells' chemoattractant abilities. The differences of cell survival and proliferation of MDSCs injected into the skeletal muscle may in part explain our improved outcome in regeneration capacity of stimulated versus non-treated MDSCs. To test this assumption, TUNEL assay can be used to determine differences in the number of apoptotic cells at the site of transplantation following injection. Apoptotic cells are revealed by using a fluorescence-conjugated dUTP to label the 3' ends of the DNA fragment generated by activated endonucleases. One can also investigate the actively-dividing cells within injected muscle by tracking the BrdU-labeled cells as representative of the mitotically active cells versus apoptotic cells at the site of injection.

A number of groups have recently shown that Akt expression, a prosurvival protein, plays an important role in myoblasts survival [196] via $p75^{\text{NTR}}$, the low affinity receptor of NGF. The $p75^{\text{NTR}}$ mediated signals are biologically important for the normal muscle development, since the absence of $p75^{\text{NTR}}$ receptor in mutant mice showed an impaired muscle strength [196]. Since Akt is known to mediate cell survival, and $p75^{\text{NTR}}$ activation can promote phosphorylation of Akt, we postulate that Akt is activated by NGF via $p75^{\text{NTR}}$ to promote the survival of the MDSCs and their transition into differentiated states. It was just reported by Shailaja et al. 2005 [196] that endogenous activation of Akt is most likely mediated by secreted NGF, and the significance of the autocrine signaling by NGF is underscored by its down regulation prior to differentiation [170]. So, we predict that the endogenous Akt activation is most likely due to expression of NGF by the engineered and stimulated MDSCs with NGF and its subsequent autocrine signaling.

It should be emphasized that high level of NGF may reflect changes in the levels of $p75^{\text{NTR}}$ expression at different stages of myogenesis. As a follow-up to the work described here, experimentation has already been initiated to further investigate the receptor levels in culture after NGF stimulation. To determine if Akt expression plays a role in the improved transplantation capacity of E- and S-MDSCs compared to C-MDSCs, levels of Akt should be monitored. Protein extract will be prepared for Western blot analysis using manufacturer recommendations with antibodies against Akt and phosphorylated Akt on the Ser 473 (Cell Signaling Technology, Beverley, MA). The Akt kinase activity will be measured using the Akt Kinase Assay Kit using GSK-3 α/β fusion protein as a substrate on immunoprecipitated Akt (Cell signaling Technology, Beverley, MA). We believe that these future experiments may provide evidence elucidating the signaling mechanisms and providing a linkage between the *in*

vitro settings within the context of muscle regeneration. This will offer insight into our current understanding of the underlying factors that promote muscle regeneration versus atrophy.

The formation of newly regenerated dystrophin-positive myofibers in dystrophic skeletal muscle does not always correlate with the physiologic performance in the injured muscle, and effective healing, however, involves the combination of both measures. In this regard, independent confirmation of physiologic measurements (e.g. contractile properties of muscle) should be performed before any conclusions regarding the long-term outcome and functionality of regenerated muscle fibers can be made. The gastrocnemius muscle should be studied under isometric conditions in order to assess specific force generation. In addition, repetitive lengthening actions, i.e. “eccentric contraction,” should be undertaken in order to assess the ability of regenerated muscle to resist contraction-induced decreases in force output. Unlike DMD patients, *mdx* mice exhibit a mild phenotype partially because of higher expression of utrophin, a protein closely related to dystrophin [197, 198] that partially compensates for lack of dystrophin [36, 199]. Indeed, double mutant mice *mdx/utr* ^{-/-} lacking both dystrophin and utrophin genes develop severe muscular dystrophy and die prematurely [200, 201], similar to outcomes observable in DMD patients. Therefore, designing a better model to study contractile properties of the muscle is currently in demand and under investigation.

8.0 SUMMARY AND CONCLUSIONS

Growth factors play important roles as signaling molecules throughout postnatal development, adult life, and aging. This study investigated the effect of nerve growth factor (NGF) on the muscle regeneration of the skeletal muscle of dystrophic (*mdx*) mice. Transplantation of muscle-derived stem cells (MDSCs) either stimulated with or genetically engineered to express NGF resulted in the regeneration of significantly more dystrophin-positive myofibers than did transplantation of control (non-treated) MDSCs. NGF did not alter the marker profile or proliferation behavior of MDSCs; however, MDSCs stimulated with NGF exhibited delayed *in vitro* differentiation, which may at least, partially explain their improved regeneration capacity observed *in vivo*.

In conclusion, these findings underscore the importance of NGF during skeletal muscle tissue remodeling and indicate that this molecule can improve the muscle regeneration capacity of muscle stem cells. Additional studies focused on NGF will substantially enhance our understanding of its mechanism and, in so doing, may lead to the development of alternate strategies for the treatment of DMD and other muscular dystrophies.

APPENDIX A

PREPLATE TECHNIQUE: ISOLATION OF THREE POPULATIONS OF MUSCLE-DERIVED CELLS

Gastrocnemius muscles of several adult-aged normal mice (3 weeks of age, C57 BL/10J; Jackson Laboratories) were obtained under aseptic techniques. A single cell suspension was obtained by digestion and enzymatic dissociation of combined muscles to obtain the appropriate number of cells. Enzymatic dissociation was performed by serial digestion of hand-minced muscles in 0.2% (by weight) collagenase-type XI solution (Sigma) for 1 hour, 0.3% dispase (Gibco-BRL) for 45 minutes, and 0.1% trypsin (Life Technologies) for 30 minutes. The final cell suspension was re-suspended in serum-supplemented Dulbecco's modified Eagle's medium (DMEM, containing 10% fetal bovine serum, 10% horse serum, 0.5% chick embryo extract by volume, and also 100 U/mL penicillin and 100 µg/mL streptomycin; Gibco-BRL), which was also used for subsequent culturing, and added to a T-75 collagen-coated flask (collagen Type I, Sigma). After 2 hours, floating cells contained within the supernatant were removed and transferred to a second T-75 flask. Fresh medium was added to the first set of adherent cells (termed preplate 1, or PP1), and this procedure was continued for PP2 through PP6 at subsequent 24 hour periods. A smaller surface area flask, T-25, was used for PP6 as the number of remaining non-adherent cells by this point was comparatively lower. This process resulted in six primary cultures of adherent cells with increasing initial adhesion times that are highly fibroblastic in nature [95, 202-204] that were subsequently used for surface protein and desmin analysis. Based on previous reports [95], the non-myogenic cells in pp2 and pp3 were removed from the cultures by replating the cells. The resulting enriched pp2 and pp3 desmin [+] cells were combined with pp4 and pp5 cells and were termed "early preplate cells" (EP). Cells in the pp6 cell population took an additional 24–72 h to attach to collagen-coated dishes after transfer from pp5 and were termed "late

preplate cells” (LP). Most of the LP cells died during the first 1–2 wks of the cultivation period, with very few of the adherent surviving cells proliferating and forming clonal colonies that are called “long-term proliferating” (LTP) cells or muscle-derived stem cells (MDSCs). A flow chart for the isolation of different population of muscle-derived-cells (EP, LP, and LTP or MDSCs) based on their adhesion characteristics to collagen coated flasks are shown below (Figure A.1).

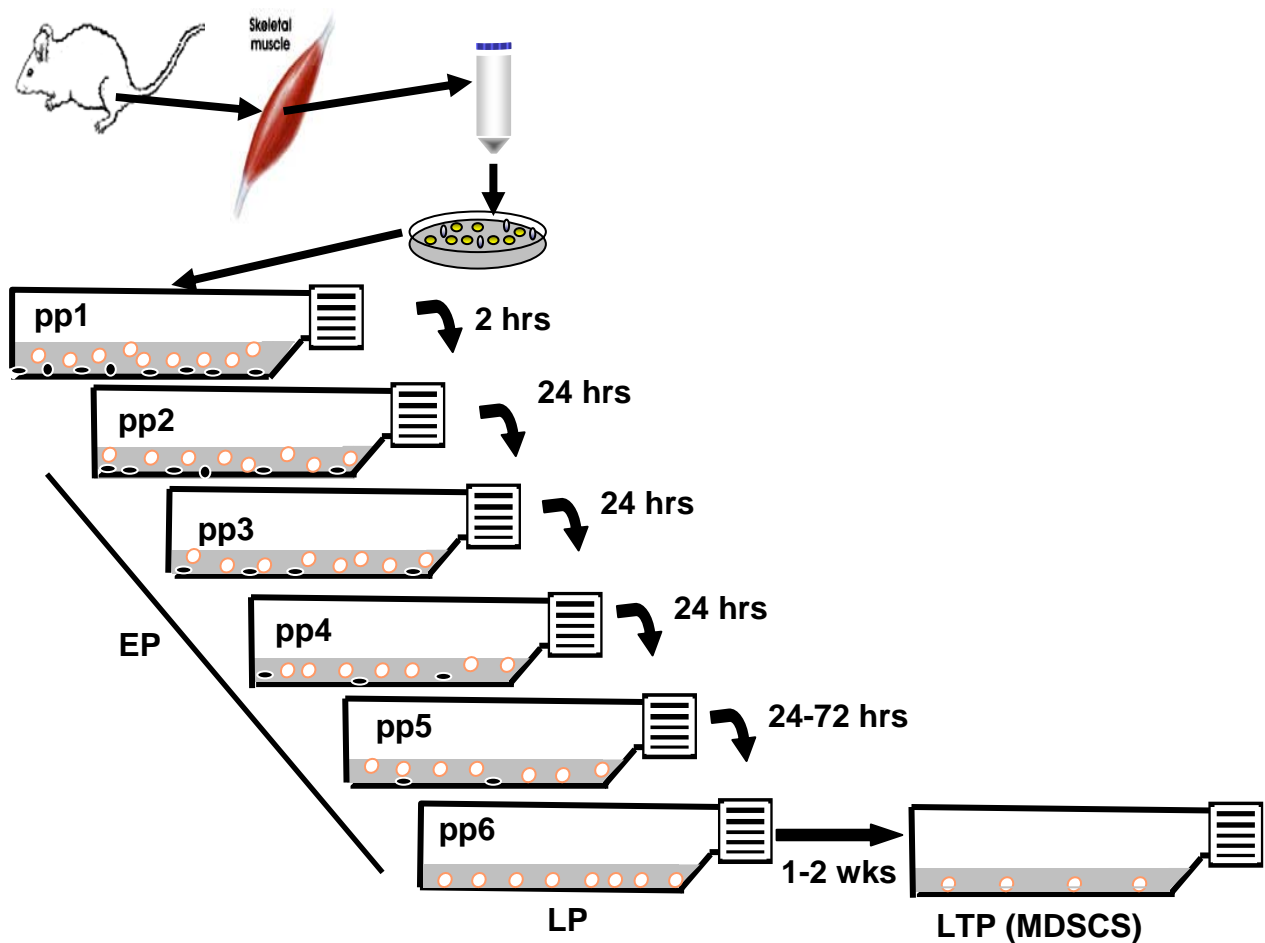


Figure A. 1 Schematic diagram of the preplating technique used for the isolation of muscle-derived cell population

APPENDIX B

NON-EXPONENTIAL GROWTH MODEL

Mathematical growth models are necessary tools that play a key role in characterizing and measuring the kinetic parameters of stem cell populations and understanding stem cell dynamics. Within heterogeneous stem cell populations such as MDSCs, a fraction of the cell population often remains in a non-dividing state. To account for this fraction in describing cell population growth, a non-exponential growth model has been proposed by Sherley [180]. To simplify the mathematical description of non-exponential growth, the following assumptions are made: 1) cells undergo asymmetric divisions, such that dividing cells are capable of giving rise to both dividing and non-dividing cells; 2) DT of the mitotically-active fraction remains constant; and 3) non-dividing cells do not re-enter the cell cycle. The validity of these assumptions has been discussed within the myogenic cell compartment [181]. Starting with an initial number of cells, N_0 , the number of cells at any subsequent doubling time interval can be described by the following equation:

$$N_1 = 2\alpha N_o + (1 - \alpha)N_o$$

where the first term represents the mitotically-active fraction (assuming the cells split to 2 daughter cells) and the second term represents the non-mitotically-active (non-dividing) fraction. Using the assumption that daughter cells that are dividing remains constant, such that at time interval = 2, we have

$$N_2 = 2\alpha(2\alpha N_o) + (1 - \alpha)(2\alpha N_o) + (1 - \alpha)N_o$$

or

$$N_i = 2\alpha^i N_o + (1-\alpha)2\alpha^{i-1} N_o + (1-\alpha)^o N_o$$

Expansion of the terms and simplification leads to the following expression

$$N_i = N_o \left[0.5 + 0.5 \sum_{i=0}^n (2\alpha)^i \right]$$

Now, if we define $i = \text{any positive value } t/DT$, and apply the identity, we have the following equation:

$$a \sum_{i=0}^n x^i = a \frac{1 - x^{n+1}}{1 - x}$$

where the cell number, N , at any time, t , depends on: 1) the initial number of cells (N_0), 2) the division time (DT) (F_D and GT , respectively in Sherley et al.) and 3) the mitotic fraction (α) or the fraction of daughter cells which are actively dividing. The Sherley model [180] includes a parameter that accounts for the presence of non-dividing cells (quiescent or senescent cells):

$$N = N_0 \left[0.5 + \frac{1 - (2\alpha)^{(t/DT)+1}}{2(1 - 2\alpha)} \right]$$

Here, we can see that if $\alpha = 1$, the equation reduces to the general exponential equation $N = N_0 2^{t/DT}$. As α approaches 0.5, the model equation becomes $N = N_0 + N_0 t / 2DT$ and there is linear growth with a slope of $N_0 / 2DT$.

It should be recognized that the phrases ‘division time’ and ‘doubling time’ are not equal ($DT \neq PDT$) [181]. Simply, division time (DT) should be understood as to the time that it takes for an individual cell to complete the cell cycle (cytokinesis) and doubling time, or more correctly population doubling time (PDT), is defined as the time it takes for a population of cells to double.

If all cells in a given population are mitotically active then, $PDT=DT$, however, if there are non-mitotic cells present within the population then $PDT \neq DT$. When non-dividing cells are present, the population doubling time is necessarily slower than the division time.

The appropriate equation to use to estimate PDT is as follows:

$$N = N_0 2^{(t/PDT)}$$

where N is the number of cells at time t , and N_0 is the initial number of cells and PDT is the population doubling time.

This comes from the more general exponential equation:

$$N = N_0 e^{kt}$$

to get the number of population doubling time, use the following equation:

$$\# \text{ doublings} = \frac{t}{PDT}$$

(e.g. if $PDT = 10$ hrs, then at time $t = 24$ hrs, you have 2.4 population doublings). When solving the first equation above for t/PDT :

$$\log \frac{N}{N_0} = \log(2^{t/PDT})$$

$$\log \frac{N}{N_0} = \frac{t}{PDT} \log 2$$

$$\frac{\log \frac{N}{N_0}}{\log 2} = \log_2 \frac{N}{N_0} = \frac{t}{PDT}$$

as a result,

$$\# \text{ of population doublings} = \log_2 \frac{N}{N_0}$$

The Sherley model [180] equation can be used to obtain PDT based on mitotic fraction, α , and DT by setting the PDT as the time t , where $N=2N_0$ and

$$\text{Population Doubling Time} = DT \left[\frac{\ln(6\alpha - 2)}{\ln(2\alpha)} - 1 \right]$$

Here, it is observed that population doubling time is now more accurately represented as a function of both α and DT.

Nonlinear Regression

```
[Parameters]
F=1
[Variables]
Nexp=col(2)
t=col(1)
[Equations]
GT=cell(3,1)
n=cell(2,1)
ep=(t/GT)+1
A=1-(2*F)^ep
B=2-4*F
N=n*(0.5+(A/B))
fit N to Nexp
[Constraints]
F>0
F<1
[Options]
```

C-MDSCs

R = 0.999 Rsqr (R^2) = 0.999 Adj Rsqr = 0.999

Standard Error of Estimate = 5.896

	Coefficient	StdError	t	P	VIF
F	0.945	0.00205	460.722	<0.001	1.000

Analysis of Variance

	DF	SS	MS	F	P
Regression	0	189225.058	189225.058	5442.733	>1e20
Residual	6	208.599	34.767		
Total	6	189433.657	31572.276		

Normality Test: Passed (P = 0.385)

Constant Variance Test: Passed (P = 0.054)

Power of performed test with alpha = 0.050: 1.000

Parameter	Value	Std.Err	CV(%)	Dependencies
alpha	9.447e-1	2.050e-3	2.171e-1	-0.0000000

E-MDSCs

R = 0.997 Rsqr (R^2) = 0.995 Adj Rsqr = 0.995

Standard Error of Estimate = 5.896

Coefficient	StdError	t	P	VIF	
F	0.923	0.00417	221.435	<0.001	1.000

Analysis of Variance:

	DF	SS	MS	F	P
Regression	0	195489.727	195489.727	1182.230	>1e20
Residual	6	992.141	165.357		
Total	6	196481.867	32746.978		

Normality Test: Passed (P = 0.278)

Constant Variance Test: Passed (P = 0.006)

Power of performed test with alpha = 0.050: 1.000

Parameter	Value	StdErr	CV(%)	Dependencies
alpha	9.231e-1	4.1690e-3	4.516e-1	-0.0000000

S-MDSCs

R = 1.000 Rsqr (R^2) = 1.000 Adj Rsqr = 01.000

Standard Error of Estimate = 2.924

	Coefficient	StdError	t	P	VIF
F	0.936	0.00115	816.573	<0.001	1.000

Analysis of Variance:

	DF	SS	MS	F	P
Regression	0	151290.897	151290.897	17700.377	>1e20
Residual	6	51.284	8.547		
Total	6	151342.181	25223.697		

Normality Test: Passed (P = 0.233)

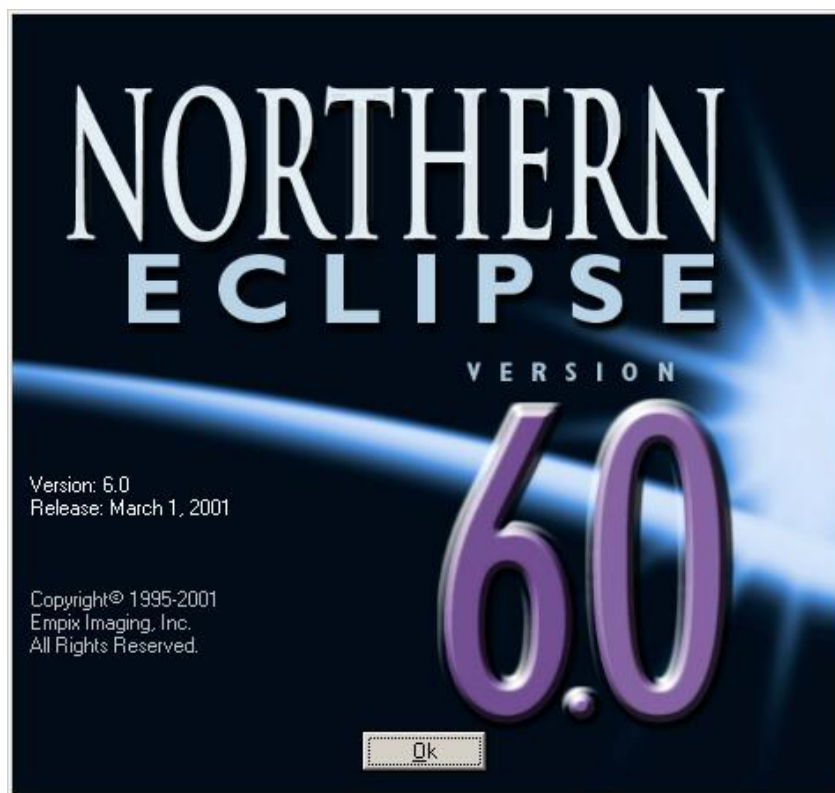
Constant Variance Test: Passed (P = 0.014)

Power of performed test with alpha = 0.050: 1.000

Parameter	Value	StdErr	CV(%)	Dependencies
alpha	9.358e-1	1.146e-3	1.225e-1	-0.0000000

APPENDIX C

DYSTROPHIN-POSITIVE MYOFIBERS ANALYSIS USING NORTHERN ECLIPSE



All images from the Northern Eclipsed software are reproduced with permission from The Empix Imaging, Inc.

Images of dystrophin-positive engraftment were taken using the Northern Eclipse software. If there was more than one image captured from the engraftment, the images were connected so that all positive fibers were measured only once. Figure A.2 shows a composite made in Adobe Photoshop 6.0 from all of the images taken from the engraftment of gastrocnemius muscle of an *mdx* mouse injected with MDSCs stimulated with NGF.

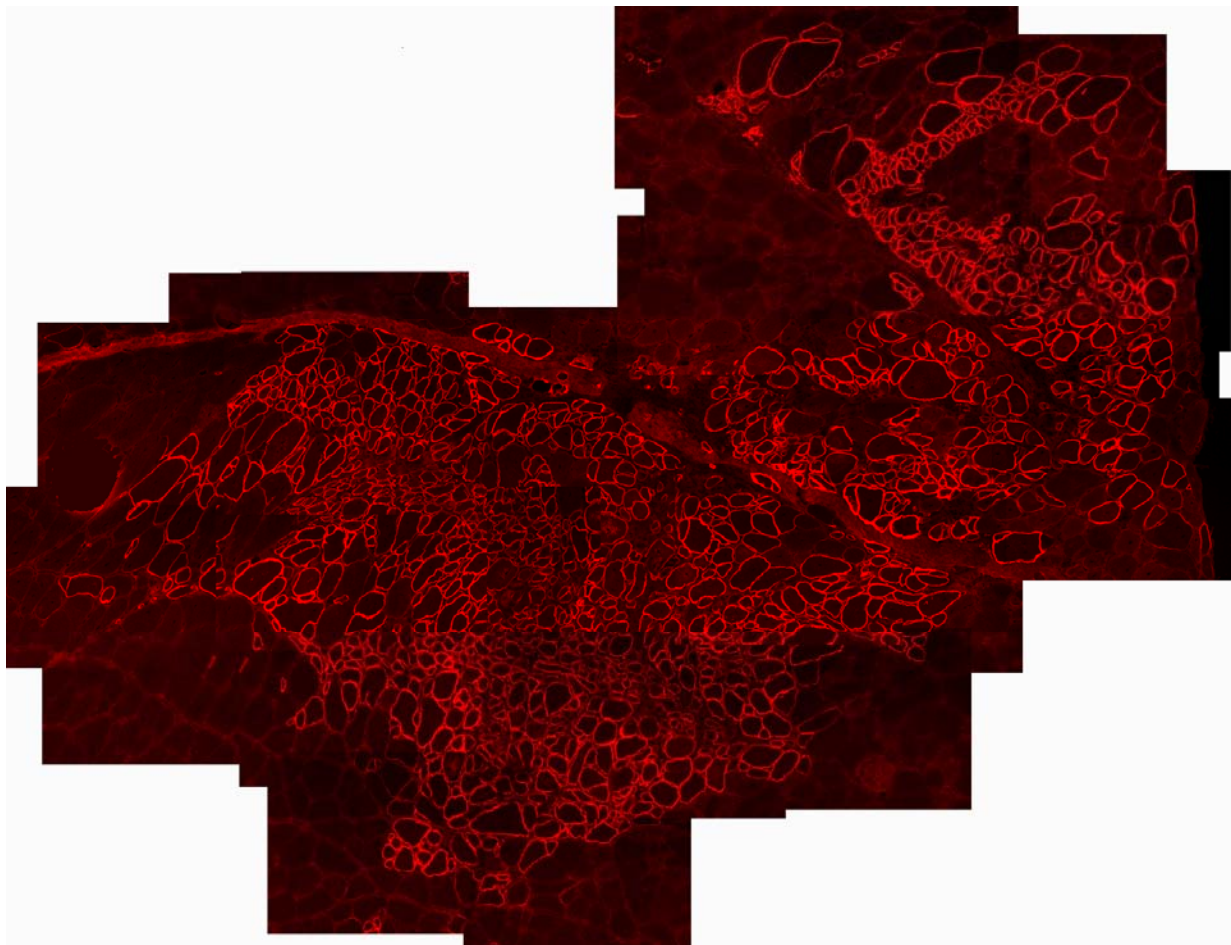


Figure A. 2 A composite of images from S-MDSCs muscle engraftment

Calibrate for Distance

Capturing a picture with known dimensions and then calibrating the software to those dimensions is known as calibration. The system is designed to calibrate pixel measurements to any unit value (i.e., microns, millimeters, and centimeters). For our purpose, we used an accurate glass scale with microns as the unit value.

An image captured from a scale is shown below (Figure A.3). In the example noted, a picture of a micrometer slide was captured from a Nikon microscope using a 40x objective. The line was drawn such that the starting point is at the top of one scale line and the ending point is at the top of the finishing scale line. Then the information such as the objective, the number of units that represent the length of the line, and unit name was entered and saved. This procedure was done for all of the objectives that were used during the experimental analysis (e.g. 10x, 20x, 40x, 60x).

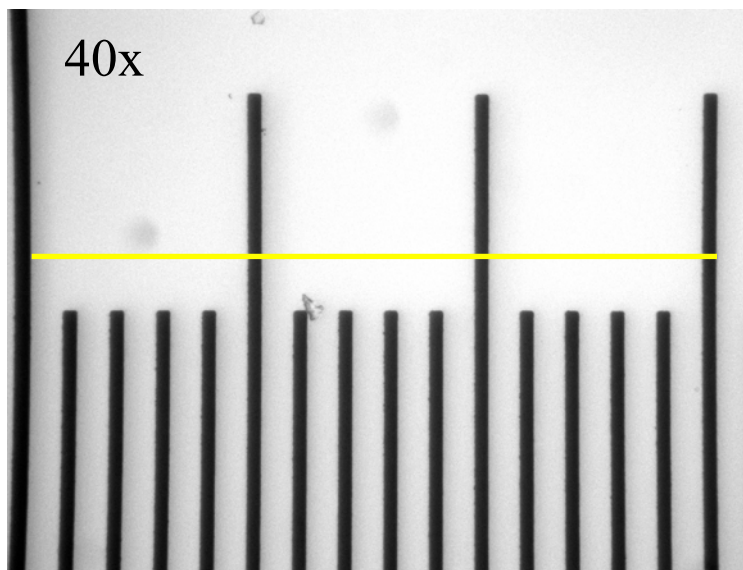


Figure A. 3 Image Calibration using micrometer slide with known dimensions

Convert To 8-bit Gray

This function is used to convert the current image into 8-bits per pixel image (1 plane of 8-bit grayscale data). When the image source is in color, the color data is converted into an image with grayscale value. This makes the image ready for thresholding.

In Toolbar under Process, choose Conversions, and then Convert to 8-bit grayscale.

Bit is the smallest unit in a binary number (binary digit) or the smallest unit of digital information recognized by a computer, and it may take the value of either zero or one (i.e. TRUE or FALSE, ON or OFF, 0 or 1, BLACK or WHITE, etc.). A pixel is represented by one or more computer bits and is the smallest spatially-digitized unit of an image. A single pixel has a single gray or color value, it is the smallest units by which the image can be collected and displayed. The sum of bits per pixel directly determines the number of colors or gray levels that can be represented. An 8-bit (1byte) image contains 28 or 256 gray levels, usually from zero (black) to 255 (white).

Data Options

In the Toolbar menu under Measure, choose Data Options. This menu allows for choosing methods of object exclusion or inclusion during measuring, morphometric data reporting choices, levels of data reporting, pixel exclusion, numeric data hole filling, and morphometric boundary options (Figure A.4).

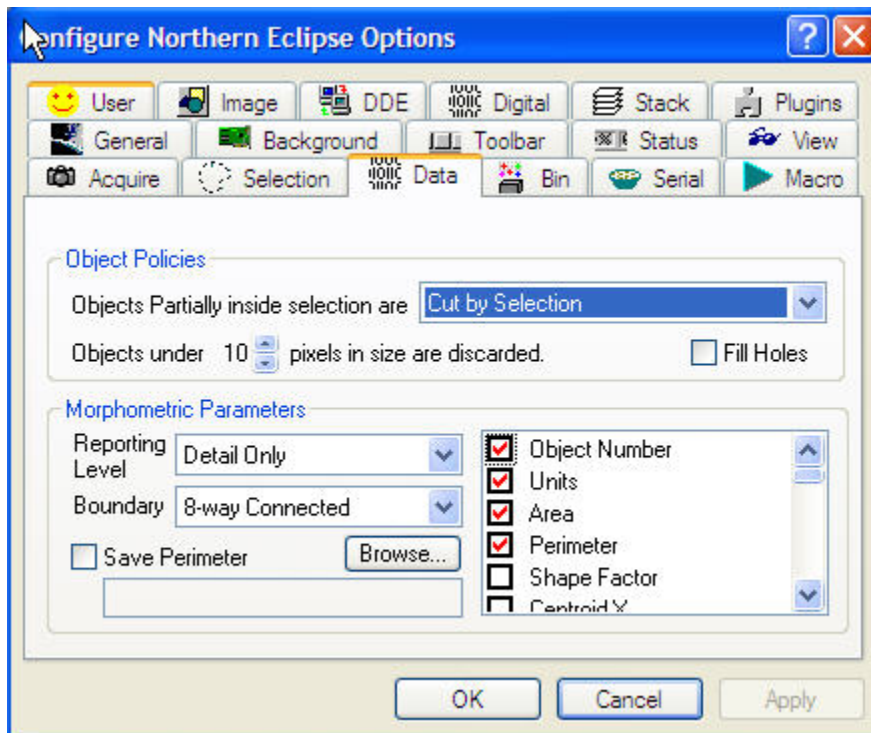


Figure A. 4 Northern Eclipse Data Options window

Object Policies

Cut by Selection: if the desired area is already selected by Trace Tool such as Rectangle Tool, this option actually cuts objects under traced areas during measuring (Figure A.5A). This selection measures all objects within the traced area and cuts objects along the trace line measuring partial objects along the cut line. The Cut by Selection option should be turned on if no thresholding is done prior to measuring.

Excluded from Selection: excludes all objects touching the lines of any traced areas during measuring (i.e. only measuring objects totally within traced areas) (Figure A.5B).

Included in Selection: includes all objects inside a traced area. Those objects touching the traced area are not counted (Figure A.5C).

Included/Excluded according to Centroid: is the most statistically correct method of counting or measuring objects, because only objects with a Centroid (center of gravity point) inside the traced region are included in the count (Figure A.5D).

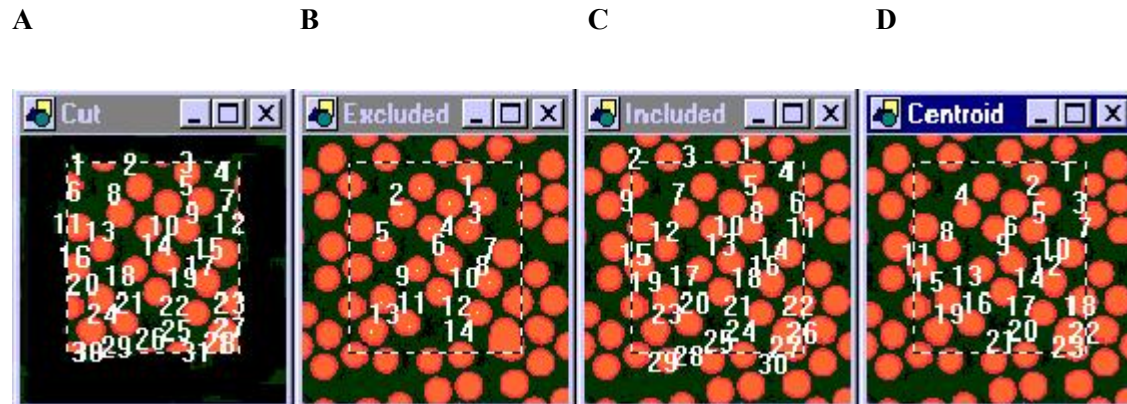


Figure A. 5 Northern Eclipse method of object exclusion or inclusion

Hint: Cut by Selection is generally not used for counting, but it can be very useful for densitometry or for objects that are not easy to threshold and therefore must be traced.

In all our measurements, we used Excluded from Selection, so only the myofibers totally within traced areas were measured.

Morphometric Parameters

The type of data to be recorded can be selected by double clicking on or off the red check marks beside the list of morphometric parameters.

For our purpose of myofiber area distribution, we used 3 groups of parameters:

Group 1: Area & Perimeter

Primitives:

Area The total number of pixels that an object occupies (Figure A.6A).

Group 2: Enclosure & Orientation

Primitives:

Diameter The longest line through an object that is parallel to its orientation (Line KL) (Figure A.6B).

Minor Axis Diameter The longest line through an object that is perpendicular to its orientation. (Line HJ) (Figure A.6B).

Derived:

Elongation $\text{Diameter} / \text{Minor Axis Diameter}$. Provides a general idea of object proportions independent from perimeter or shape (Figure A.6B).

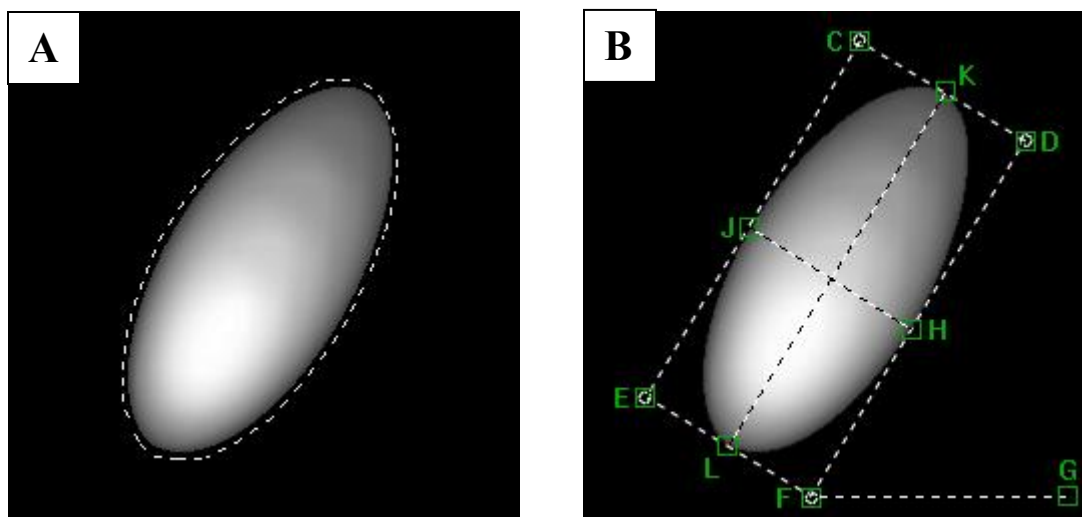


Figure A. 6 Northern Eclipse morphometric parameters

Group 3: Other Parameters

Object # A unique number that refers to the number of objects being counted. In our case, object # is the number of dystrophin-positive myofibers.

Units The units of the calibrated measurements. Our unit of calibration is microns.

Bin Classification The name of the Bin that an object is classified as. We created a new bin named “myofiber analysis”.

Boundary

This option allows the choice of an **8-way Connected** or **4-way Connected** morphometric measuring algorithm to be used. The Boundary method will be required by the user to determine when very thin, ambiguous objects need to be deciphered.

Bin Classifier Options

In Tool bar under Measure choose Bin Classifier Options.

Binning is a method of including or excluding certain objects by means of the objects morphometric characteristics (e.g. area, perimeter, and shape factor). Sorting, or data exclusion, takes place during the object measurement operations with the goal of selecting or rejecting objects that fall into preset morphometric ranges (e.g. measure all objects greater than 500 microns, or measure all objects with a shape factor greater than 0.7 etc.). We added two new bins referred to as “small fibers” and “large fibers” (Figure A.7).

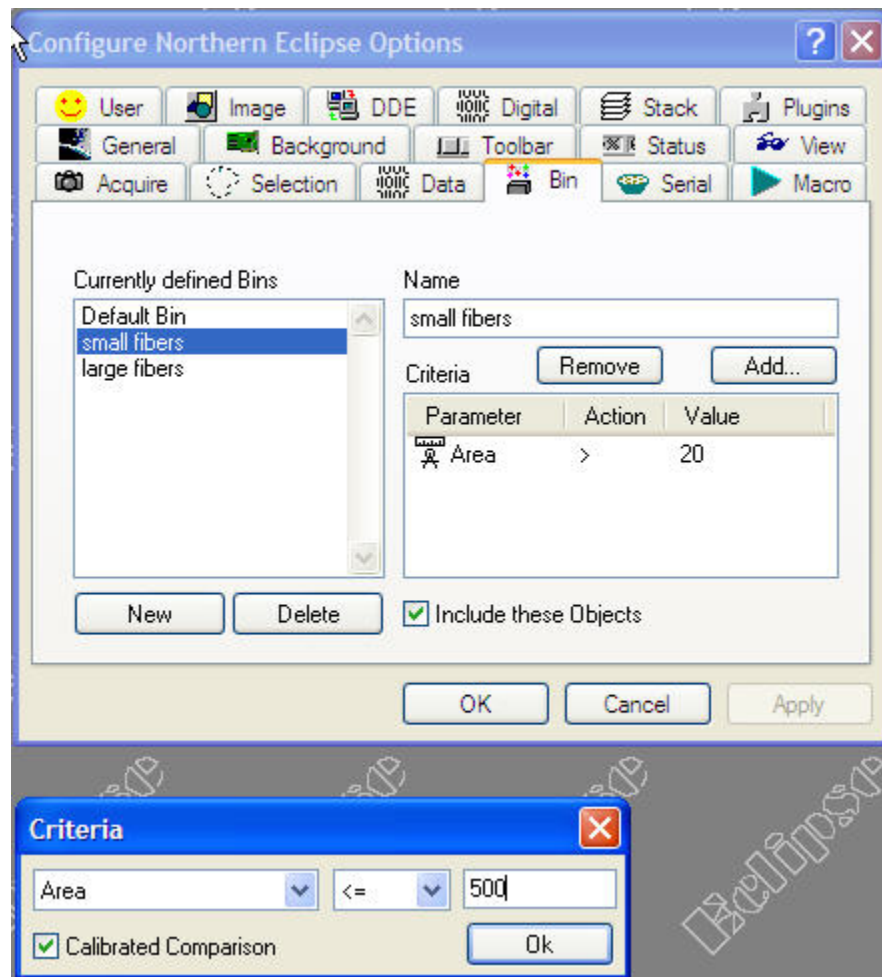


Figure A. 7 Northern Eclipse Bin Classifier Options

For large Fibers:

Area < 2000

Area > 500

For small fibers:

Area \leq 500

Area > 20

We checked the **Include these Objects** check box so that all the data with new bin category criteria will be included. We un-checked the Default Bin so that other parameters would not be included in our measurements.

Note: The above numbers were modified for each engraftment based on the quality of the image and fiber size distribution.

Threshold



This function is used to select objects in an image by specifying range(s) of values that differentiate it from the rest of the image. This process is alternatively known as binarization, segmentation, or object detection. Each pixel is tested independently and it is either selected or rejected according to the same criteria. The goal is to adjust the range(s) only until the pixels in the object are selected. This happens differently depending upon whether the image is monochrome or color.

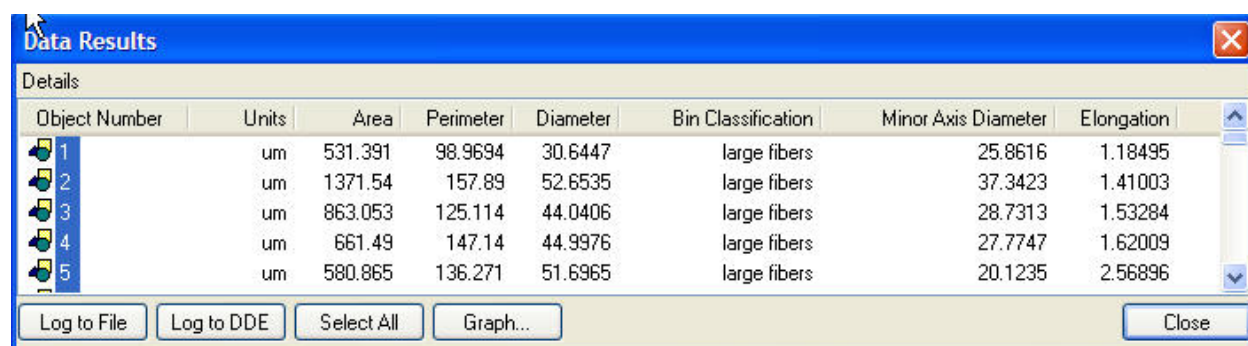
A range of intensities that corresponds to the gray values in the object can be chosen so that the gray values can be seen in the main status bar by moving the mouse over the image before calling this function. The display will change as the values are adjusted, showing the

selected pixels in red/white and the unselected pixels in cyan/black. The range will be between 0 and 255 for 8-bit images and 0 to 65535 for 16-bit images.

Occasionally, the range that selects the desired object also selects debris or unwanted objects. If they are smaller, larger, or have a different shape than the desired criteria, then bin classification can be used to classify and not include those objects that fall within that bin. Alternatively, the objects can be classified so that objects that do not fall within the created bin are not included. Finally, the unwanted objects can be ignored and deleted if necessary.



The last step is measuring selected objects and obtaining the raw data. An example of our raw data created in the Data Results window is shown below in Figure A.8.



Object Number	Units	Area	Perimeter	Diameter	Bin Classification	Minor Axis Diameter	Elongation
1	um	531.391	98.9694	30.6447	large fibers	25.8616	1.18495
2	um	1371.54	157.89	52.6535	large fibers	37.3423	1.41003
3	um	863.053	125.114	44.0406	large fibers	28.7313	1.53284
4	um	661.49	147.14	44.9976	large fibers	27.7747	1.62009
5	um	580.865	136.271	51.6965	large fibers	20.1235	2.56896

Figure A. 8 Northern Eclipse Data Results window

The count values were logged to an Excel spreadsheet by clicking on **Log to DDE**. Data was analyzed on the selected parameters and statistical analysis was performed as previously described.

APPENDIX D

PROCEDURES FOR QUANTIZATION OF DYSTROPHIN-POSITIVE MYOFIBER USING NORTHERN ECLIPSE

1. Open Northern Eclipse
2. Open your saved image (TIFF format)
3. In Toolbar choose Process
 - Conversion
 - Convert to 8-bit grayscale
4. In Toolbar choose Measure
 - Calibrate for distance

Note: Select the right calibration from the already calibrated scales. If the image is taken with a different microscope (e.g. Nikon or Leica), make sure that the correct calibration is chosen. In order to check the microscope used to take the image, right click on image and click on Image Info. Look at dimensions and consider the following points:

If the dimension is 1280x1024, the image has been taken on Leica with the Retiga 1300 camera. Consequently, choose calibration for Leica.

If the dimension is 1360x1024, the image has been taken in Nikon with the Retiga Exi camera. Here, choose calibration for Nikon.

5. Setting up the parameters
 - A) Go to “View”
 - View Options
 - “Data” tab

Object Policies

Select Objects Partially inside selected are

Object under 10 pixels in size are discarded

(This options is for eliminating debris or not defined fibers due to their small size, so the # is changed based on the engraftment by user)

Morphometric Parameters

Reporting level

Boundary

Put a check mark on the desired parameters listed:

For our purpose, we used Object #, Units, Area, Perimeter, Diameter, Bin Classification, Minor Axis Diameter, and Elongation.

B) Choose “Bin” tab

Add a new bin by clicking on

Name the new bin as desire

Criteria:

→ Click on

→ Choose

→ Scroll down and add $>$, $<$, \leq , \geq , based on myofibers area

For Example:

Area < 2000

Area > 500

These criteria will select large fibers between 500 to 2000 microns.

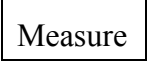
Note: Click on if there are any changes need to be made. Then, enter new criteria. Highlight the bin you need to get rid of and Click on under Currently defined Bins. Check mark ☒ “Include these Objects” only for the new bin created. Un-check for Default and delete any **other bins that may exist**.

Warning: The **Include these Objects** check box is an important check box to consider when making measurements with Northern Eclipse. In each new bin category, the criteria chosen can either be included or not included depending on this check box. Be careful when un-checking the Default Bin. It is possible to exclude any measurements from being made and if your system is a multi-user system, it may be wise to turn the Default Bin parameters back on or the next person using the system may not be getting the results they expect.

C) Click on button in Toolbar.

You will need to select a range of intensities that corresponds to the gray values in the object. The gray values can be seen in the main status bar by moving the mouse over the image before calling this function. The display will change as you adjust the values, showing you the selected pixels in red/white and unselected pixels in cyan/black. The range will be between 0 and 255 for 8-bit images. In our case, the myofibers should have defined boundaries. If the threshold point is at low pixel intensity, red/white will flood the myofibers and the myofiber number will be underrepresented. If the threshold is at high pixel intensity, the connected components will decrease and we will not be representing small fibers. One way of dealing with composites with very different sizes of myofibers is to divide the analysis into two sets. First, set the criteria in

your bin set up to count large fibers (Area >1000). Later change the criteria to measure the small myofibers (Area >100, <1000). Note that the threshold levels will also require adjustment between the two measurements.

D) Click on  button in Toolbar.

The data will be created according to chosen parameters the in Data Result Window. By clicking on top of each parameter, the layout of the information can be changed so that the data can be listed in ascending or descending order. Each number can also be clicked individually and examined to see which myofiber corresponds to that number. In order to get rid of a measured myofiber, close the Data Result Window, go to the image, right click on the number or box on that fiber, and “Remove Object”.

At last,

E)  if you are want to record the data to an excel spreadsheet.

If Excel cannot be found, be sure it has been loaded onto the computer first. Also, be sure that Excel is run at least once prior to linking through DDE. Once the DDE link has been established, all subsequent data logging will use this connection. Book1 will then be launched, and the data will go to sheet1 (unless other wise specified).

BIBLIOGRAPHY

1. Decary, S., Mouly, V., Hamida, C.B., Sautet, A., Barbet, J.P., and Butler-Browne, G.S. (1997). Replicative potential and telomere length in human skeletal muscle: implications for satellite cell-mediated gene therapy. *Hum Gene Ther* 8, 1429-1438.
2. Schmalbruch, H., and Lewis, D.M. (2000). Dynamics of nuclei of muscle fibers and connective tissue cells in normal and denervated rat muscles. *Muscle Nerve* 23, 617-626.
3. Rappolee, D.A., and Werb, Z. (1992). Macrophage-derived growth factors. *Curr Top Microbiol Immunol* 181, 87-140.
4. Tidball, J.G. (1995). Inflammatory cell response to acute muscle injury. *Med Sci Sports Exerc* 27, 1022-1032.
5. Fielding, R.A., Manfredi, T.J., Ding, W., Fiatarone, M.A., Evans, W.J., and Cannon, J.G. (1993). Acute phase response in exercise. III. Neutrophil and IL-1 beta accumulation in skeletal muscle. *Am J Physiol* 265, R166-172.
6. Orimo, S., Hiyamuta, E., Arahata, K., and Sugita, H. (1991). Analysis of inflammatory cells and complement C3 in bupivacaine-induced myonecrosis. *Muscle Nerve* 14, 515-520.
7. Almekinders, L.C., and Gilbert, J.A. (1986). Healing of experimental muscle strains and the effects of nonsteroidal antiinflammatory medication. *Am J Sports Med* 14, 303-308.
8. Lescaudron, L., Peltekian, E., Fontaine-Perus, J., Paulin, D., Zampieri, M., Garcia, L., and Parrish, E. (1999). Blood borne macrophages are essential for the triggering of muscle regeneration following muscle transplant. *Neuromuscul Disord* 9, 72-80.
9. Merly, F., Lescaudron, L., Rouaud, T., Crossin, F., and Gardahaut, M.F. (1999). Macrophages enhance muscle satellite cell proliferation and delay their differentiation. *Muscle Nerve* 22, 724-732.

10. Robertson, T.A., Maley, M.A., Grounds, M.D., and Papadimitriou, J.M. (1993). The role of macrophages in skeletal muscle regeneration with particular reference to chemotaxis. *Exp Cell Res* 207, 321-331.
11. Champion, D.R. (1984). The muscle satellite cell: a review. *Int Rev Cytol* 87, 225-251.
12. Grounds, M.D., White, J.D., Rosenthal, N., and Bogoyevitch, M.A. (2002). The role of stem cells in skeletal and cardiac muscle repair. *J Histochem Cytochem* 50, 589-610.
13. Hawke, T.J., and Garry, D.J. (2001). Myogenic satellite cells: physiology to molecular biology. *J Appl Physiol* 91, 534-551.
14. Darr, K.C., and Schultz, E. (1987). Exercise-induced satellite cell activation in growing and mature skeletal muscle. *J Appl Physiol* 63, 1816-1821.
15. Snow, M.H. (1977). Myogenic cell formation in regenerating rat skeletal muscle injured by mincing. II. An autoradiographic study. *Anat Rec* 188, 201-217.
16. Snow, M.H. (1978). An autoradiographic study of satellite cell differentiation into regenerating myotubes following transplantation of muscles in young rats. *Cell Tissue Res* 186, 535-540.
17. Blaveri, K., Heslop, L., Yu, D.S., Rosenblatt, J.D., Gross, J.G., Partridge, T.A., and Morgan, J.E. (1999). Patterns of repair of dystrophic mouse muscle: studies on isolated fibers. *Dev Dyn* 216, 244-256.
18. Engel, A.G. (1986). Duchenne dystrophy. In *Myology*, Volume 2, A.G. Engel and B.Q. Banker, eds. (New York: McGraw-Hill), pp. 1185-1202.
19. Hoffman, E.P., Brown, R.H., Jr., and Kunkel, L.M. (1987). Dystrophin: the protein product of the Duchenne muscular dystrophy locus. *Cell* 51, 919-928.
20. Hoffman, E.P., Brown, R.H., and Kunkel, L.M. (1992). Dystrophin: the protein product of the Duchene muscular dystrophy locus. 1987. *Biotechnology* 24, 457-466.
21. Koenig, M., Hoffman, E.P., Bertelson, C.J., Monaco, A.P., Feener, C., and Kunkel, L.M. (1987). Complete cloning of the Duchenne muscular dystrophy (DMD) cDNA and preliminary genomic organization of the DMD gene in normal and affected individuals. *Cell* 50, 509-517.

22. Menke, A., and Jockusch, H. (1991). Decreased osmotic stability of dystrophin-less muscle cells from the mdx mouse. *Nature* 349, 69-71.
23. Hutter, O.F., Burton, F.L., and Bovell, D.L. (1991). Mechanical properties of normal and mdx mouse sarcolemma: bearing on function of dystrophin. *J Muscle Res Cell Motil* 12, 585-589.
24. Petrof, B.J., Stedman, H.H., Shrager, J.B., Eby, J., Sweeney, H.L., and Kelly, A.M. (1993). Adaptations in myosin heavy chain expression and contractile function in dystrophic mouse diaphragm. *Am J Physiol* 265, C834-841.
25. Gorospe, J.R., and Hoffman, E.P. (1992). Duchenne muscular dystrophy. *Curr Opin Rheumatol* 4, 794-800.
26. Sicinski, P., Geng, Y., Ryder-Cook, A.S., Barnard, E.A., Darlison, M.G., and Barnard, P.J. (1989). The molecular basis of muscular dystrophy in the mdx mouse: a point mutation. *Science* 244, 1578-1580.
27. Arikawa, E., Ishihara, T., Nonaka, I., Sugita, H., and Arahata, K. (1991). Immunocytochemical analysis of dystrophin in congenital muscular dystrophy. *J Neurol Sci* 105, 79-87.
28. Coulton, G.R., Morgan, J.E., Partridge, T.A., and Sloper, J.C. (1988). The mdx mouse skeletal muscle myopathy: I. A histological, morphometric and biochemical investigation. *Neuropathol Appl Neurobiol* 14, 53-70.
29. Pastoret, C., and Sebillé, A. (1995). Age-related differences in regeneration of dystrophic (mdx) and normal muscle in the mouse. *Muscle Nerve* 18, 1147-1154.
30. Tanabe, Y., Esaki, K., and Nomura, T. (1986). Skeletal muscle pathology in X chromosome-linked muscular dystrophy (mdx) mouse. *Acta Neuropathol (Berl)* 69, 91-95.
31. Cohn, R.D., Henry, M.D., Michele, D.E., Barresi, R., Saito, F., Moore, S.A., Flanagan, J.D., Skwarchuk, M.W., Robbins, M.E., Mendell, J.R., Williamson, R.A., and Campbell, K.P. (2002). Disruption of DAG1 in differentiated skeletal muscle reveals a role for dystroglycan in muscle regeneration. *Cell* 110, 639-648.
32. Pastoret, C., and Sebillé, A. (1993). Further aspects of muscular dystrophy in mdx mice. *Neuromuscul Disord* 3, 471-475.

33. Pastoret, C., and Sebille, A. (1995). mdx mice show progressive weakness and muscle deterioration with age. *J Neurol Sci* 129, 97-105.
34. Partridge, T.A., Morgan, J.E., Coulton, G.R., Hoffman, E.P., and Kunkel, L.M. (1989). Conversion of mdx myofibres from dystrophin-negative to -positive by injection of normal myoblasts. *Nature* 337, 176-179.
35. Vilquin, J.T., Wagner, E., Kinoshita, I., Roy, R., and Tremblay, J.P. (1995). Successful histocompatible myoblast transplantation in dystrophin-deficient mdx mouse despite the production of antibodies against dystrophin. *J Cell Biol* 131, 975-988.
36. Law, D.J., Allen, D.L., and Tidball, J.G. (1994). Talin, vinculin and DRP (utrophin) concentrations are increased at mdx myotendinous junctions following onset of necrosis. *J Cell Sci* 107 (Pt 6), 1477-1483.
37. Gussoni, E., Soneoka, Y., Strickland, C.D., Buzney, E.A., Khan, M.K., Flint, A.F., Kunkel, L.M., and Mulligan, R.C. (1999). Dystrophin expression in the mdx mouse restored by stem cell transplantation. *Nature* 401, 390-394.
38. Karpati, G., Pouliot, Y., Zubrzycka-Gaarn, E., Carpenter, S., Ray, P.N., Worton, R.G., and Holland, P. (1989). Dystrophin is expressed in mdx skeletal muscle fibers after normal myoblast implantation. *Am J Pathol* 135, 27-32.
39. Huard, J., Bouchard, J.P., Roy, R., Malouin, F., Dansereau, G., Labrecque, C., Albert, N., Richards, C.L., Lemieux, B., and Tremblay, J.P. (1992). Human myoblast transplantation: preliminary results of 4 cases. *Muscle Nerve* 15, 550-560.
40. Huard, J., Roy, R., Bouchard, J.P., Malouin, F., Richards, C.L., and Tremblay, J.P. (1992). Human myoblast transplantation between immunohistocompatible donors and recipients produces immune reactions. *Transplant Proc* 24, 3049-3051.
41. Karpati, G., Holland, P., and Worton, R.G. (1992). Myoblast transfer in DMD: problems in the interpretation of efficiency. *Muscle Nerve* 15, 1209-1210.
42. Tremblay, J.P., Malouin, F., Roy, R., Huard, J., Bouchard, J.P., Satoh, A., and Richards, C.L. (1993). Results of a triple blind clinical study of myoblast transplantations without immunosuppressive treatment in young boys with Duchenne muscular dystrophy. *Cell Transplant* 2, 99-112.

43. Partridge, T.A. (1991). Invited review: myoblast transfer: a possible therapy for inherited myopathies? *Muscle Nerve* 14, 197-212.
44. Morgan, J.E., Pagel, C.N., Sherratt, T., and Partridge, T.A. (1993). Long-term persistence and migration of myogenic cells injected into pre-irradiated muscles of mdx mice. *J Neurol Sci* 115, 191-200.
45. Miller, R.G., Sharma, K.R., Pavlath, G.K., Gussoni, E., Mynhier, M., Lanctot, A.M., Greco, C.M., Steinman, L., and Blau, H.M. (1997). Myoblast implantation in Duchenne muscular dystrophy: the San Francisco study. *Muscle Nerve* 20, 469-478.
46. Mendell, J.R., Kissel, J.T., Amato, A.A., King, W., Signore, L., Prior, T.W., Sahenk, Z., Benson, S., McAndrew, P.E., Rice, R., and et al. (1995). Myoblast transfer in the treatment of Duchenne's muscular dystrophy. *N Engl J Med* 333, 832-838.
47. Smythe, G.M., Hodgetts, S.I., and Grounds, M.D. (2000). Immunobiology and the future of myoblast transfer therapy. *Mol Ther* 1, 304-313.
48. Huard, J., Verreault, S., Roy, R., Tremblay, M., and Tremblay, J.P. (1994). High efficiency of muscle regeneration after human myoblast clone transplantation in SCID mice. *J Clin Invest* 93, 586-599.
49. Huard, J., Roy, R., Guerette, B., Verreault, S., Tremblay, G., and Tremblay, J.P. (1994). Human myoblast transplantation in immunodeficient and immunosuppressed mice: evidence of rejection. *Muscle Nerve* 17, 224-234.
50. Fan, Y., Maley, M., Beilharz, M., and Grounds, M. (1996). Rapid death of injected myoblasts in myoblast transfer therapy. *Muscle Nerve* 19, 853-860.
51. Guerette, B., Asselin, I., Skuk, D., Entman, M., and Tremblay, J.P. (1997). Control of inflammatory damage by anti-LFA-1: increase success of myoblast transplantation. *Cell Transplant* 6, 101-107.
52. Beauchamp, J.R., Morgan, J.E., Pagel, C.N., and Partridge, T.A. (1999). Dynamics of myoblast transplantation reveal a discrete minority of precursors with stem cell-like properties as the myogenic source. *J Cell Biol* 144, 1113-1122.
53. Hodgetts, S.I., Beilharz, M.W., Scalzo, A.A., and Grounds, M.D. (2000). Why do cultured transplanted myoblasts die in vivo? DNA quantification shows enhanced survival of donor male myoblasts in host mice depleted of CD4+ and CD8+ cells or Nk1.1+ cells. *Cell Transplant* 9, 489-502.

54. Skuk, D., Goulet, M., Roy, B., and Tremblay, J.P. (2000). Myoblast transplantation in whole muscle of nonhuman primates. *J Neuropathol Exp Neurol* 59, 197-206.
55. Kinoshita, I., Huard, J., and Tremblay, J.P. (1994). Utilization of myoblasts from transgenic mice to evaluate the efficacy of myoblast transplantation. *Muscle Nerve* 17, 975-980.
56. Pavlath, G.K., Rando, T.A., and Blau, H.M. (1994). Transient immunosuppressive treatment leads to long-term retention of allogeneic myoblasts in hybrid myofibers. *J Cell Biol* 127, 1923-1932.
57. Quantin, B., Perricaudet, L.D., Tajbakhsh, S., and Mandel, J.L. (1992). Adenovirus as an expression vector in muscle cells in vivo. *Proc Natl Acad Sci U S A* 89, 2581-2584.
58. Ragot, T., Vincent, N., Chafey, P., Vigne, E., Gilgenkrantz, H., Couton, D., Cartaud, J., Briand, P., Kaplan, J.C., Perricaudet, M., and et al. (1993). Efficient adenovirus-mediated transfer of a human minidystrophin gene to skeletal muscle of mdx mice. *Nature* 361, 647-650.
59. Huard, J., Lochmuller, H., Acsadi, G., Jani, A., Holland, P., Guerin, C., Massie, B., and Karpati, G. (1995). Differential short-term transduction efficiency of adult versus newborn mouse tissues by adenoviral recombinants. *Exp Mol Pathol* 62, 131-143.
60. van Deutekom, J.C., Cao, B., Pruchnic, R., Wickham, T.J., Kovesdi, I., and Huard, J. (1999). Extended tropism of an adenoviral vector does not circumvent the maturation-dependent transducibility of mouse skeletal muscle. *J Gene Med* 1, 393-399.
61. van Deutekom, J.C., Hoffman, E.P., and Huard, J. (1998). Muscle maturation: implications for gene therapy. *Mol Med Today* 4, 214-220.
62. Acsadi, G., Jani, A., Huard, J., Blaschuk, K., Massie, B., Holland, P., Lochmuller, H., and Karpati, G. (1994). Cultured human myoblasts and myotubes show markedly different transducibility by replication-defective adenovirus recombinants. *Gene Ther* 1, 338-340.
63. Acsadi, G., Jani, A., Massie, B., Simoneau, M., Holland, P., Blaschuk, K., and Karpati, G. (1994). A differential efficiency of adenovirus-mediated in vivo gene transfer into skeletal muscle cells of different maturity. *Hum Mol Genet* 3, 579-584.

64. Vincent, N., Ragot, T., Gilgenkrantz, H., Couton, D., Chafey, P., Gregoire, A., Briand, P., Kaplan, J.C., Kahn, A., and Perricaudet, M. (1993). Long-term correction of mouse dystrophic degeneration by adenovirus-mediated transfer of a minidystrophin gene. *Nat Genet* 5, 130-134.
65. Hannallah, D., Peterson, B., Lieberman, J.R., Fu, F.H., and Huard, J. (2002). Gene therapy in orthopaedic surgery. *J Bone Joint Surg Am* 84-A, 1046-1061.
66. Robbins, P.D., and Ghivizzani, S.C. (1998). Viral vectors for gene therapy. *Pharmacol Ther* 80, 35-47.
67. Evans, C.H., and Robbins, P.D. (1995). Possible orthopaedic applications of gene therapy. *J Bone Joint Surg Am* 77, 1103-1114.
68. Wolff, J.A., Ludtke, J.J., Acsadi, G., Williams, P., and Jani, A. (1992). Long-term persistence of plasmid DNA and foreign gene expression in mouse muscle. *Hum Mol Genet* 1, 363-369.
69. van Deutekom, J.C., Floyd, S.S., Booth, D.K., Oligino, T., Krisky, D., Marconi, P., Glorioso, J.C., and Huard, J. (1998). Implications of maturation for viral gene delivery to skeletal muscle. *Neuromuscul Disord* 8, 135-148.
70. Dunkley, M.G., Love, D.R., Davies, K.E., Walsh, F.S., Morris, G.E., and Dickson, G. (1992). Retroviral-mediated transfer of a dystrophin minigene into mdx mouse myoblasts in vitro. *FEBS Lett* 296, 128-134.
71. Huard, J., Acsadi, G., Jani, A., Massie, B., and Karpati, G. (1994). Gene transfer into skeletal muscles by isogenic myoblasts. *Hum Gene Ther* 5, 949-958.
72. Bosch, P., Musgrave, D.S., Lee, J.Y., Cummins, J., Shuler, T., Ghivizzani, T.C., Evans, T., Robbins, T.D., and Huard (2000). Osteoprogenitor cells within skeletal muscle. *J Orthop Res* 18, 933-944.
73. Musgrave, D.S., Bosch, P., Ghivizzani, S., Robbins, P.D., Evans, C.H., and Huard, J. (1999). Adenovirus-mediated direct gene therapy with bone morphogenetic protein-2 produces bone. *Bone* 24, 541-547.
74. Musgrave, D.S., Bosch, P., Lee, J.Y., Pelinkovic, D., Ghivizzani, S.C., Whalen, J., Niyibizi, C., and Huard, J. (2000). Ex vivo gene therapy to produce bone using different cell types. *Clin Orthop*, 290-305.

75. Smith, B.F., Hoffman, R.K., Giger, U., and Wolfe, J.H. (1990). Genes transferred by retroviral vectors into normal and mutant myoblasts in primary cultures are expressed in myotubes. *Mol Cell Biol* 10, 3268-3271.
76. Barr, E., and Leiden, J.M. (1991). Systemic delivery of recombinant proteins by genetically modified myoblasts. *Science* 254, 1507-1509.
77. Dhawan, J., Pan, L.C., Pavlath, G.K., Travis, M.A., Lanctot, A.M., and Blau, H.M. (1991). Systemic delivery of human growth hormone by injection of genetically engineered myoblasts. *Science* 254, 1509-1512.
78. Salminen, A., Elson, H.F., Mickley, L.A., Fojo, A.T., and Gottesman, M.M. (1991). Implantation of recombinant rat myocytes into adult skeletal muscle: a potential gene therapy. *Hum Gene Ther* 2, 15-26.
79. Yao, S.N., and Kurachi, K. (1992). Expression of human factor IX in mice after injection of genetically modified myoblasts. *Proc Natl Acad Sci U S A* 89, 3357-3361.
80. Dai, Y., Roman, M., Naviaux, R.K., and Verma, I.M. (1992). Gene therapy via primary myoblasts: long-term expression of factor IX protein following transplantation in vivo. *Proc Natl Acad Sci U S A* 89, 10892-10895.
81. Floyd, S.S., Jr., Clemens, P.R., Ontell, M.R., Kochanek, S., Day, C.S., Yang, J., Hauschka, S.D., Balkir, L., Morgan, J., Moreland, M.S., Feero, G.W., Epperly, M., and Huard, J. (1998). Ex vivo gene transfer using adenovirus-mediated full-length dystrophin delivery to dystrophic muscles. *Gene Ther* 5, 19-30.
82. Evans, C.H., and Robbins, P.D. (1999). Gene therapy of arthritis. *Intern Med* 38, 233-239.
83. Simonson, G.D., Groskreutz, D.J., Gorman, C.M., and MacDonald, M.J. (1996). Synthesis and processing of genetically modified human proinsulin by rat myoblast primary cultures. *Hum Gene Ther* 7, 71-78.
84. Jiao, S., Gurevich, V., and Wolff, J.A. (1993). Long-term correction of rat model of Parkinson's disease by gene therapy. *Nature* 362, 450-453.
85. Miller, D.G., Adam, M.A., and Miller, A.D. (1990). Gene transfer by retrovirus vectors occurs only in cells that are actively replicating at the time of infection. *Mol Cell Biol* 10, 4239-4242.

86. Partridge, T.A. (2002). Cells that participate in regeneration of skeletal muscle. *Gene Ther* 9, 752-753.
87. Bischoff, R. (1986). A satellite cell mitogen from crushed adult muscle. *Dev Biol* 115, 140-147.
88. Bischoff, R. (1994). The satellite cell and muscle regeneration. In *Myology: Basic and Clinical*, 2 Edition, A.G. Engel and C. Franzini-Armstrong, eds. (New York: McGraw-Hill), pp. 97-118.
89. Asakura, A., Komaki, M., and Rudnicki, M. (2001). Muscle satellite cells are multipotential stem cells that exhibit myogenic, osteogenic, and adipogenic differentiation. *Differentiation* 68, 245-253.
90. Wada, M.R., Inagawa-Ogashiwa, M., Shimizu, S., Yasumoto, S., and Hashimoto, N. (2002). Generation of different fates from multipotent muscle stem cells. *Development* 129, 2987-2995.
91. Schultz, E., and McCormick, K.M. (1994). Skeletal muscle satellite cells. *Rev Physiol Biochem Pharmacol* 123, 213-257.
92. Miller, J.B., Schaefer, L., and Dominov, J.A. (1999). Seeking muscle stem cells. *Curr Top Dev Biol* 43, 191-219.
93. Cornelison, D.D., and Wold, B.J. (1997). Single-cell analysis of regulatory gene expression in quiescent and activated mouse skeletal muscle satellite cells. *Dev Biol* 191, 270-283.
94. Baroffio, A., Hamann, M., Bernheim, L., Bochaton-Piallat, M.L., Gabbiani, G., and Bader, C.R. (1996). Identification of self-renewing myoblasts in the progeny of single human muscle satellite cells. *Differentiation* 60, 47-57.
95. Qu, Z., Balkir, L., van Deutekom, J.C., Robbins, P.D., Pruchnic, R., and Huard, J. (1998). Development of approaches to improve cell survival in myoblast transfer therapy. *J Cell Biol* 142, 1257-1267.
96. Qu-Petersen, Z., Deasy, B., Jankowski, R., Ikezawa, M., Cummins, J., Pruchnic, R., Mytinger, J., Cao, B., Gates, C., Wernig, A., and Huard, J. (2002). Identification of a novel population of muscle stem cells in mice: potential for muscle regeneration. *J Cell Biol* 157, 851-864.

97. Lee, J.Y., Qu-Petersen, Z., Cao, B., Kimura, S., Jankowski, R., Cummins, J., Usas, A., Gates, C., Robbins, P., Wernig, A., and Huard, J. (2000). Clonal isolation of muscle-derived cells capable of enhancing muscle regeneration and bone healing. *J Cell Biol* 150, 1085-1100.
98. Jankowski, R.J., Deasy, B.M., and Huard, J. (2002). Muscle-derived stem cells. *Gene Ther* 9, 642-647.
99. Bittner, R.E., Schofer, C., Weipoltshammer, K., Ivanova, S., Streubel, B., Hauser, E., Freilinger, M., Hoyer, H., Elbe-Burger, A., and Wachtler, F. (1999). Recruitment of bone-marrow-derived cells by skeletal and cardiac muscle in adult dystrophic mdx mice. *Anat Embryol (Berl)* 199, 391-396.
100. Ferrari, G., Cusella-De Angelis, G., Coletta, M., Paolucci, E., Stornaiuolo, A., Cossu, G., and Mavilio, F. (1998). Muscle regeneration by bone marrow-derived myogenic progenitors. *Science* 279, 1528-1530.
101. LaBarge, M.A., and Blau, H.M. (2002). Biological progression from adult bone marrow to mononucleate muscle stem cell to multinucleate muscle fiber in response to injury. *Cell* 111, 589-601.
102. Asakura, A., Seale, P., Girgis-Gabardo, A., and Rudnicki, M.A. (2002). Myogenic specification of side population cells in skeletal muscle. *J Cell Biol* 159, 123-134.
103. Jankowski, R.J., Deasy, B.M., Cao, B., Gates, C., and Huard, J. (2002). The role of CD34 expression and cellular fusion in the regeneration capacity of myogenic progenitor cells. *J Cell Sci* 115, 4361-4374.
104. Torrente, Y., Tremblay, J.P., Pisati, F., Belicchi, M., Rossi, B., Sironi, M., Fortunato, F., El Fahime, M., D'Angelo, M.G., Caron, N.J., Constantin, G., Paulin, D., Scarlato, G., and Bresolin, N. (2001). Intraarterial injection of muscle-derived CD34(+)Sca-1(+) stem cells restores dystrophin in mdx mice. *J Cell Biol* 152, 335-348.
105. Clarke, D.L., Johansson, C.B., Wilbertz, J., Veress, B., Nilsson, E., Karlstrom, H., Lendahl, U., and Frisen, J. (2000). Generalized potential of adult neural stem cells. *Science* 288, 1660-1663.
106. Galli, R., Borello, U., Gritti, A., Minasi, M.G., Bjornson, C., Coletta, M., Mora, M., De Angelis, M.G., Fiocco, R., Cossu, G., and Vescovi, A.L. (2000). Skeletal myogenic potential of human and mouse neural stem cells. *Nat Neurosci* 3, 986-991.

107. Young, H.E., Duplaa, C., Young, T.M., Floyd, J.A., Reeves, M.L., Davis, K.H., Mancini, G.J., Eaton, M.E., Hill, J.D., Thomas, K., Austin, T., Edwards, C., Cuzzourt, J., Parikh, A., Groom, J., Hudson, J., and Black, A.C., Jr. (2001). Clonogenic analysis reveals reserve stem cells in postnatal mammals: I. Pluripotent mesenchymal stem cells. *Anat Rec* 263, 350-360.
108. Young, H.E., Steele, T.A., Bray, R.A., Hudson, J., Floyd, J.A., Hawkins, K., Thomas, K., Austin, T., Edwards, C., Cuzzourt, J., Duenzl, M., Lucas, P.A., and Black, A.C., Jr. (2001). Human reserve pluripotent mesenchymal stem cells are present in the connective tissues of skeletal muscle and dermis derived from fetal, adult, and geriatric donors. *Anat Rec* 264, 51-62.
109. Goldring, K., Partridge, T., and Watt, D. (2002). Muscle stem cells. *J Pathol* 197, 457-467.
110. Seale, P., and Rudnicki, M.A. (2000). A new look at the origin, function, and "stem-cell" status of muscle satellite cells. *Dev Biol* 218, 115-124.
111. Trippel, S.B. (1997). Growth factors as therapeutic agents. *Instr Course Lect* 46, 473-476.
112. Florini, J.R., Roberts, A.B., Ewton, D.Z., Falen, S.L., Flanders, K.C., and Sporn, M.B. (1986). Transforming growth factor-beta. A very potent inhibitor of myoblast differentiation, identical to the differentiation inhibitor secreted by Buffalo rat liver cells. *J Biol Chem* 261, 16509-16513.
113. Florini, J.R., and Magri, K.A. (1989). Effects of growth factors on myogenic differentiation. *Am J Physiol* 256, C701-711.
114. Allen, J.B., Manthey, C.L., Hand, A.R., Ohura, K., Ellingsworth, L., and Wahl, S.M. (1990). Rapid onset synovial inflammation and hyperplasia induced by transforming growth factor beta. *J Exp Med* 171, 231-247.
115. Florini, J.R., Ewton, D.Z., and Magri, K.A. (1991). Hormones, growth factors, and myogenic differentiation. *Annu Rev Physiol* 53, 201-216.
116. Alameddine, H.S., Dehaupas, M., and Fardeau, M. (1989). Regeneration of skeletal muscle fibers from autologous satellite cells multiplied in vitro. An experimental model for testing cultured cell myogenicity. *Muscle Nerve* 12, 544-555.

117. Hurme, T., and Kalimo, H. (1992). Activation of myogenic precursor cells after muscle injury. *Med Sci Sports Exerc* 24, 197-205.
118. Schultz, E., Jaryszak, D.L., and Valliere, C.R. (1985). Response of satellite cells to focal skeletal muscle injury. *Muscle Nerve* 8, 217-222.
119. Schultz, E. (1989). Satellite cell behavior during skeletal muscle growth and regeneration. *Med Sci Sports Exerc* 21, S181-186.
120. Joseph-Silverstein, J., Consigli, S.A., Lyser, K.M., and Ver Pault, C. (1989). Basic fibroblast growth factor in the chick embryo: immunolocalization to striated muscle cells and their precursors. *J Cell Biol* 108, 2459-2466.
121. Anderson, J.E., Liu, L., and Kardami, E. (1991). Distinctive patterns of basic fibroblast growth factor (bFGF) distribution in degenerating and regenerating areas of dystrophic (mdx) striated muscles. *Dev Biol* 147, 96-109.
122. Barnard, W., Bower, J., Brown, M.A., Murphy, M., and Austin, L. (1994). Leukemia inhibitory factor (LIF) infusion stimulates skeletal muscle regeneration after injury: injured muscle expresses lif mRNA. *J Neurol Sci* 123, 108-113.
123. Ross, R., Raines, E.W., and Bowen-Pope, D.F. (1986). The biology of platelet-derived growth factor. *Cell* 46, 155-169.
124. Jennische, E., and Hansson, H.A. (1987). Regenerating skeletal muscle cells express insulin-like growth factor I. *Acta Physiol Scand* 130, 327-332.
125. Clarke, M.S., Khakee, R., and McNeil, P.L. (1993). Loss of cytoplasmic basic fibroblast growth factor from physiologically wounded myofibers of normal and dystrophic muscle. *J Cell Sci* 106 (Pt 1), 121-133.
126. Kinoshita, I., Vilquin, J.T., and Tremblay, J.P. (1995). Pretreatment of myoblast cultures with basic fibroblast growth factor increases the efficacy of their transplantation in mdx mice. *Muscle Nerve* 18, 834-841.
127. Kasemkijwattana, C., Menetrey, J., Somogyi, G., Moreland, M.S., Fu, F.H., Buranapanitkit, B., Watkins, S.C., and Huard, J. (1998). Development of approaches to improve the healing following muscle contusion. *Cell Transplant* 7, 585-598.
128. Kasemkijwattana, C., Menetrey, J., and Day, C.S. (1998). Biologic intervention in muscle healing and regeneration. *Sports Med Arthrosc Rev* 6, 95-102.

129. Kasemkijwattana, C., Menetrey, J., Bosch, P., Somogyi, G., Moreland, M.S., Fu, F.H., Buranapanitkit, B., Watkins, S.S., and Huard, J. (2000). Use of growth factors to improve muscle healing after strain injury. *Clin Orthop*, 272-285.
130. Menetrey, J., Kasemkijwattana, C., Day, C.S., Bosch, P., Vogt, M., Fu, F.H., Moreland, M.S., and Huard, J. (2000). Growth factors improve muscle healing in vivo. *J Bone Joint Surg Br* 82, 131-137.
131. Huard, J., Li, Y., and Fu, F.H. (2002). Muscle injuries and repair: current trends in research. *J Bone Joint Surg Am* 84-A, 822-832.
132. Li, Y., Cummins, J., and Huard, J. (2001). Muscle injury and repair. *Curr Opin Orthop* 12, 409-415.
133. Lyles, J.M., Amin, W., Bock, E., and Weill, C.L. (1993). Regulation of NCAM by growth factors in serum-free myotube cultures. *J Neurosci Res* 34, 273-286.
134. McFarland, D.C., Pesall, J.E., and Gilkerson, K.K. (1993). The influence of growth factors on turkey embryonic myoblasts and satellite cells in vitro. *Gen Comp Endocrinol* 89, 415-424.
135. Allen, R.E., and Boxhorn, L.K. (1989). Regulation of skeletal muscle satellite cell proliferation and differentiation by transforming growth factor-beta, insulin-like growth factor I, and fibroblast growth factor. *J Cell Physiol* 138, 311-315.
136. Harrington, M.A., Daub, R., Song, A., Stasek, J., and Garcia, J.G. (1992). Interleukin 1 alpha mediated inhibition of myogenic terminal differentiation: increased sensitivity of Ha-ras transformed cultures. *Cell Growth Differ* 3, 241-248.
137. Olson, E.N., Sternberg, E., Hu, J.S., Spizz, G., and Wilcox, C. (1986). Regulation of myogenic differentiation by type beta transforming growth factor. *J Cell Biol* 103, 1799-1805.
138. Yablonka-Reuveni, Z., Balestreri, T.M., and Bowen-Pope, D.F. (1990). Regulation of proliferation and differentiation of myoblasts derived from adult mouse skeletal muscle by specific isoforms of PDGF. *J Cell Biol* 111, 1623-1629.
139. Levi-Montalcini, R. (1987). The nerve growth factor 35 years later. *Science* 237, 1154-1162.

140. Thoenen, H., Bandtlow, C., and Heumann, R. (1987). The physiological function of nerve growth factor in the central nervous system: comparison with the periphery. *Rev Physiol Biochem Pharmacol* 109, 145-178.
141. Edwards, R.H., Selby, M.J., Garcia, P.D., and Rutter, W.J. (1988). Processing of the native nerve growth factor precursor to form biologically active nerve growth factor. *J Biol Chem* 263, 6810-6815.
142. Ayer-LeLievre, C., Olson, L., Ebendal, T., Hallbook, F., and Persson, H. (1988). Nerve growth factor mRNA and protein in the testis and epididymis of mouse and rat. *Proc Natl Acad Sci U S A* 85, 2628-2632.
143. Brodie, C., and Sampson, S.R. (1987). Nerve growth factor supports growth of rat skeletal myotubes in culture. *Brain Res* 435, 393-397.
144. Aloe, L., Skaper, S.D., Leon, A., and Levi-Montalcini, R. (1994). Nerve growth factor and autoimmune diseases. *Autoimmunity* 19, 141-150.
145. Aloe, L., Tuveri, M.A., and Levi-Montalcini, R. (1992). Nerve growth factor and distribution of mast cells in the synovium of adult rats. *Clin Exp Rheumatol* 10, 203-204.
146. Bonini, S., Lambiase, A., Bonini, S., Angelucci, F., Magrini, L., Manni, L., and Aloe, L. (1996). Circulating nerve growth factor levels are increased in humans with allergic diseases and asthma. *Proc Natl Acad Sci U S A* 93, 10955-10960.
147. Lambiase, A., Bonini, S., Bonini, S., Micera, A., Magrini, L., Bracci-Laudiero, L., and Aloe, L. (1995). Increased plasma levels of nerve growth factor in vernal keratoconjunctivitis and relationship to conjunctival mast cells. *Invest Ophthalmol Vis Sci* 36, 2127-2132.
148. Laudiero, L.B., Aloe, L., Levi-Montalcini, R., Buttinelli, C., Schilter, D., Gillesen, S., and Otten, U. (1992). Multiple sclerosis patients express increased levels of beta-nerve growth factor in cerebrospinal fluid. *Neurosci Lett* 147, 9-12.
149. Bracci-Laudiero, L., Aloe, L., Levi-Montalcini, R., Galeazzi, M., Schilter, D., Scully, J.L., and Otten, U. (1993). Increased levels of NGF in sera of systemic lupus erythematosus patients. *Neuroreport* 4, 563-565.
150. Brodie, C., and Sampson, S.R. (1990). Nerve growth factor and fibroblast growth factor influence post-fusion expression of Na-channels in cultured rat skeletal muscle. *J Cell Physiol* 144, 492-497.

151. Bocchini, G., and Angeletti, P.U. (1996). The nerve growth factor: purification as a 30,000 molecular-weight protein. *Proc Natl Acad Sci* *64*, 787-794.
152. Hempstead, B.L., Martin-Zanca, D., Kaplan, D.R., Parada, L.F., and Chao, M.V. (1991). High-affinity NGF binding requires coexpression of the trk proto-oncogene and the low-affinity NGF receptor. *Nature* *350*, 678-683.
153. Bothwell, M. (1995). Functional interactions of neurotrophins and neurotrophin receptors. *Annu Rev Neurosci* *18*, 223-253.
154. Kaplan, D.R., and Miller, F.D. (1997). Signal transduction by the neurotrophin receptors. *Curr Opin Cell Biol* *9*, 213-221.
155. Chao, M.V., and Hempstead, B.L. (1995). p75 and Trk: a two-receptor system. *Trends Neurosci* *18*, 321-326.
156. Lee, F.S., Kim, A.H., Khursigara, G., and Chao, M.V. (2001). The uniqueness of being a neurotrophin receptor. *Curr Opin Neurobiol* *11*, 281-286.
157. Patapoutian, A., and Reichardt, L.F. (2001). Trk receptors: mediators of neurotrophin action. *Curr Opin Neurobiol* *11*, 272-280.
158. Miller, F.D., and Kaplan, D.R. (2002). Neurobiology. TRK makes the retrograde. *Science* *295*, 1471-1473.
159. Miller, F.D., and Kaplan, D.R. (2001). Neurotrophin signalling pathways regulating neuronal apoptosis. *Cell Mol Life Sci* *58*, 1045-1053.
160. Deasy, B.M., Qu-Peterson, Z., Greenberger, J.S., and Huard, J. (2002). Mechanisms of muscle stem cell expansion with cytokines. *Stem Cells* *20*, 50-60.
161. Duchenne, G.B. (1868). Researches sur la paralysie musculaire pseudo-hyperophrque ou paralysie myo-sclerotique. *Arch. Gen. Med.* *11*, 179, 305, 421, 552.
162. Arahata, K., Ishiura, S., Ishiguro, T., Tsukahara, T., Suhara, Y., Eguchi, C., Ishihara, T., Nonaka, I., Ozawa, E., and Sugita, H. (1988). Immunostaining of skeletal and cardiac muscle surface membrane with antibody against Duchenne muscular dystrophy peptide. *Nature* *333*, 861-863.

163. Bonilla, E., Samitt, C.E., Miranda, A.F., Hays, A.P., Salviati, G., DiMauro, S., Kunkel, L.M., Hoffman, E.P., and Rowland, L.P. (1988). Duchenne muscular dystrophy: deficiency of dystrophin at the muscle cell surface. *Cell* 54, 447-452.
164. Watkins, S.C., Hoffman, E.P., Slayter, H.S., and Kunkel, L.M. (1988). Immunoelectron microscopic localization of dystrophin in myofibres. *Nature* 333, 863-866.
165. Hoffman, E.P., Monaco, A.P., Feener, C.C., and Kunkel, L.M. (1987). Conservation of the Duchenne muscular dystrophy gene in mice and humans. *Science* 238, 347-350.
166. Anderson, J.E., Ovalle, W.K., and Bressler, B.H. (1987). Electron microscopic and autoradiographic characterization of hindlimb muscle regeneration in the mdx mouse. *Anat Rec* 219, 243-257.
167. Grounds, M.D. (1991). Towards understanding skeletal muscle regeneration. *Pathol Res Pract* 187, 1-22.
168. Weiss, A., and Schlessinger, J. (1998). Switching signals on or off by receptor dimerization. *Cell* 94, 277-280.
169. Rende, M. (1998). Nerve growth factor (NGF) stimulates myoblast fusion into myotubes in a rat myogenic cell line (L6): A novel autocrine role for NGF in muscle development. In: *Proceedings of the 28th Annual Meeting of Society for Neuroscience*. 801.10.
170. Rende, M., Brizi, E., Conner, J., Treves, S., Censier, K., Provenzano, C., Taglialatela, G., Sanna, P.P., and Donato, R. (2000). Nerve growth factor (NGF) influences differentiation and proliferation of myogenic cells in vitro via TrKA. *Int J Dev Neurosci* 18, 869-885.
171. Ou, J.Y., Chambers, J., and Wheeler, E.F. (1999). Myoblasts differentiation is accompanied by expression of the NGF receptors: effects of NGF on the proliferation and differentiation of myoblasts. In: *proceedings of the 29th Annual Meeting of the Society for Neuroscience*. Abs. 94.15.
172. Capsoni, S., Ruberti, F., Di Daniel, E., and Cattaneo, A. (2000). Muscular dystrophy in adult and aged anti-NGF transgenic mice resembles an inclusion body myopathy. *J Neurosci Res* 59, 553-560.
173. Ruberti, F., Capsoni, S., Comparini, A., Di Daniel, E., Franzot, J., Gonfloni, S., Rossi, G., Berardi, N., and Cattaneo, A. (2000). Phenotypic knockout of nerve growth factor in adult transgenic mice reveals severe deficits in basal forebrain cholinergic neurons, cell death in the spleen, and skeletal muscle dystrophy. *J Neurosci* 20, 2589-2601.

174. Wheeler, E.F., Gong, H., Grimes, R., Benoit, D., and Vazquez, L. (1998). p75^{NTR} and Trk receptors are expressed in reciprocal patterns in a wide variety of non-neural tissues during rat embryonic development, indicating independent receptor functions. *J Comp Neurol* 391, 407-428.
175. Zhao, J., Yoshioka, K., Miike, T., Kageshita, T., and Arao, T. (1991). Nerve growth factor receptor immunoreactivity on the tunica adventitia of intramuscular blood vessels in childhood muscular dystrophies. *Neuromuscul Disord* 1, 135-141.
176. Baron, P., Scarpini, E., Meola, G., Santilli, I., Conti, G., Pleasure, D., and Scarlato, G. (1994). Expression of the low-affinity NGF receptor during human muscle development, regeneration, and in tissue culture. *Muscle Nerve* 17, 276-284.
177. Evans, C.H., and Robbins, P.D. (1994). The interleukin-1 receptor antagonist and its delivery by gene transfer. *Receptor* 4, 9-15.
178. Peng, H., Wright, V., Usas, A., Gearhart, B., Shen, H.C., Cummins, J., and Huard, J. (2002). Synergistic enhancement of bone formation and healing by stem cell-expressed VEGF and bone morphogenetic protein-4. *J Clin Invest* 110, 751-759.
179. Deasy, B.M., Jankowski, R.J., and Huard, J. (2001). Muscle-derived stem cells: characterization and potential for cell-mediated therapy. *Blood Cells Mol Dis* 27, 924-933.
180. Sherley, J.L., Stadler, P.B., and Stadler, J.S. (1995). A quantitative method for the analysis of mammalian cell proliferation in culture in terms of dividing and non-dividing cells. *Cell Prolif* 28, 137-144.
181. Deasy, B.M., Jankowski, R.J., Payne, T.R., Cao, B., Goff, J.P., Greenberger, J.S., and Huard, J. (2003). Modeling stem cell population growth: incorporating terms for proliferative heterogeneity. *Stem Cells* 21, 536-545.
182. Greenberger, J.S., Goff, J.P., Bush, J., Bahnson, A., Koebler, D., Athanassiou, H., Domach, M., and Houck, R.K. (2000). Expansion of hematopoietic stem cells in vitro as a model system for human tissue engineering. *Orthop Clin North Am* 31, 499-510.
183. Kinoshita, I., Vilquin, J.T., Guerette, B., Asselin, I., Roy, R., and Tremblay, J.P. (1994). Very efficient myoblast allotransplantation in mice under FK506 immunosuppression. *Muscle Nerve* 17, 1407-1415.

184. DiMario, J., Buffinger, N., Yamada, S., and Strohman, R.C. (1989). Fibroblast growth factor in the extracellular matrix of dystrophic (mdx) mouse muscle. *Science* 244, 688-690.
185. White, T.P., and Esser, K.A. (1989). Satellite cell and growth factor involvement in skeletal muscle growth. *Med Sci Sports Exerc* 21, S158-163.
186. Acosta, C.G., Fabrega, A.R., Masco, D.H., and Lopez, H.S. (2001). A sensory neuron subpopulation with unique sequential survival dependence on nerve growth factor and basic fibroblast growth factor during development. *J Neurosci* 21, 8873-8885.
187. Shitaka, Y., and Saito, H. (1994). The effect of basic fibroblast growth factor (bFGF) and nerve growth factor (NGF) on the survival of septal neurons transplanted into the third ventricle in rats. *Jpn J Pharmacol* 64, 27-33.
188. Kushima, Y., Nishio, C., Nonomura, T., and Hatanaka, H. (1992). Effects of nerve growth factor and basic fibroblast growth factor on survival of cultured septal cholinergic neurons from adult rats. *Brain Res* 598, 264-270.
189. McCallister, W.V., Tang, P., Smith, J., and Trumble, T.E. (2001). Axonal regeneration stimulated by the combination of nerve growth factor and ciliary neurotrophic factor in an end-to-side model. *J Hand Surg [Am]* 26, 478-488.
190. Salvatori, G., Ferrari, G., Mezzogiorno, A., Servidei, S., Coletta, M., Tonali, P., Giavazzi, R., Cossu, G., and Mavilio, F. (1993). Retroviral vector-mediated gene transfer into human primary myogenic cells leads to expression in muscle fibers in vivo. *Hum Gene Ther* 4, 713-723.
191. Anderson, W.F. (1992). Human gene therapy. *Science* 256, 808-813.
192. Miller, A.R., Skotzko, M.J., Rhoades, K., Belldegrun, A.S., Tso, C.L., Kaboo, R., McBride, W.H., Jacobs, E., Kohn, D.B., Moen, R., and et al. (1992). Simultaneous use of two retroviral vectors in human gene marking trials: feasibility and potential applications. *Hum Gene Ther* 3, 619-624.
193. Meakin, S.O., and Shooter, E.M. (1992). The nerve growth factor family of receptors. *Trends Neurosci* 15, 323-331.
194. Barde, Y.A. (1989). Trophic factors and neuronal survival. *Neuron* 2, 1525-1534.

195. Toti, P., Villanova, M., Vatti, R., Schuerfeld, K., Stumpo, M., Barbagli, L., Malandrini, A., and Costantini, M. (2003). Nerve growth factor expression in human dystrophic muscles. *Muscle Nerve* 27, 370-373.
196. Reddypalli, S., Roll, K., Lee, H., Lundell, M., Rodriguez-Barea, E., and Wheeler, E.F. (2005). p75^{NTR}-mediated signaling promotes the survival of myoblasts and influences muscle strength. In *Journal of Cellular Physiology*.
197. Tinsley, J.M., Blake, D.J., Roche, A., Fairbrother, U., Riss, J., Byth, B.C., Knight, A.E., Kendrick-Jones, J., Suthers, G.K., Love, D.R., and et al. (1992). Primary structure of dystrophin-related protein. *Nature* 360, 591-593.
198. Blake, D.J., Tinsley, J.M., and Davies, K.E. (1996). Utrophin: a structural and functional comparison to dystrophin. *Brain Pathol* 6, 37-47.
199. Pons, F., Nicholson, L.V., Robert, A., Voit, T., and Leger, J.J. (1993). Dystrophin and dystrophin-related protein (utrophin) distribution in normal and dystrophin-deficient skeletal muscles. *Neuromuscul Disord* 3, 507-514.
200. Grady, R.M., Teng, H., Nichol, M.C., Cunningham, J.C., Wilkinson, R.S., and Sanes, J.R. (1997). Skeletal and cardiac myopathies in mice lacking utrophin and dystrophin: a model for Duchenne muscular dystrophy. *Cell* 90, 729-738.
201. Deconinck, A.E., Rafael, J.A., Skinner, J.A., Brown, S.C., Potter, A.C., Metzinger, L., Watt, D.J., Dickson, J.G., Tinsley, J.M., and Davies, K.E. (1997). Utrophin-dystrophin-deficient mice as a model for Duchenne muscular dystrophy. *Cell* 90, 717-727.
202. Richler, C., and Yaffe, D. (1970). The in vitro cultivation and differentiation capacities of myogenic cell lines. *Dev Biol* 23, 1-22.
203. Rando, T.A., and Blau, H.M. (1994). Primary mouse myoblast purification, characterization, and transplantation for cell-mediated gene therapy. *J Cell Biol* 125, 1275-1287.
204. Qu, Z., and Huard, J. (2000). Matching host muscle and donor myoblasts for myosin heavy chain improves myoblast transfer therapy. *Gene Ther* 7, 428-437.